

**CALCIUM REGULATION OF INHIBITORY SYNAPTIC TRANSMISSION**

By

Courtney Lauren Williams

A DISSERTATION

Presented to the Neuroscience Graduate Program

and the Oregon Health and Science University

School of Medicine

In partial fulfillment of

the requirements for the degree of

Doctor of Philosophy

October 2016

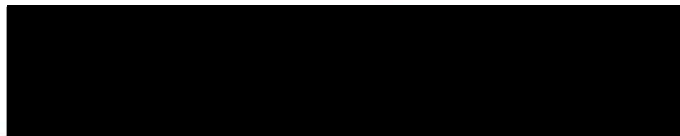
School of Medicine  
Oregon Health & Science University


---

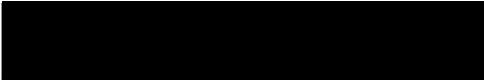
CERTIFICATE OF APPROVAL

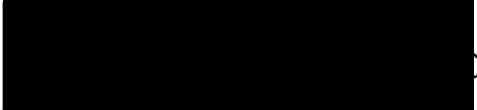
---

This is to certify that the Ph.D. dissertation of  
COURTNEY WILLIAMS  
has been approved on October 21, 2016

  
Advisor, Stephen M. Smith, M.B., B.S., Ph.D.

  
Member and Chair, Craig Jahr, Ph.D.

  
Member, Michael Andresen, Ph.D.

  
Member, Laurence Trussell, Ph.D.

  
Member, Henriette Von Gersdorff, Ph.D.

## TABLE OF CONTENTS

---

LIST OF TABLES AND FIGURES	iii
ACKNOWLEDGEMENTS	v
ABSTRACT	vi
INTRODUCTION	1
Ca <sup>2+</sup> dependence of spontaneous and evoked release	2
Stochastic VACC activity and spontaneous release	4
Ca <sup>2+</sup> domain coupling and synaptic properties	6
VACC-independent mechanisms impacting spontaneous release	7
G protein-coupled receptors mediate Ca <sup>2+</sup> dependence of spontaneous release	9
Divergence in synaptic vesicle release machinery	11
Spontaneous and evoked release use distinct vesicle pools	13
Figures	16
CHAPTER 1	21
Abstract	21
Results	22
Methods	27
Figures	30
CHAPTER 2	40
Abstract	40
Introduction	41
Results	43

Discussion	50
Methods	57
Figures	62
CHAPTER 3	74
Abstract	74
Introduction	75
Methods	76
Results	79
Discussion	85
Figures	91
SUMMARY & CONCLUSIONS	101
Functional significance of tight VACC coupling and cooperativity for spontaneous release	102
Differences in spontaneous release mechanisms at excitatory and inhibitory synapses	106
Consequences of segregation of vesicle pools for spontaneous and evoked release	108
Physiological and pathophysiological importance of spontaneous neurotransmission	112
Conclusions	115
REFERENCES	112

## LIST OF TABLES AND FIGURES

---

### INTRODUCTION

Table 1: Heterogeneity in VACC dependence of spontaneous Release of glutamate and GABA from central synapses	16
Figure 1: Ca <sup>2+</sup> domains	17
Figure 2: Simplified model of vesicle release machinery protein interactions	18
Figure 3: Synaptic vesicles arise from three hypothesised pools	19
Figure 4: Possible vesicle pool scenarios for the origin of spontaneous release	20

### CHAPTER 1

Figure 5: VACCs mediate Ca <sup>2+</sup> -dependent increases in mIPSC frequency	31
Figure 6: Presynaptic hyperpolarization reduces mIPSC frequency	33
Figure 7: Pharmacological dissection of the identity of VACCs mediating spontaneous GABA release	34
Figure 8: The percentage of the total VACC currents carried by GV1a- (1 $\mu$ M) and Aga-IVa (300 nM)-sensitive components were unchanged by the order of toxin application	36
Figure 9: VACC-vesicle coupling is attenuated by BAPTA-AM but not EGTA-AM	37
Figure 10: Exemplary experiments showing the effects of fast and slow Ca <sup>2+</sup> chelation on VACC-vesicle coupling at basal and elevated [Ca <sup>2+</sup> ] <sub>o</sub>	39

### CHAPTER 2

Figure 11: Cd <sup>2+</sup> has distinct actions on spontaneous release Of glutamate and GABA in acute neocortical slices	62
---	----

Figure 12: Cd <sup>2+</sup> had a lower affinity for spontaneous release than evoked release or VACC currents in cultured neocortical neurons	64
Figure 13: Voltage-dependence of Cd <sup>2+</sup> block of VACC currents	66
Figure 14: The selective VACC blocker, MVIIC, substantially reduces spontaneous release of GABA but was ineffective on spontaneous release of glutamate	68
Figure 15: Cd <sup>2+</sup> reduces spontaneous release of GABA and glycine but not glutamate in acute auditory brainstem slices	70
Figure 16: Cd <sup>2+</sup> does not reduce mEPSC frequency in neocortical culture, even in an alternative extracellular solution	72

### CHAPTER 3

Figure 17: Ca <sup>2+</sup> enhancement of spontaneous glutamate and GABA release	91
Figure 18: Diltiazem selectively blocks L-type VACCs	92
Figure 19: L-type VACCs contribute to release of evoked and spontaneous release of GABA	93
Figure 20: VACCs trigger stimulus-evoked release of GABA through Ca <sup>2+</sup> microdomain coupling	94
Figure 21: mechanisms of vesicle pool distinction	95
Figure 22: Selective depletion of the spontaneous recycling pool by inhibiting vesicle refilling	96
Figure 23: The dependence of synaptic depression on stimulation Frequency and estimation of RRP sizes	98
Figure 24: Selective depletion of the evoked recycling pool by inhibiting vesicle refilling	99

## ACKNOWLEDGEMENTS

---

There are many people who I would like to thank for their guidance, encouragement, and friendship during the course of this project. First to thank is my advisor Dr. Stephen M. Smith for his excellent mentorship and support. I could not have asked for a better mentor than Steve. I would like to thank Drs. Craig Jahr, Michael Andresen, Laurence Trussell, and Henrike von Gersdorff for their participation in committees, suggested experiments, and advising on this dissertation. I also owe my thanks to Briana Knight, Wenyen Chen, Glynis Mathiesen, Timur Tsintsadze, and the other members of the Smith lab over the course of this project for their assistance in daily tasks that made this work possible and discussions during lab meetings. Without the aid of my friends Madalynn Erb, Maria Purice, and Caitlin Monaghan my first year course work would have been much more difficult. This project would not have been possible without funding from the National Institute of Neurological Diseases and Stroke, the Tartar Trust Fellowship program, the Neuroscience Graduate Program training grant, and the Pulmonary Critical Care Medicine training grant. Finally, I would like to thank my friends and family for their encouragement, support, and patience during the course of my graduate studies.

## ABSTRACT

---

Synaptic transmission is a process through which neurotransmitter is released from vesicles and triggers a subsequent postsynaptic voltage change. Such interneuronal communication lies at the heart of brain function and is relevant to neurological diseases. The key step in synaptic transmission, vesicle fusion, is driven by highly localized  $\text{Ca}^{2+}$  entry through presynaptic voltage-activated  $\text{Ca}^{2+}$  channels (VACCs), which open in response to an action potential. However, vesicle fusion can also occur spontaneously in the absence of an action potential, and the role of VACCs in regulating this form of release is not understood. This lack of knowledge is a major obstacle to fully understanding the process of neurotransmitter release and its underlying regulatory mechanisms.

Recent findings indicate that action potential-evoked and spontaneous synaptic transmission may be mechanistically distinct. At central synapses, evoked and spontaneous release have been distinguished by differences in vesicle pools used,  $\text{Ca}^{2+}$  sensors for exocytosis, and spatial separation of postsynaptic receptors. The central role of  $\text{Ca}^{2+}$  in triggering vesicle fusion and the apparent differences between evoked and spontaneous synaptic transmission raise the question: does the extracellular  $[\text{Ca}^{2+}]$  ( $[\text{Ca}^{2+}]_o$ ) affect all forms of neurotransmitter release by the same mechanism? This work shows VACCs play a major role in the spontaneous release of the inhibitory neurotransmitter, GABA, but do not trigger spontaneous release of the excitatory neurotransmitter, glutamate, in cortical neurons. Additionally, VACCs are more tightly coupled to vesicle release machinery for spontaneous release than for evoked release at inhibitory terminals. Finally, spontaneous and evoked release at inhibitory nerve



terminals arises from distinct vesicle pools that can be depleted independently. Taken together, these findings provide insight into the mechanisms by which  $\text{Ca}^{2+}$  regulates both spontaneous and evoked release of GABA.

## INTRODUCTION

---

Neurons rely on chemical synaptic transmission to convey and process information. In chemical synaptic transmission, the mechanisms by which action potentials and VAPCs trigger release of neurotransmitter, which is packaged in single vesicles, have been a focal point of inquiry (Neher & Sakaba 2008; Sudhof 2011). Two other forms of neurotransmitter release are used by the nervous system: spontaneous release, which occurs in the absence of an action potential (Ramirez & Kavalali 2011; Pang et al. 2011); and asynchronous release, which is loosely coupled to an action potential (Hefft & Jonas 2005). Just as for synchronous release,  $Ca^{2+}$  plays a vital role in regulating these two alternative forms of synaptic transmission (Peters et al. 2010; Yang et al. 2010; Yao et al. 2011; Xu et al. 2009; Vyleta & Smith 2011; Groffen et al. 2010). It has been presumed that spontaneous and asynchronous release arise from the same vesicle pools and are regulated by similar processes as evoked release (Zucker 2005). However, the situation is much more complex. Mounting evidence shows that spontaneous and synchronous release pathways are distinct (Peters et al. 2010; Yao et al. 2011; Vyleta & Smith 2011; Groffen et al. 2010; Sara et al. 2005), arise from independent vesicle pools (Sara et al. 2005; Fredj & Burrone 2009), utilize disparate release machinery (Yao et al. 2011; Groffen et al. 2010; Sun et al. 2007; Ramirez et al. 2012), and potentially mediate discrete physiological functions (Autry et al. 2011; Xu et al. 2012; Sutton et al. 2006; Gideons et al.

2014). Herein are discussed the multifarious activities of  $\text{Ca}^{2+}$  in the regulation of these various release mechanisms at the synapse. We focus on three key aspects of synaptic transmission: sources of  $\text{Ca}^{2+}$  mediating release, vesicle release machinery, and vesicle pools for different modes of transmission.

### **$\text{Ca}^{2+}$ dependence of Spontaneous and Evoked Release**

Spontaneous release was first described at the frog neuromuscular junction with the observation of small, subthreshold depolarizations of the postsynaptic membrane, occurring in the absence of stimulation (Fatt et al. 1950; Fatt & Katz 1952). These events had similar time courses to end-plate potentials (EPPs)—which are evoked by action potentials in the motor neuron—but, being around 100 times smaller, were termed miniature end-plate potentials (mEPPs) or minis (Fatt & Katz 1952). Decreasing external  $[\text{Ca}^{2+}]$  ( $[\text{Ca}^{2+}]_o$ ) resulted in step-like reductions in EPP amplitude, with each step about the same size as a mEPP, indicating that synaptic transmission arises from the release of discrete quanta of acetylcholine and is  $\text{Ca}^{2+}$ -dependent (del Castillo & Katz 1954). These findings were confirmed by the observation of fusion of discrete vesicles of neurotransmitters with the presynaptic membrane using electron microscopy (Heuser et al. 1979; Heuser & Reese 1973).

Since these investigations, spontaneous neurotransmission has frequently been studied as a simple proxy for examining properties of action potential-evoked release, including quantal content and numbers of postsynaptic receptors. Even in these early studies, however, differences in spontaneous and

evoked neurotransmission were apparent in the disparities in their  $\text{Ca}^{2+}$  dependence (Katz & Miledi 1968; Katz & Miledi 1969).  $\text{Ca}^{2+}$  entry is the initiation step for fast synaptic transmission (Katz & Miledi 1967; Borst & Sakmann 1996). Dodge and Rahamimoff observed that evoked release is proportional to the fourth power of  $[\text{Ca}^{2+}]_o$  at the frog neuromuscular junction, which has since been confirmed in a number of preparations (Dodge & Rahamimoff 1967; Augustine & Charlton 1986; Borst & Sakmann 1996). The slope of the log-log transform of the concentration-effect relationship ( $n$ ) reflects the high intrinsic  $\text{Ca}^{2+}$  cooperativity of activation of the exocytotic machinery, and represents a minimum number of  $\text{Ca}^{2+}$  binding steps required to trigger vesicle fusion—in this case 4-5 (Matveev et al. 2011). This contrasts with the relatively weak dependence of spontaneous release on  $[\text{Ca}^{2+}]_o$  observed at the neuromuscular junction (Fatt & Katz 1952). The slope of the log-log plot for spontaneous release was only 0.21–0.41, much lower than for evoked release (Matthews & Wickelgren 1977; Boyd & Martin 1956; Hubbard et al. 1968; Hubbard 1961). At neocortical excitatory and inhibitory synapses, spontaneous release was also weakly dependent on external  $\text{Ca}^{2+}$  ( $n = 0.45\text{--}0.63$ ) (Williams et al. 2012; Vyleta & Smith 2011; Groffen et al. 2010). However, in contrast, glutamate and GABA release have been reported to be more strongly dependent on  $[\text{Ca}^{2+}]_o$  at neocortical synapses by others ( $n = 1.47$  and  $1.49$ , respectively) (Xu et al. 2009). Despite some disagreement on specifics, the majority of studies agree that spontaneous release is  $\text{Ca}^{2+}$  dependent, albeit with a weaker dose-response relationship for  $[\text{Ca}^{2+}]_o$ . This raises the question,

how do changes in  $[Ca^{2+}]_o$  affect spontaneous neurotransmission in the absence of a synchronizing action potential? The two major possible pathways I discuss here are stochastic opening of VACCs and release of  $Ca^{2+}$  from intracellular stores.

### **Stochastic VACC activity and spontaneous release**

Evoked vesicle fusion is triggered by  $Ca^{2+}$  entry predominantly via N-, P/Q- or R-type VACCs (Wheeler et al. 1994; Jun et al. 1999). Despite the high intrinsic cooperativity, evoked release is astoundingly sensitive to  $Ca^{2+}$  and can be triggered by only 1 or 2 VACCs per vesicle at some synapses (Bucurenciu et al. 2010; Shahrezaei et al. 2006; Stanley 1993). Thus stochastic activation of VACCs could provide the mechanism for spontaneous release at rest (Matthews & Wickelgren 1977). Spontaneous activation of a VACC at the resting membrane potential will result in a very differently shaped transient in  $[Ca^{2+}]_i$  than an action potential evoked VACC opening. The upper limit for the driving force for  $Ca^{2+}$  will be higher for spontaneous release when the membrane is at rest. This can be calculated using the Nernst equation (eq. 1) to calculate the reversal potential for  $Ca^{2+}$  ( $V_{eq}$ ) and the electrochemical driving force ( $V_{DF}$ ; eq.2).

$$\text{eq.1} \quad V_{eq} = \frac{RT}{zF} \ln\left(\frac{[Ca^{2+}]_o}{[Ca^{2+}]_i}\right)$$

$$\text{eq.2} \quad V_{DF} = V_m - V_{eq}$$

The equilibrium potential for  $Ca^{2+}$  is estimated to be 134 mV, using physiological values for  $[Ca^{2+}]_o$  (1.1 mM), intracellular  $[Ca^{2+}]$  ( $[Ca^{2+}]_i$ , around 50 nM), and temperature ( $T$ , 37°C); as well as the gas constant ( $R$ ), the Faraday constant ( $F$

), and a valence ( $z$ ) of +2 (Nilsson et al. 1993; Maravall et al. 2000). The electrochemical driving force ( $V_{DF}$ ) is then calculated to be -204 mV at a resting membrane potential ( $V_m$ ) of -70 mV, indicating a strong force for influx through randomly opening channels.  $V_{DF}$  will be lower for stimulus-evoked release because the membrane is more depolarized.

Studies show that VACCs are important physiological triggers for spontaneous release at central synapses (Table 1; Goswami et al. 2012; Ermolyuk et al. 2013; Williams et al. 2012). The frequency of spontaneous release events at these synapses may be dependent several factors including the number and type of VACC, the  $\text{Ca}^{2+}$  domain coupling for the channels and release machinery, the concentration of intracellular  $\text{Ca}^{2+}$  buffers, or the resting membrane potential. For example, R-type channels in particular may be a good candidate for regulation of spontaneous release because of their lower activation voltage (Ermolyuk et al. 2013). Additionally, cholecystinin-expressing interneurons exhibit higher spontaneous release rates compared to parvalbumin-expressing interneurons in the dentate gyrus, which has been attributed to differences in relative number of VACC in the active zone (Goswami et al. 2012).

If stochastic opening of VACCs is the gateway for  $\text{Ca}^{2+}$  entry that triggers spontaneous vesicle fusion, it raises the question: are there enough VACC openings to account for the observed frequency of spontaneous neurotransmission? The frequency of random VACC openings in the inhibitory

terminals synapsing with a single neocortical neuron ( $Fr_o$ ) was estimated using eq. 3 to attempt to answer this question (Smith et al. 2012).

$$\text{eq.3} \quad Fr_o = N_T \times Pr_i \times N_{VACC} \times \frac{P_{VACC}}{T}$$

Where  $N_T$  was the number nerve terminals per neuron,  $Pr_i$  was the proportion of synapses that are inhibitory,  $N_{VACC}$  was the number of VACC per terminal,  $P_{VACC}$  was the probability that a VACC was open and  $T$  was the average channel open time at the membrane potential. The estimate of the average  $Fr_o$  was more than 100 times greater than the average measured mIPSC frequency (513  $s^{-1}$  versus 4.4  $s^{-1}$ , respectively), indicating that there are 100-fold more VACC openings than vesicle fusion events at inhibitory synapses (Smith et al. 2012).

### **Ca<sup>2+</sup> domain coupling and synaptic properties**

The diffusion distance for Ca<sup>2+</sup> from VACCs to Ca<sup>2+</sup> sensors for release, or Ca<sup>2+</sup> domain, is an essential determinant of synaptic properties (Figure 1; Eggermann et al. 2011). Two functional distances have been defined for Ca<sup>2+</sup> domains: nanodomains (distances < 100 nm) and microdomains (distances > 100 nm) (Eggermann et al. 2011). A Ca<sup>2+</sup> nanodomain (Bucurenciu et al. 2008; Christie et al. 2010; Meinrenken et al. 2002) to promote higher release probability and temporal precision of neurotransmission, as tighter coupling minimizes the diffusion component of the synaptic delay (Bucurenciu et al. 2008; Christie et al. 2010; Meinrenken et al. 2002). In contrast, Ca<sup>2+</sup> microdomains allow for more modulation by Ca<sup>2+</sup> buffers, possibly enabling presynaptic forms of synaptic plasticity (Ahmed & Siegelbaum 2009).

Ca<sup>2+</sup> domain size has major implications for spontaneous transmission. A nanodomain topography may allow for an increase in the frequency of spontaneous exocytosis (Stanley 1997). In this arrangement, stochastic opening of single VACCs—which lead to brief, local elevations in [Ca<sup>2+</sup>]<sub>i</sub>—could directly trigger fusion of synaptic vesicles (Figure 1). However, simultaneous opening of multiple VACCs—and the generation of a more global, longer lasting rise in [Ca<sup>2+</sup>]<sub>i</sub>—may be required to trigger spontaneous vesicle fusion in a microdomain coupling configuration. In the extreme case, where the Ca<sup>2+</sup> domain is very large, spontaneous release could be controlled by basal [Ca<sup>2+</sup>]<sub>i</sub>, instead of the transient changes like those occurring following the opening of VACCs. To date, spontaneous release has been shown to be triggered by both microdomains and nanodomains at different central synapses (Goswami et al. 2012; Williams et al. 2012; Ermolyuk et al. 2013).

### **VACC-independent mechanisms impacting spontaneous release**

In spite of observations that VACCs regulate spontaneous release of neurotransmitter at some synapses, it is clear that spontaneous release does not always require VACCs for release (Table 1). In cerebellum, blockade of VACCs with Cd<sup>2+</sup> does not affect spontaneous release from inhibitory terminals (Llano & Gerschenfeld 1993). Neocortical excitatory synapses do not require Ca<sup>2+</sup> entry via VACCs to trigger spontaneous release of glutamate (Vyleta & Smith 2011). Spontaneous release is also independent of tight coupling to VACCs at the calyx of held synapse (Dai et al. 2015). Furthermore, several studies that disrupt



recruitment of VACCs to release sites or association of VACCs to fusion proteins have shown a decrease in stimulus evoked release but an increase in spontaneous release (Mochida et al. 1996; Long et al. 2008). Even at neocortical inhibitory terminals where VACCs trigger spontaneous fusion, approximately 40% of spontaneous release remains in saturating concentrations of  $\text{Cd}^{2+}$ , defining a portion of spontaneous release that is independent of VACCs (Williams et al. 2012).

At some synapses  $\text{Ca}^{2+}$  release from intracellular stores may control spontaneous neurotransmission. Cerebellar interneurons produce large-amplitude miniature inhibitory postsynaptic currents (mIPSCs) in the presence of tetrodotoxin (TTX) (Llano et al. 2000). These multivesicular spontaneous events are independent of VACC activity, but may arise from release of  $\text{Ca}^{2+}$  via ryanodine receptors on presynaptic  $\text{Ca}^{2+}$  stores (Llano et al. 2000). In hippocampus, depletion of  $\text{Ca}^{2+}$  from stores activates store-operated  $\text{Ca}^{2+}$  channels, and can thereby influence spontaneous glutamate release (Emptage et al. 2001). Caffeine has also been shown to modulate spontaneous release of glutamate in neocortical neurons through stimulation of  $\text{Ca}^{2+}$ -induced  $\text{Ca}^{2+}$  release (CICR)—a process by which  $\text{Ca}^{2+}$  promotes its own release from intracellular stores (Vyleta & Smith 2008).

Another possible source for  $\text{Ca}^{2+}$  regulation of spontaneous release is the  $\text{Na}^+$ - $\text{Ca}^{2+}$  exchanger (NCX), which normally functions in removal of  $\text{Ca}^{2+}$  from nerve terminals (Nachshen et al. 1986; Sanchez-Armass & Blaustein 1987).

$[Ca^{2+}]_o$  could enhance spontaneous fusion by promoting reverse-mode NCX activity ( $Na^+$  efflux,  $Ca^{2+}$  influx) (Smith et al. 2012). If this occurs, direct inhibition of NCX-mediated  $Ca^{2+}$  transport should attenuate the enhancement of spontaneous fusion by elevation of  $[Ca^{2+}]_o$ . KB-R7943 inhibits forward- and reverse-mode NCX currents, and spontaneous release of glutamate is significantly increased by KB-R7943 in neocortical cultures, consistent with the hypothesis that NCX can increase basal  $[Ca^{2+}]_i$  and spontaneous fusion through a forward transport mechanism (Watano et al. 1996; Kimura et al. 1999; Vyleta & Smith 2011; Smith et al. 2012).

### **G protein-coupled receptors mediate $Ca^{2+}$ dependence of spontaneous release**

G protein-coupled receptors (GPCRs) may also mediate a portion of the  $Ca^{2+}$  dependence of spontaneous vesicle fusion. One example is the  $Ca^{2+}$ -sensing receptor (CaSR), which is activated by increases in  $[Ca^{2+}]_o$  and  $[Mg^{2+}]_o$  and is expressed at presynaptic terminals in the central nervous system (Brown et al. 1993; Chen et al. 2010). CaSR canonically couples to  $G_q$  proteins and signals by activation of phospholipase-C (PLC)—hydrolysing phosphatidylinositol-(4,5)-bisphosphate ( $PIP_2$ ) into inositol-1,4,5-trisphosphate ( $IP_3$ ) and diacylglycerol (DAG) (Smith et al. 2012). Cinacalcet, an allosteric CaSR agonist, increases miniature frequency at both excitatory and inhibitory neocortical synapses (Vyleta & Smith 2011; Smith et al. 2012). Multiple lines of evidence indicate that CaSR activation strongly stimulates spontaneous

glutamate release at neocortical synapses, which are also unaffected by block of VACCs (Vyleta & Smith 2011). For example,  $\text{Ga}^{3+}$  and  $\text{Mg}^{2+}$ —CaSR agonists and VACC blockers—increase spontaneous release of glutamate (Vyleta & Smith 2011). In addition, CaSR null mutants have a lower miniature excitatory postsynaptic current (mEPSC) frequency over the range of  $[\text{Ca}^{2+}]_o$  to which CaSR responds (Vyleta & Smith 2011; Smith et al. 2012). Interestingly, CaSR stimulation also inhibits the activity of a nonselective cation channel in nerve terminals and impairs evoked excitatory transmission in neocortical neurons, indicating inverse regulation of spontaneous and activity-dependent transmission at the same synapse, though likely through distinct pathways (Chen et al. 2010; Phillips et al. 2008).

In neocortical cultures, CaSR accounts for about 30% of basal spontaneous glutamate release, but it is unknown which pathways regulate the remaining 70% of spontaneous glutamate release (Smith et al. 2012). At least a portion of the underlying mechanisms must be  $\text{Ca}^{2+}$ -sensitive, since spontaneous glutamate release is still dependent on increases in  $[\text{Ca}^{2+}]_o$  in neocortical cultures made from CaSR knockout mice (Vyleta & Smith 2011). Several other GPCRs modulate spontaneous release (Ramirez & Kavalali 2011). Exogenous phorbol esters and DAG—which activate or participate in a protein kinase C-dependent pathway—augment both spontaneous and evoked release through allosteric modification of  $\text{Ca}^{2+}$  sensing release machinery or VACCs (Swartz et al. 1993; Lou et al. 2005; Waters & Smith 2000; Ramirez & Kavalali 2011; Malenka et al. 1986;

Virmani et al. 2005). Activation of Group II metabotropic glutamate receptors in cerebellar brain slices reduces spontaneous release of GABA onto Purkinje cells (Glitsch 2006). Likewise, activation of GABA<sub>B</sub> or cannabinoid receptors reduces spontaneous release at cerebellar synapses (Yamasaki 2006; Dittman & Regehr 1996). Cannabinoid receptor activation also increases spontaneous release in the dentate gyrus, showing that there is brain region-specific variability in these regulatory mechanisms (Hofmann et al. 2011).

### **Divergence in synaptic vesicle release machinery**

The vesicle membrane contains a variety of proteins that participate in exocytosis (Figure 2; Takamori et al. 2006; Weingarten et al. 2014; Wilhelm et al. 2014).

Some of these vesicle associated proteins have been shown to participate in trafficking of vesicles into segregated pools, indicating that vesicles may have distinct molecular identities related to their function (Crawford & Kavalali 2015).

Many of these proteins are important in the process of exocytosis, which is initiated by the binding of vesicular soluble NSF attachment protein receptor (v-SNARE) proteins to target membrane SNARE (t-SNARE) proteins to form a fusion complex (Figure 2; Crawford & Kavalali 2015). The canonical v-SNARE, synaptobrevin 2 binds to t-SNAREs syntaxin 1 and synaptosomal associated protein of 25 kDa (SNAP-25) in order to bring the vesicular membrane in close proximity to the plasma membrane (Figure 2; Südhof 2013). For evoked release, fusion occurs when Ca<sup>2+</sup> binds the Ca<sup>2+</sup> sensor synaptotagmin 1 (Figure 2; Südhof 2013). Furthermore, a variety of other synaptic proteins, many of which are

localized in the vesicle membrane, have been shown to regulate fusion (Sudhof 2011; Crawford & Kavalali 2015).

Studies have found several differences in release machinery and vesicle associated proteins for spontaneous and evoked release. Deletion of synaptobrevin 2 in cultured mouse hippocampal neurons and the *Drosophila* neuromuscular junction abolishes activity-dependent release but only reduces spontaneous release (Schoch et al. 2001; Deák et al. 2004; Broadie et al. 1995; Deitcher et al. 1998; Saitoe et al. 2001; Deak et al. 2006). Similarly, application of tetanus toxin, which cleaves synaptobrevin 2, severely impairs evoked neurotransmission while having a small effect on spontaneous release (Schiavo et al. 1992; Herreros et al. 1995). Other machinery proteins show preference for spontaneous release. For example, the v-SNARE vps10p tail interactor 1a (vti1a) and vesicular associated membrane protein 7 (VAMP7) are major participants in spontaneous but not evoked vesicle recycling (Crawford & Kavalali 2015; Ramirez et al. 2012; Hua et al. 2011). Reelin, a glycoprotein, enhances spontaneous neurotransmission by recruiting VAMP7-expressing vesicles (Bal et al. 2013). Complexin—a SNARE complex-binding protein—activates Ca<sup>2+</sup>-dependent exocytosis (Figure 2; Brose 2008; McMahon et al. 1995). Complexin null mutations in *Drosophila* and double knockdown of complexins 1 and 2 in mouse neurons markedly increases spontaneous release, suggesting that complexins act as a clamp to prevent spontaneous vesicle fusion (Yang et al. 2013; Huntwork & Littleton 2007).

Ca<sup>2+</sup> sensors that bind Ca<sup>2+</sup> to catalyze vesicle fusion also differ for spontaneous and evoked release at some synapses. Synaptotagmin 1 and 2 both sense Ca<sup>2+</sup> via their two C-terminal C2 domains (Fernández-Chacón et al. 2001; Pang et al. 2006). Loss of either synaptotagmin 1 or 2 impairs activity-dependent transmission but increases spontaneous release, leading to a hypothesis that synaptotagmins, like complexins, may also have a clamping function (Maximov & Südhof 2005; Liu et al. 2009; Wierda & Sorensen 2014). Other studies have shown that synaptotagmin does function as a Ca<sup>2+</sup> sensor for spontaneous release, but deletion of synaptotagmin allows for activation of a second Ca<sup>2+</sup> sensor that has an apparent higher Ca<sup>2+</sup> affinity (Xu et al. 2009). Double C2 domain (DOC2) family proteins have also been shown to selectively maintain spontaneous release, though there is disagreement about whether DOC2 proteins function in a Ca<sup>2+</sup>-dependent or-independent manner (Groffen et al. 2010; Pang et al. 2011). Taken together, the observed actions of complexins, synaptotagmins, and DOC2 proteins suggest that there may be important mechanisms that selectively regulate the probability of spontaneous vesicle fusion events.

### **Spontaneous and evoked release use distinct vesicle pools**

Most models of synaptic transmission divide synaptic vesicles into three functional pools: the readily releasable pool (RRP)—which contains vesicles docked at the active zone and primed for release, a recycling pool—containing vesicles that mobilize on depletion of the RRP, and a reserve pool—containing, vesicles that are difficult to mobilize and may function to maintain the recycling

pool (Figure 3; Zucker 1989; Denker & Rizzoli 2010; Rizzoli & Betz 2005). The assumption that spontaneous and evoked release share the same vesicle population provides testable hypotheses about the relationship between these two forms of synaptic transmission (Figure 4). If both forms of transmission arise from the same vesicle pool, the spontaneous release rate should be proportional to the number of vesicles in the RRP, and evoked release should be reduced by exhaustion of spontaneously recycling vesicles (Kavalali 2015). These assumptions have been tested using manipulations to impair presynaptic function in a use-dependent manner. Inhibiting vesicle refilling of spontaneously recycling vesicles with vacuolar ATPase inhibitors impairs spontaneous release, but only modestly reduces evoked release (Nosyreva et al. 2013; Ertunc et al. 2007; Sara et al. 2005). Experiments using the styryl dye, FM2-10 show that vesicles that are stained in the absence of activity are resistant to destaining during stimulation (Sara et al. 2005). Other work has shown that dynamin inhibition causes depletion of vesicles within the RRP and use-dependent loss of evoked release, while the spontaneous recycling pool is independent of dynamin activity (Chung et al. 2010). In vivo imaging experiments in *Drosophila* larvae have shown that while individual synapses can participate in both evoked and spontaneous neurotransmission, synapses show a preference for one mode of transmission over the other (Peled et al. 2014; Melom et al. 2013).

Evidence suggests that trafficking pathways that maintain spontaneous and evoked synaptic transmission are divergent and there are several mechanism

by which this could occur (Figure 4). The molecular differences in membrane associated proteins may contribute to this divergence from parallel pathways, as there appear to be both overlapping and nonoverlapping distributions of vesicle associated proteins (Figure 4). Studies that aim to biochemically characterize the various population of synaptic vesicles and super-resolution imaging experiments will be needed in the future to help construct a more concrete picture of vesicle pool heterogeneity and its function in neurotransmission.



## FIGURES

**Table 1: Heterogeneity in VACC-dependence of spontaneous release of glutamate and GABA from central synapses.**

Synapse	VACC dependence?	Reference
GABAergic synapses from hippocampal granule cells in rat hippocampal slices	yes	(Goswami et al. 2012)
GABAergic synapses in mouse neocortical culture	yes	(Williams et al. 2012)
GABA release from rat medial preoptic nerve	yes	(Druzin et al. 2002)
GABAergic synapses in dissociated rat basolateral amygdala neurons	yes	(Koyama et al. 1999)
Glutamatergic synapses in rat hippocampal cultures	yes	(Ermolyuk et al. 2013)
Glutamatergic synapses in slices of hamster and rat spinal laminae I and II	yes	(Bao et al. 1998)
Glutamate release from juvenile mouse calyx of held	yes	(Dai et al. 2015)
Glutamatergic and GABAergic synapses onto mouse cerebellar purkinje cells	no	(Yamasaki 2006)
Glutamatergic synapses in rat hippocampal cultures	no	(Abenavoli et al. 2002)
Glutamatergic synapses in rat hippocampal slice culture	no	(Scanziani et al. 1992)
Glutamatergic synapses in mouse neocortical culture	no	(Vyleta & Smith 2011)

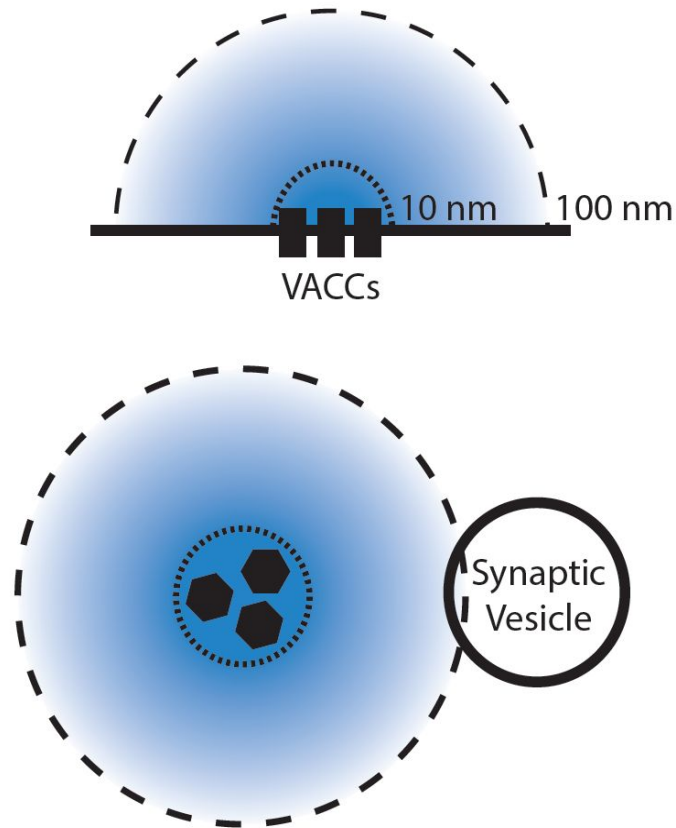


**Figure 1: Ca<sup>2+</sup> domains.** (Upper panel) Illustration of Ca<sup>2+</sup> domain (blue gradient) created by Ca<sup>2+</sup> influx through a cluster of VACCs as viewed from the side. The dashed lines represent the boundaries of a Ca<sup>2+</sup> nanodomain from 10-100 nm away from the Ca<sup>2+</sup> source. (Lower panel) Top-down view of the same Ca<sup>2+</sup> domain with a synaptic vesicle. Illustration adapted from (Stanley 2016).

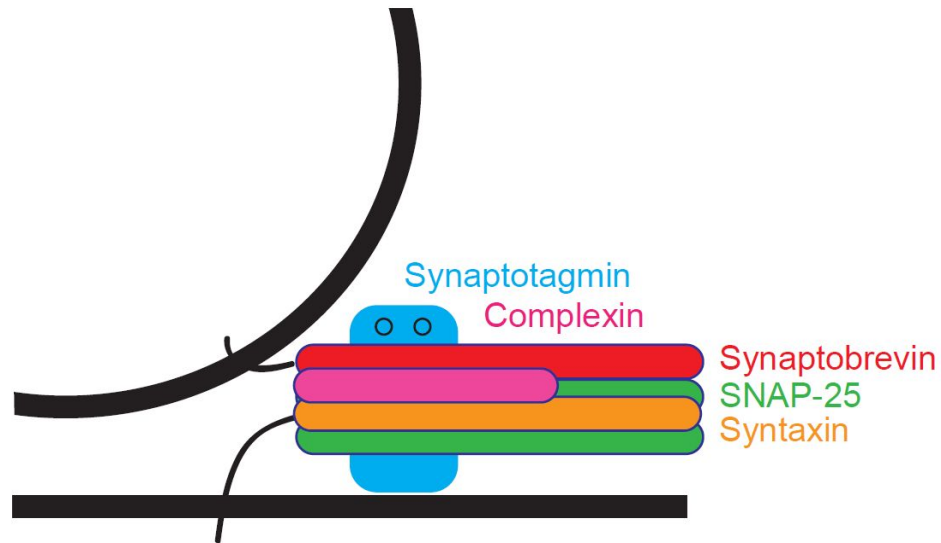


**Figure 2: Simplified model of synaptic vesicle release machinery protein**

**interactions.** The core of the vesicle release apparatus is the SNARE complex. The neuronal SNARE complex is formed by interactions between the v-SNARE, synaptobrevin (red), and the t-SNAREs, SNAP-25 (green) and syntaxin (orange). Each rod shape represents a SNARE motif. Synaptobrevin and syntaxin both have a single SNARE motif and SNAP-25 has two. Synaptotagmin (blue) acts as a  $\text{Ca}^{2+}$  sensor for exocytosis via its two C2 domains (circles). Complexin (pink) stabilizes SNARE complex formation and assists synaptotagmin. Illustration adapted from (Rizo et al. 2015).

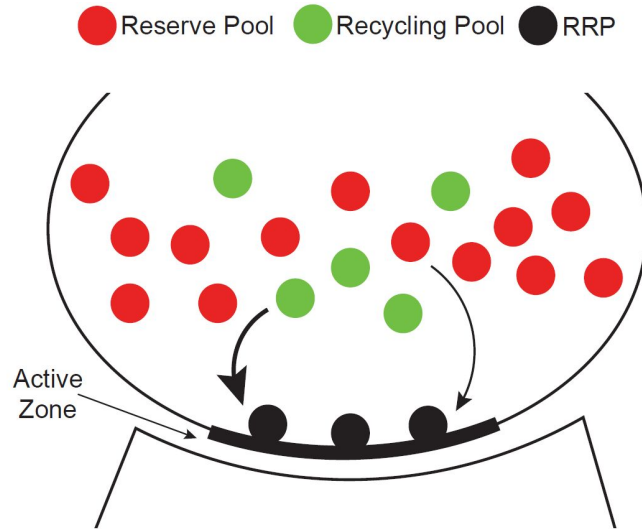


**Figure 3: Synaptic vesicles arise from three theoretical pools.** These pools consist of a RRP (black), recycling pool (green), and a reserve pool (red). RRP vesicles are docked and primed for release at the active zone. Recycling vesicles are recruited for release upon moderate stimulation (indicated by the thick arrow), while reserve vesicles are only released under high intensity stimulation (indicated by the thin arrow). Illustration adapted from (Denker & Rizzoli 2010).

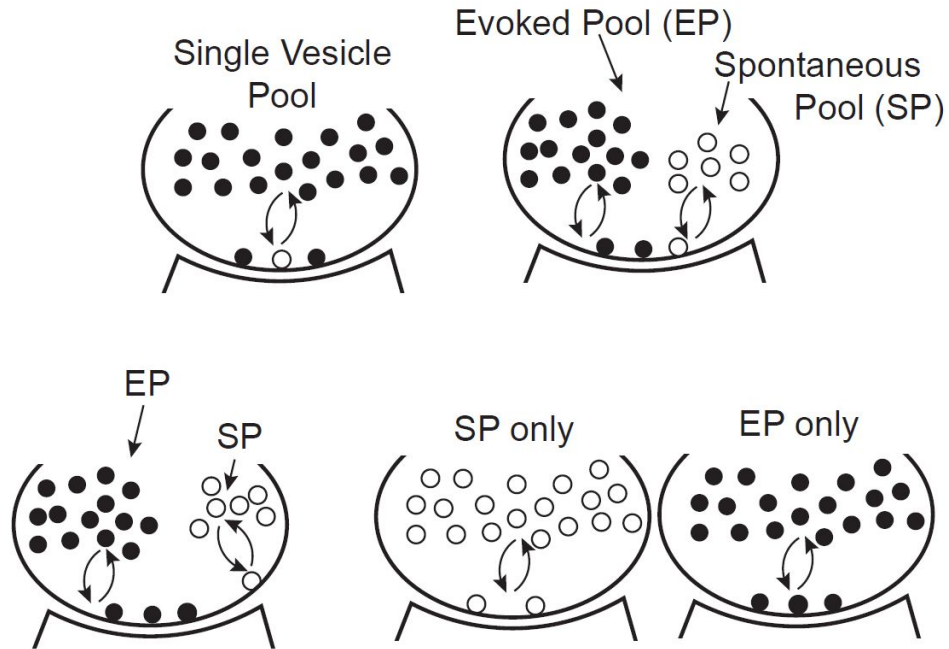


**Figure 4: Possible vesicle pool scenarios for the origin of spontaneous**

**release.** Spontaneous and evoked release may arise from the same vesicle pools and be released at the same active zones (top left). Some evidence that spontaneously released vesicles may arise from an independently recycling pool. There are three main possible mechanisms by which this may occur: (1) spontaneous and evoked pools recycle independently but are released from the same active zone (top right), (2) spontaneous and evoked pool recycle independently and spontaneous release occurs at a distant site from the active zone (bottom left), and (3) spontaneous and evoked release take place at different nerve terminals (bottom right). Adapted from (Wasser & Kavalali 2009).

## CHAPTER 1

---

### **Co-activation of multiple tightly-coupled calcium channels triggers spontaneous release of GABA**

Courtney Williams,<sup>1</sup> Wenyan Chen,<sup>1</sup> Chia-Hsueh Lee, Daniel Yaeger, Nicholas P. Vyleta,<sup>2</sup> and Stephen M. Smith<sup>3</sup>

Division of Pulmonary & Critical Care Medicine, Oregon Health & Science University, Portland, OR 97239

<sup>3</sup>Correspondence should be addressed to: Dr. Stephen M. Smith, Division of Pulmonary & Critical Care Medicine, 3181, SW Sam Jackson Park Road, UHN-67, O.H.S.U., Portland, OR 97239, USA., Telephone: (503) 494-2736, Fax: (503) 494-7368, Email: [smisteph@ohsu.edu](mailto:smisteph@ohsu.edu)

<sup>1</sup>These authors contributed equally

<sup>2</sup>Current address: Institute of Science and Technology, Austria

### **ABSTRACT**

VACCs mediate Ca<sup>2+</sup> influx to trigger action potential-evoked neurotransmitter release but the mechanism by which Ca<sup>2+</sup> regulates spontaneous transmission is unclear. Here we show VACCs are the major physiological triggers for

spontaneous release at murine neocortical inhibitory synapses. Moreover, despite the absence of a synchronizing action potential, we find that spontaneous fusion of a GABA-containing vesicle requires the activation of multiple tightly-coupled VACCs of variable type.

## **RESULTS**

Spontaneous and evoked neurotransmission, two forms of interneuronal communication, have been proposed to rely on different signaling mechanisms and to mediate physiologically distinct functions (Sara et al. 2005; Autry et al. 2011). While it is well-established that presynaptic action potentials activate VACCs, triggering  $\text{Ca}^{2+}$  influx and synchronous release of neurotransmitter, how  $[\text{Ca}^{2+}]_o$  is coupled to spontaneous release remains controversial. Although increasing  $[\text{Ca}^{2+}]_o$  enhances spontaneous neurotransmission at excitatory neocortical synapses, blocking of VACCs or buffering of  $[\text{Ca}^{2+}]_i$  has no effect on spontaneous release (Vyleta & Smith 2011). In contrast, at GABAergic cortical synapses mutation of  $\text{Ca}^{2+}$  sensors, such as synaptotagmin-1, impacts spontaneous release, suggesting a major role for  $\text{Ca}^{2+}$  influx (Xu et al. 2009). Here we show that, in contrast to regulation of excitatory synapses, spontaneous release from inhibitory synapses is dependent on VACCs and that single vesicle fusion requires coincident activation of multiple closely packed VACCs.

We examined how  $[\text{Ca}^{2+}]_o$  is coupled to spontaneous release of GABA by recording mIPSCs in cultured neocortical neurons. Changing  $[\text{Ca}^{2+}]_o$  from 1.1

mM, altered mIPSC frequency in a reversible and concentration-dependent manner (Figure 5a-c, n = 6). The steepness of the concentration-effect relationship was much lower (slope = 0.45) compared to evoked release but similar to that for mEPSCs (Vyleta & Smith 2011; Lou et al. 2005). Application of  $\text{Cd}^{2+}$  (100  $\mu\text{M}$ ), a VACC blocker, reduced mIPSC frequency by  $56 \pm 7\%$  (n = 6) from the basal level when  $[\text{Ca}^{2+}]_o$  was 1.1 mM (Figure 5d). At 6 mM  $\text{Ca}^{2+}$  mIPSC frequency was  $185 \pm 46\%$  above basal level and relatively reduced by  $56 \pm 8\%$  following  $\text{Cd}^{2+}$  application. These data indicate VACCs trigger spontaneous GABA release at both physiological and elevated  $[\text{Ca}^{2+}]_o$ . Stochastic VACC activity should be decreased by presynaptic hyperpolarization. Reduction of external  $[\text{K}^+]$  from 4 to 1 mM, to hyperpolarize the nerve terminals, reversibly reduced mIPSC frequency by  $34 \pm 8\%$  (Figure 6, n = 6) but had little effect when VACC were blocked by  $\text{Cd}^{2+}$ . These data demonstrate that, in contrast to glutamatergic excitatory synapses, VACCs elicit spontaneous GABA release at neocortical synapses (Vyleta & Smith 2011).

Evoked GABA release is regulated by VACC subtypes in the order P/Q->N->R-types at cortical synapses (Cao & Tsien 2005). To determine which VACCs regulate spontaneous GABA release, we applied specific channel type blockers while recording mIPSCs. Blockade of N-type channels with a saturating dose of  $\omega$ -conotoxin-GVIA (GVIA, 1  $\mu\text{M}$ ) reduced mIPSC frequency by  $32 \pm 7\%$  (n = 9; Figure 7a,b; Boland et al. 1994). Subsequent addition of a saturating concentration of the P/Q-type blocker  $\omega$ -Aga-toxin-IVA (Aga-IVA, 300 nM)



reduced mIPSC frequency by  $11 \pm 4\%$  suggesting a larger contribution by N- than P/Q-type VACCs (Figure 7a,b;  $p = 0.015$ ).  $\text{Cd}^{2+}$  reduced mIPSC frequency a further  $23 \pm 8\%$  (Figure 7a,b), indicating contributions by L- or R-type VACCs. On average,  $33 \pm 6\%$  of mIPSCs were  $\text{Cd}^{2+}$  resistant suggesting that other regulatory mechanisms also contribute to spontaneous GABA release (Vyleta & Smith 2011). Taken together these data indicate that P/Q- and N- type VACCs are important triggers of mIPSCs.

At most synapses the simultaneous activation of multiple VACCs has been implicated as necessary to trigger single vesicle fusion during evoked release whereas it has been proposed that spontaneous release results from the activation of a single VACC (Stanley 1997; Bucurenciu et al. 2010; Eggermann et al. 2011). If each fusion event depends on the opening of a single channel the impact of the block of P/Q- or N-type VACCs with slowly dissociating toxins will be independent of each other. Conversely, if multiple channels are involved, cooperativity will result in proportionately smaller reductions in release probability as the total fraction of VACC blocked is increased (Mintz et al. 1995). Consistent with multiple channel involvement, the relative effectiveness of 300 nM Aga-IVa and 1  $\mu\text{M}$  GVIA was reversed when the order of toxin application was switched ( $32 \pm 7\%$  versus  $3 \pm 3\%$ ,  $p = 0.050$ ; Figure 7c,d). This was not due to interneuronal variability of the proportion of mIPSCs independent of VACCs, as the reversal in the apparent effectiveness of GVIA and Aga-IVa was also evident when we compared the toxin's actions on the  $\text{Cd}^{2+}$ -sensitive fraction (Figure 7e).

In other words GVIA and Aga-IVA were more effective at reducing mIPSC frequency when the neuron had not already been exposed to saturating doses of the other blocker ( $p = 0.008$  and  $p = 0.018$  respectively; Figure 7e). At higher doses Aga-IVA cross-reacts with N-type channels (Sidach & Mintz 2000). To test if cross-reactivity was responsible for the reduced effects of the second toxin applications on mIPSC frequency we directly measured VACC current block in these neurons. The percentage of the total VACC currents carried by  $1 \mu\text{M}$  GVIA- and  $300 \text{ nM}$  Aga-IVA-sensitive fractions were unchanged by the order of toxin application (Figure 8) indicating cross-reactivity was not responsible for the reduced effect of the second toxin application (Figure 7). Collectively, the data obtained from channel-type specific toxins show that each fusion event was dependent on multiple VACCs *and* that different VACC types cooperate to trigger fusion of a single vesicle.

How close are these VACCs to the vesicle? One hypothesis is that VACCs are not tightly associated with vesicles but cooperate to raise bulk  $[\text{Ca}^{2+}]_i$  which increases mIPSC frequency. BAPTA and EGTA, have similar affinities for  $\text{Ca}^{2+}$  but BAPTA has a  $\sim 40$  times faster rate of binding so that at mM concentrations BAPTA will impact signaling if the mean diffusion distance for  $\text{Ca}^{2+}$  is as short as  $10\text{--}20 \text{ nm}$ , whereas EGTA will only have an effect if the path length is relatively long ( $>100 \text{ nm}$ ; Eggermann et al. 2011). Application of cell-permeant I BAPTA-AM ( $50 \mu\text{M}$ ) substantially reduced the  $[\text{Ca}^{2+}]_o$ -dependent increase in mIPSC frequency (Figures 9a,b, 10a;  $p = 0.007$ ,  $n = 8$ ;) indicating this  $\text{Ca}^{2+}$  buffer

attenuated the  $[Ca^{2+}]_i$  transient when  $[Ca^{2+}]_o$  was 6 mM. In contrast, EGTA-AM (50  $\mu$ M) did not change the response to increases in  $[Ca^{2+}]_o$  (Figures 9a,c, 10a;  $p = 0.391$ ,  $n = 6$ ). At physiological  $[Ca^{2+}]_o$  BAPTA reduced mIPSC frequency by  $24 \pm 7\%$  ( $n=14$ ) while EGTA was ineffective (Figures 9d,e, 10a;  $1 \pm 6\%$ ,  $n = 16$ ;  $p = 0.009$ ). Application of  $Cd^{2+}$  after BAPTA exposure reduced mIPSC frequency further (Figures 9d,f, 10b; by  $65 \pm 7\%$ ,  $n = 7$ ). Given that the final intracellular concentrations of the two buffers are likely to have been similar, these combined data strongly indicate that VACCs triggered spontaneous GABA-release via tightly coupled vesicles and not by changing bulk  $[Ca^{2+}]_i$  (Eggermann et al. 2011; Neher & Sakaba 2008). Interestingly, action potential-evoked release of a single GABA-containing vesicle relies on a vesicle-VACC coupling distance of 10–20 nm and activation of up to three VACCs (Bucurenciu et al. 2010).

An important physiological consequence of the requirement that multiple VACC openings combine to trigger each mIPSC will be a lower basal rate of spontaneous GABA release due to the low probability of coincident VACC openings. The mechanism synchronizing the activation of multiple VACCs remains unclear. Based on somatic VACC currents, stochastic synchronization seems unlikely, although it cannot be ruled out, since the membrane potential ( $-78 \pm 2$  mV;  $n = 17$ ) sits at the foot of the VACC current activation curve (Figure 8). Another possibility is that nerve terminal VACCs are linked via their C-termini, leading to coupled gating similar to the mechanism proposed to synchronize L-type VACC activity (Navedo et al. 2010). The importance of VACCs

as triggers for spontaneous GABA release is surprising in the light of our earlier findings that spontaneous glutamate release is not initiated by Ca<sup>2+</sup> influx, and indicates a substantial difference between the regulation of GABAergic and glutamatergic synapses in the neocortex (Vyleta & Smith 2011). Further research is required to identify the constituents at the active zone responsible for the differential regulation of inhibitory and excitatory spontaneous release and to determine if this phenomenon extends to other regions of the brain.

## **METHODS**

### **Neuronal cell culture**

Neocortical neurons were isolated from postnatal day 1–2 mouse pups as described previously (Phillips et al. 2008). All animal procedures were approved by Oregon Health & Science University's Institutional Animal Care and Use Committee in accordance with the U.S. Public Health Service Policy on Humane Care and Use of Laboratory Animals and the National Institutes of Health Guide for the Care and Use of Laboratory Animals. Animals were decapitated following general anesthetic with isoflurane and then the cerebral cortices were removed. Cortices were incubated in trypsin and DNase and then dissociated with a heat polished pipette. Dissociated cells were cultured in MEM plus 5% FBS on glass coverslips. Cytosine arabinoside (4 μM) was added 48 hours after plating to limit glial division. Cells were used after a minimum of 14 days in culture.

### **Electrophysiological recordings**

Cells were visualized with an Olympus IX70 inverted microscope. Recordings were made in whole-cell voltage clamp mode in neurons voltage-clamped at  $-70$  mV. Voltages were corrected for liquid junction potentials (Hughes et al. 1987). In general and except where stated in the text, extracellular solution contained the following (in mM): 150 NaCl, 4 KCl, 10 HEPES, 10 glucose, 1.1 MgCl<sub>2</sub>, pH 7.35 with NaOH. CaCl<sub>2</sub> was 1.1 mM unless otherwise indicated. Recordings of mIPSCs were made in the presence of tetrodotoxin (TTX; 1  $\mu$ M) and CNQX (10  $\mu$ M) to block Na<sup>+</sup> channels and AMPA receptors, respectively. Recordings of mIPSCs were made using a potassium chloride-rich intracellular solution containing the following (in mM): 118 KCl, 9 EGTA, 10 HEPES, 4 MgCl<sub>2</sub>, 1 CaCl<sub>2</sub>, 4 NaATP, 0.3 NaGTP, 14 creatinine phosphate, pH 7.2 with KOH. Electrodes had resistances of 3–7 M $\Omega$ . VACC currents were isolated using cesium methane-sulfonate rich solution as described previously<sup>3</sup>. Currents were recorded with a HEKA EPC9/2 amplifier and filtered at 1 kHz using a Bessel filter and sampled at 10 kHz. Series Resistance (R<sub>s</sub>) was monitored, and recordings were discarded if R<sub>s</sub> changed significantly during the course of a recording. R<sub>s</sub> was compensated to  $\sim$ 70% in recordings of VACC currents.

### **Solution Application**

Solutions were gravity fed through a glass capillary (1.2 mm outer diameter) placed  $\sim$ 1 mm from the patch pipette tip. Toxin (Alomone Labs) stock solutions were all made at 1000X concentration with distilled water and stored at  $-20$  °C. Cytochrome C (0.1 mg/ml) was also added to Aga-IVa-containing solutions to

minimize non-selective toxin binding to the apparatus. BAPTA-AM (Invitrogen) was dissolved in DMSO at 50 mM stock concentration. Before use, extracellular solution was incubated at 30°C while undergoing ultrasonic agitation for ≥30 min to ensure BAPTA-AM dissolved completely. EGTA-AM (Invitrogen) was dissolved in DMSO at 50 mM stock concentration.

### **Analysis**

Data were acquired on a PIII computer and analyzed with IgorPro (Wavemetrics) and Minianalysis (Synaptosoft) software using a threshold crossing algorithm. Miniature IPSC data were normalized to the basal level by dividing the mIPSC frequency measured over each ten second interval by the average mIPSC frequency over 100–200 s at the beginning of the experiment. Steady-state mIPSC frequency changes were the averages measured over ≥60 seconds as a percentage of the basal level. In some experiments (Figure 7e) reductions in mIPSC frequency were described as a percentage of the Cd<sup>2+</sup>-sensitive component by comparing the response to blockers as a fraction of the difference between the basal mIPSC rate and the mIPSC rate following application of Cd<sup>2+</sup> (100 μM). Exemplar plots of mIPSC frequency versus time are shown as supplementary information (Figure 8) to illustrate the variability of basal mIPSC frequency rates which presumably reflect differences in the number of synapses and release probability. The average basal mIPSC frequency was  $5.3 \pm 0.6 \text{ s}^{-1}$  (n = 61).

### **Statistical Analysis**

Data values are reported as mean  $\pm$  SEM. Pairwise comparison of data were performed using Student's t test or Mann-Whitney U-test if the data were not normally distributed (Microsoft EXCEL or Sigmaplot). We used two-way repeated measures ANOVAs to examine the impact of BAPTA-AM and EGTA-AM on the mIPSC frequency at different external calcium levels. Subsequent pairwise comparisons were performed with the Holm-Sidak method (Sigmaplot). Curve fitting was carried out using IgorPro (Wavemetrics).

### **ACKNOWLEDGEMENTS**

We thank Drs. Michael Andresen and Kamran Khodakhah for helpful comments. The work was supported by the NIH (DA027110 and GM097433) and OCTRI. CW and NPV were supported by T32HL033808 from the National Heart, Lung, and Blood Institute.

### **AUTHOR CONTRIBUTIONS**

CW conducted the calcium chelation, specific toxin- block of mIPSC and VACC currents, and VACC gating experiments and participated in writing the manuscript. WYC conducted the calcium chelation, Cd<sup>2+</sup> and specific toxin- block of mIPSC and VACC currents, and hyperpolarization experiments. CHL conducted the [Ca<sup>2+</sup>]-effect experiments. DY conducted the Cd<sup>2+</sup> block of mIPSC and hyperpolarization experiments. NPV provided cell cultures and participated in writing the manuscript. SMS designed experiments, analyzed data, and wrote the manuscript.

## FIGURES

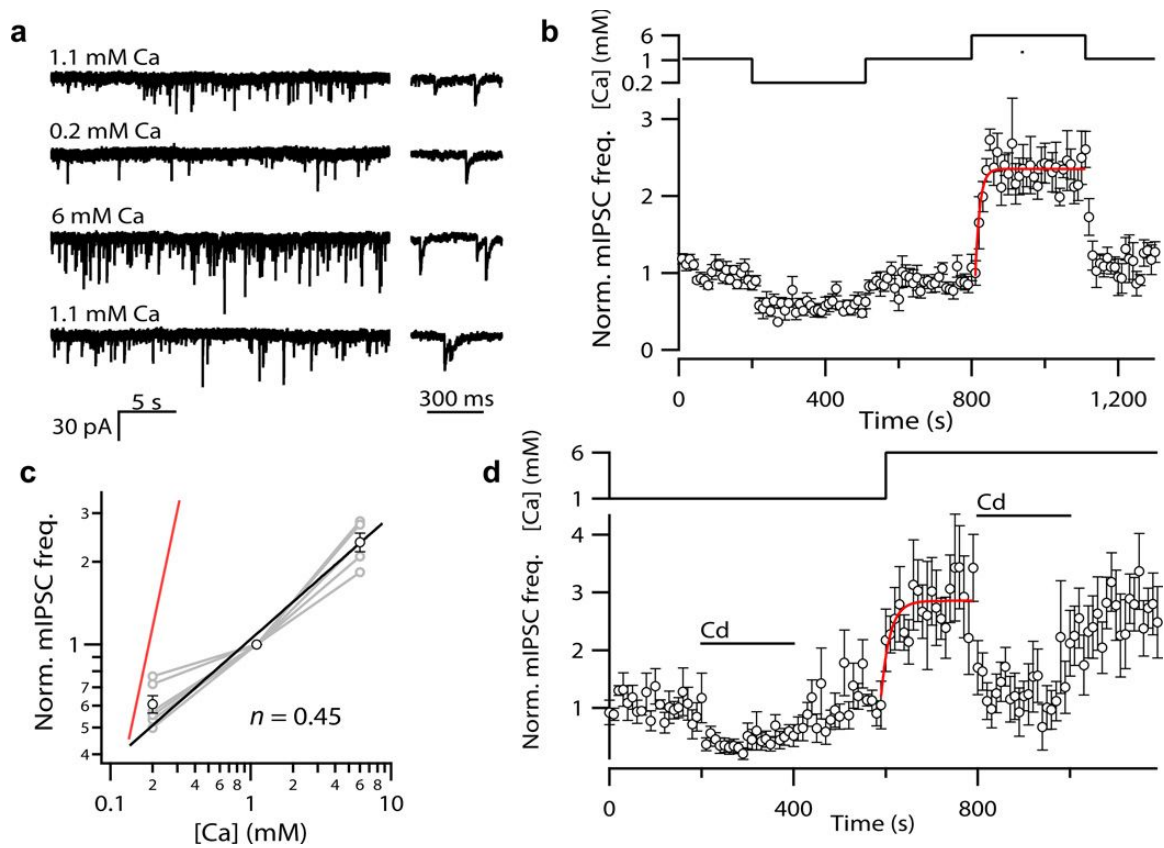


### Figure 5: VACCs mediate $\text{Ca}^{2+}$ -dependent increases in mIPSC frequency.

**a**, Exemplary traces of mIPSCs at 0.2, 1.1 and 6 mM  $[\text{Ca}^{2+}]_o$ . Insets show expanded timescales. **b**, Average normalized plot of mIPSC frequency versus time ( $\pm$  SEM in this and subsequent figures;  $n = 6$ ). Response to increased  $[\text{Ca}^{2+}]_o$  was well described by an exponential function (red curve,  $\tau = 12$  s). **c**, log-log plot of the concentration-effect relationship for normalized mIPSC frequency versus  $[\text{Ca}^{2+}]_o$ . Responses from individual neurons are indicated in gray ( $n = 6$ ) and mean values are plotted in black. The data were fit with a line which had a slope of 0.45. A line with slope of 4 is shown in red for comparison (Dodge & Rahamimoff 1967). **d**,  $\text{Cd}^{2+}$  reversibly reduces mIPSC frequency at physiological and elevated  $[\text{Ca}^{2+}]_o$  in this average plot of normalized mIPSC



frequency versus time ( $n = 6$ ). Response to increased  $[Ca^{2+}]_o$  was described by an exponential function ( $\tau = 19$  s).

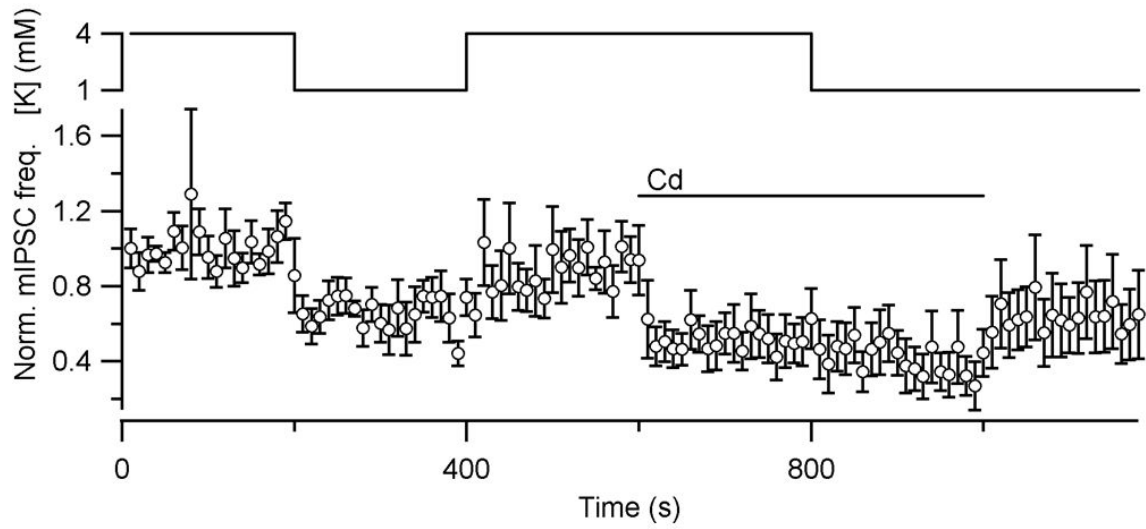


**Figure 6: Presynaptic hyperpolarization reduces mIPSC frequency.** Average plot of normalized mIPSC frequency versus time showing that mIPSC frequency is reversibly reduced by lowering external  $[K^+]$ . Reduction of external  $[K^+]$  had little impact in the presence of  $Cd^{2+}$ .

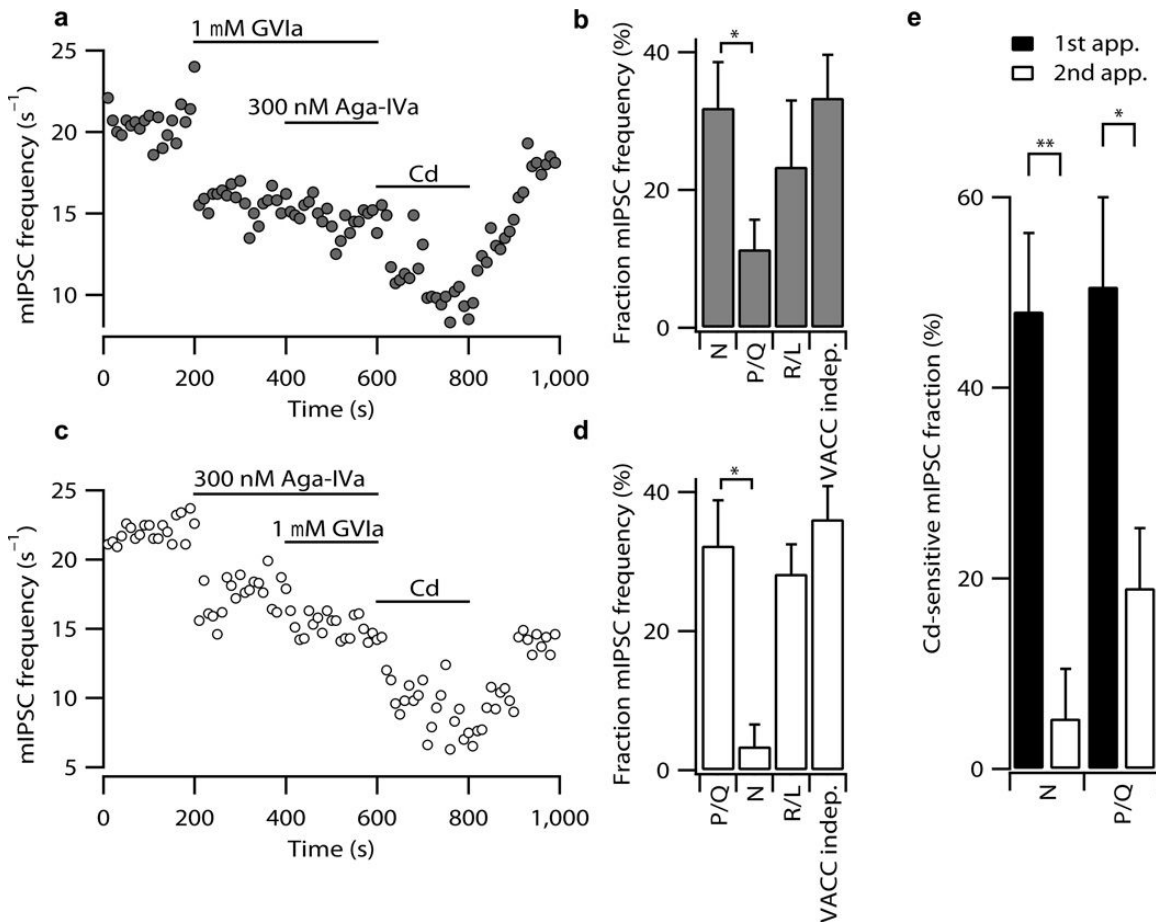


**Figure 7: Pharmacological dissection of the identity of VACCs mediating**

**spontaneous GABA release.** **a**, Plot of mIPSC frequency versus time from an exemplary experiment indicating effects of GVla, Aga-IVa, and Cd<sup>2+</sup> in this order (at 1 μM, 300 nM, and 100 μM respectively in this and all other experiments). **b**, Bar graph indicating average effects on mIPSC frequency of these blockers when applied sequentially. **c**, Plot of mIPSC frequency versus time from an exemplary experiment indicating effects of Aga-IVa, GVla, and Cd<sup>2+</sup> in this order. **d**, Bar graph indicating average effects on normalized mIPSC frequency of application of Aga-IVa, GVla, and Cd<sup>2+</sup>. **e**, Effect of varying the order of application of Aga-IVa and GVla on the Cd<sup>2+</sup>-sensitive fraction of mIPSC frequency. The second application was always in the presence of a saturating dose the other blocker at steady state. Frequency of mIPSCs were reduced differently

by first (filled bars) and second (open) applications of GVIa ( $48 \pm 8\%$  vs  $5 \pm 5\%$ ,  $n = 9$  vs  $4$ ;  $p = 0.008$ ) and Aga-IVa ( $51 \pm 9\%$  vs  $19 \pm 6\%$ ,  $n = 4$  vs  $9$ ;  $p = 0.018$ ). Here and in subsequent figures \* and \*\* describe p-values of  $\leq 0.05$  and  $< 0.01$ .

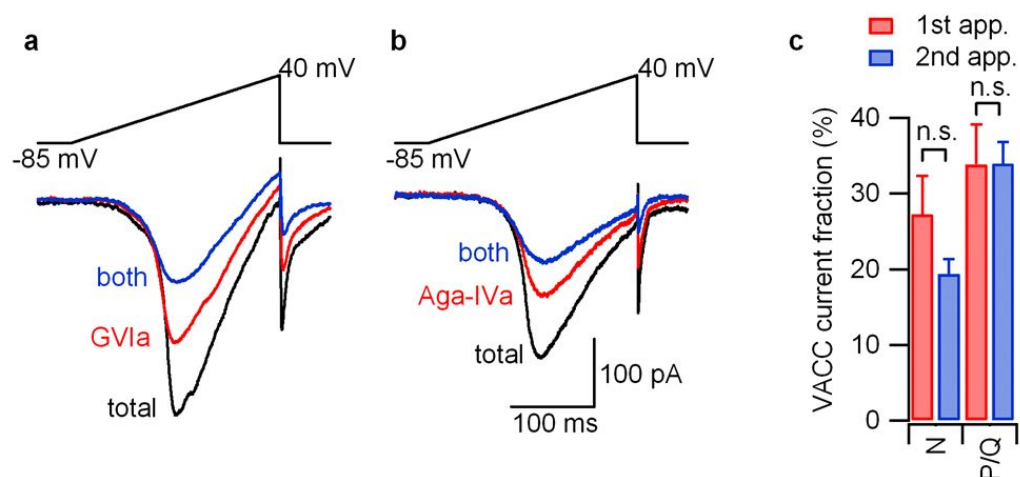


**Figure 8: The percentage of the total VACC currents carried by GV1a- (1  $\mu$ M) and Aga-IVa (300 nM)-sensitive components were unchanged by the order of toxin application. a, Recording of the average steady state VACC currents activated by a voltage-ramp protocol (0.5 mV/ms) after subtraction of the Cd<sup>2+</sup>-sensitive component. The total VACC current (black) was reduced by 1  $\mu$ M GV1a (red) and further by GV1a plus 300 nM Aga-IVa (blue). b, Another recording of the VACC currents activated by a voltage-ramp protocol (0.5 mV/ms) after subtraction of the Cd<sup>2+</sup>-sensitive component. The total VACC current (black) was reduced by 300 nM Aga-IVa (red) and further by Aga-IVa plus 1  $\mu$ M GV1a (blue). c, Bar graph of average fraction of the total peak VACC currents sensitive to GV1a (N-type) or Aga-IVa (P/Q-type) when the toxins were applied first (red) or after the other toxin (blue) (p = 0.18 for GV1a, n = 5; p = 0.99 for Aga-IVa, n = 5).**

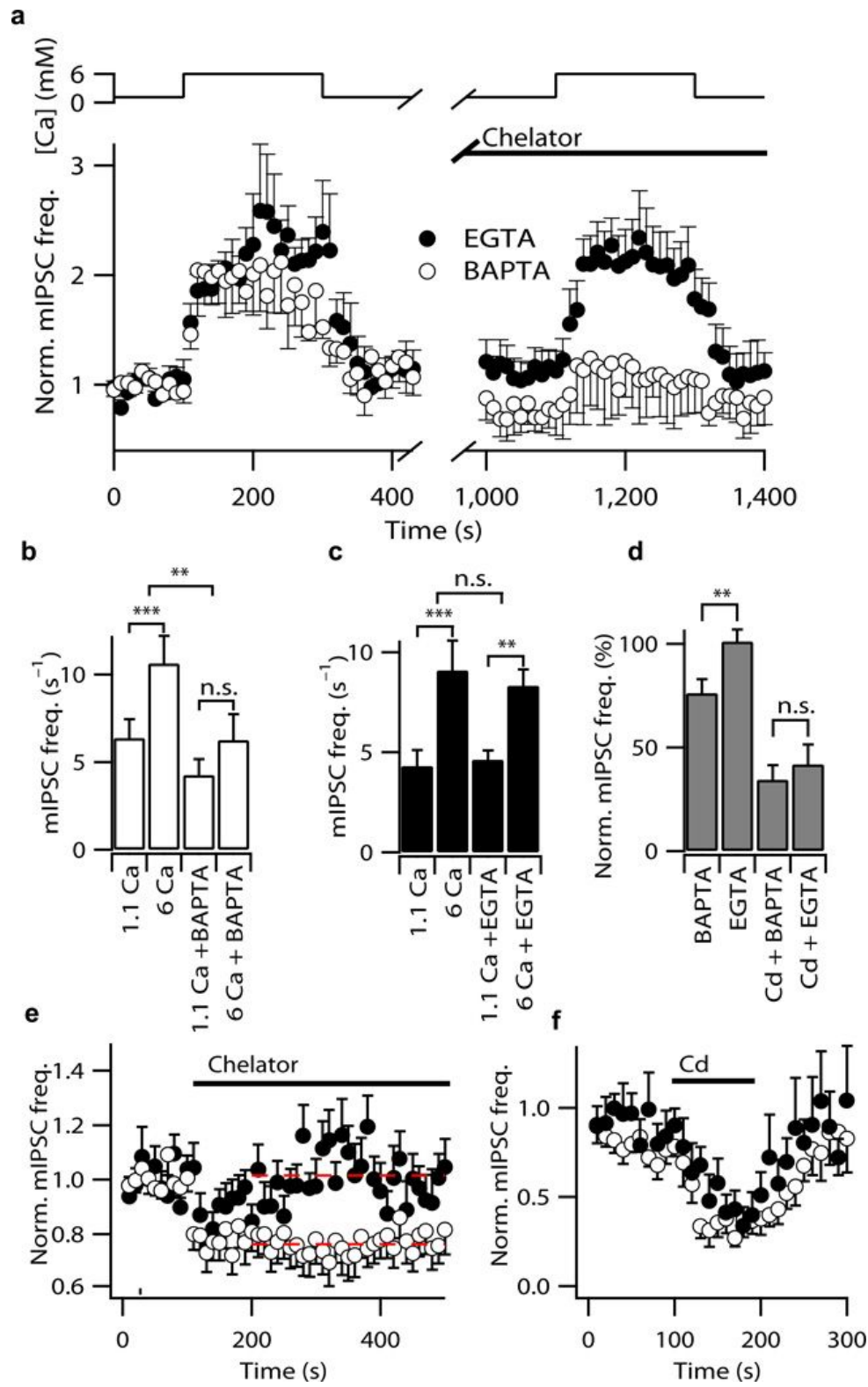


**Figure 9: VACC-vesicle coupling is attenuated by BAPTA-AM but not**

**EGTA-AM.** **a**, Application of 50  $\mu\text{M}$  BAPTA-AM (open circles,  $n = 9$ ), but not 50  $\mu\text{M}$  EGTA-AM (filled,  $n = 6$ ), decreases the response to 6 mM  $\text{Ca}^{2+}$  in this plot of normalized average mIPSC frequency versus time. The thick black line indicates chelator application. **b, c**, Bar graph of steady-state mIPSC frequency from the same experiments as a in 1.1 or 6 mM  $[\text{Ca}^{2+}]_o$  and in the absence and presence of BAPTA-AM (b, open bars) or EGTA-AM (c, filled). Here \*\*\* describes p-values  $< 0.001$ . **d**, Bar graph of normalized steady-state mIPSC frequency (200–500 s) in either BAPTA-AM (50  $\mu\text{M}$ ,  $n = 14$ ) or EGTA-AM (50  $\mu\text{M}$ ,  $n = 17$ ; left hand columns).  $\text{Cd}^{2+}$  inhibition of the mIPSC frequency following BAPTA-AM ( $n = 7$ ) or EGTA-AM ( $n = 7$ ) exposure is illustrated in the right hand columns. **e**, Plot of normalized average mIPSC frequency versus time from the same experiments in d showing the effect of BAPTA-AM (open circles) and EGTA-AM (filled) on basal mIPSC frequency. Broken red lines indicate the average mIPSC frequency after 100s of chelator application. **f**, Plot of normalized average mIPSC frequency showing the action of  $\text{Cd}^{2+}$  after 400s of chelator application for the same experiments as in e.

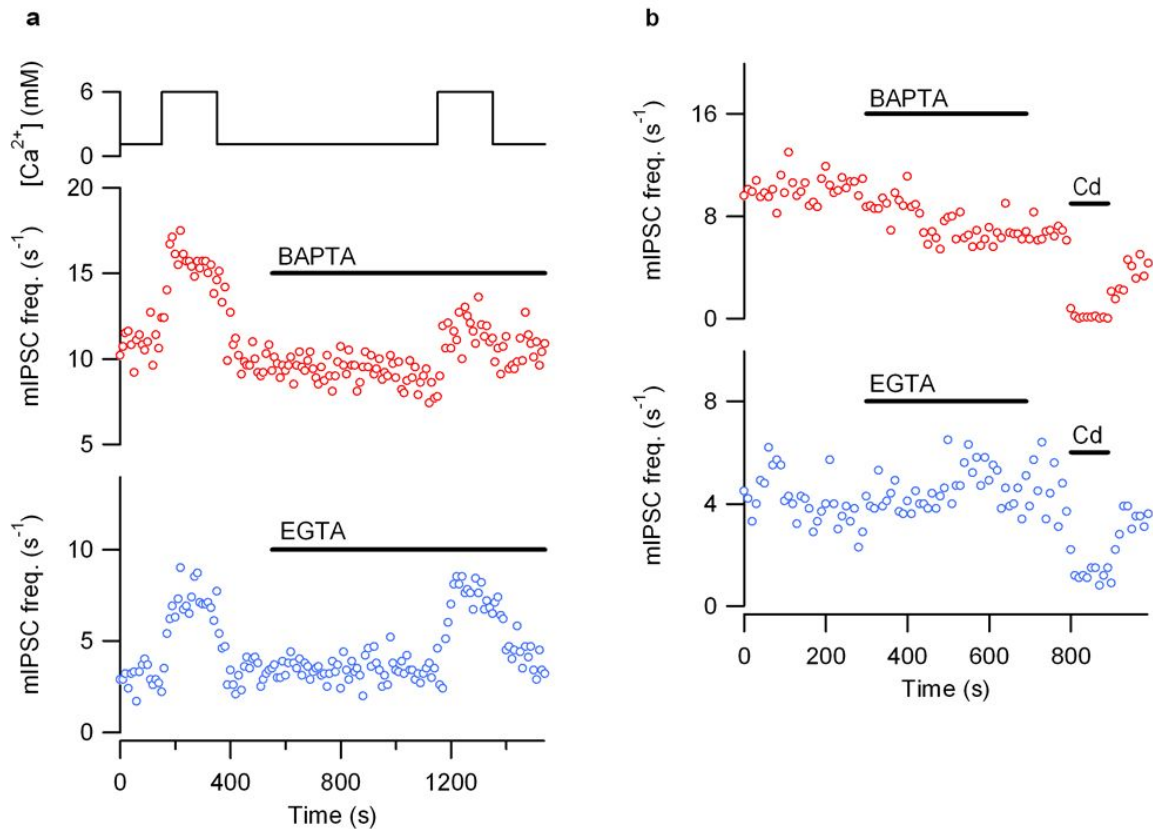


**Figure 10: Exemplary experiments showing the effects of fast and slow  $Ca^{2+}$  chelation on VACC-vesicle coupling at basal and elevated  $[Ca^{2+}]_o$ .** **a**, 2 diary plots of mIPSC frequency versus time for two exemplary experiments. mIPSC frequency is reversibly increased by 6 mM  $Ca^{2+}$ . 10 min application of 50  $\mu$ M BAPTA-AM (red) decreases the response to 6 mM  $Ca^{2+}$ . 10 min application of 50  $\mu$ M EGTA-AM (blue) does not significantly reduce the response to 6 mM  $Ca^{2+}$ . **b**, Diary plots of mIPSC frequency versus time from two exemplary experiments. Application of 50  $\mu$ M BAPTA-AM (red) reduces steady-state basal mIPSC frequency but does not prevent the decrease resulting from VACC block by 100  $\mu$ M  $Cd^{2+}$  after 400s of chelator application. Application of 50  $\mu$ M EGTA-AM (blue) does not significantly reduce steady-state basal mIPSC frequency nor does it prevent the decrease resulting from VACC block by 100  $\mu$ M  $Cd^{2+}$  after 400s of chelator application.



## CHAPTER 2

---

### **Distinct Actions of Voltage-activated Ca<sup>2+</sup> Channel Block on Spontaneous Release at Excitatory and Inhibitory Central Synapses**

Timur Tsintsadze<sup>1,2,4</sup>, Courtney Williams<sup>1,2,4</sup>, Dennis Weingarten<sup>3</sup>, Henrique Von Gersdorff<sup>3</sup>, and Stephen M. Smith<sup>1,2</sup>

<sup>1</sup>Department of Medicine, Division of Pulmonary & Critical Care Medicine, Oregon Health & Science University, Portland, Oregon, 97239, USA.

<sup>2</sup>Section of Pulmonary & Critical Care Medicine, VA Portland Health Care System, Portland, Oregon, USA.

<sup>3</sup>Vollum Institute, Oregon Health & Science University, Portland, Oregon, 97239, USA.

<sup>4</sup>These authors contributed equally

Address correspondence to: Stephen M. Smith, *VA Portland Health Care System*, 3710 SW U.S. Veterans Hospital Road, R&D 24, Portland, OR 97239.  
Phone: 503 220 8262 extension 52361; E-mail: [smisteph@ohsu.edu](mailto:smisteph@ohsu.edu).

### **ABSTRACT**

At chemical synapses, VACCs mediate Ca<sup>2+</sup> influx to trigger action potential-evoked neurotransmitter release. However, the mechanisms by which

$\text{Ca}^{2+}$  regulates spontaneous transmission have not been fully determined. We have shown that VACCs are a major trigger of spontaneous release at neocortical inhibitory synapses, but in stark contrast, VACCs do not regulate spontaneous release at excitatory synapses. Recently, VACC blockers were reported to reduce spontaneous release of glutamate, and it was hypothesized that the distinct effects on excitatory and inhibitory synapses may have resulted from off target actions of  $\text{Cd}^{2+}$ , a non-specific VACC blocker, or other variations in experimental conditions. Interestingly, these contrasting results indicate either conservation of regulatory mechanisms or fundamental differences in the underlying mechanisms of release across inhibitory and excitatory synapses. Here we report that VACC blockers inhibit spontaneous release at inhibitory but not excitatory terminals, and that this pattern is observed in culture and slice neocortical preparations, as well as in synapses from acute slices of the auditory brainstem. The voltage-dependence of  $\text{Cd}^{2+}$  block of VACCs accounts for the apparent discrepancy between the potency of  $\text{Cd}^{2+}$  on VACC current amplitudes, evoked release, and spontaneous release of GABA. These findings indicate fundamental differences between the regulation of spontaneous release at inhibitory and excitatory synapses by stochastic VACC activity that extend beyond the cortex to the brainstem.

## **INTRODUCTION**

Spontaneous release of neurotransmitter supports synapse maturation and maintenance, homeostasis, and plasticity (Jensen et al. 1999; McKinney et al.

1999; Kombian et al. 2000; Verhage et al. 2000; Sutton & Schuman 2006). Regulation of neuronal excitability and action potential firing by spontaneous release are additional examples of the physiological importance of this form of transmission (Cohen & Miles 2000; Carter & Regehr 2002). The recent proposal that different vesicle pools underlie spontaneous and evoked release and that these mediate distinct functions has emphasized the importance of precisely understanding both forms of transmission (Autry et al. 2011; Kavalali et al. 2011).

VACCs are well established as key triggers of evoked synaptic transmission, but this is less clear for spontaneous release where the probability of VACC activation is low because of the hyperpolarized resting membrane potential (Matthews & Wickelgren 1977; Llinas et al. 1989; Wheeler et al. 1994). We determined, in cultured cortical neurons, that spontaneous release of glutamate was independent of VACCs while spontaneous release of GABA was strongly regulated by VACC (Vyleta & Smith 2011; Williams et al. 2012). These surprising results indicated there are substantial differences between key regulatory mechanisms at excitatory and inhibitory synapses and point to further differences between vesicle regulation for spontaneous and evoked release. In contrast, it was proposed that a substantial fraction of spontaneous release of glutamate is VACC-dependent at small and large central synapses consistent with the more conservative proposal that inhibitory and excitatory release mechanisms are similarly regulated (Ermolyuk et al. 2013; Dai et al. 2015). In this study we have set out to re-address the question of whether VACCs regulate

spontaneous release of GABA and glutamate differently at central synapses. We have extended our experiments to acute neocortical slices in addition to cell culture, tested if the actions of  $\text{Cd}^{2+}$  on spontaneous release can be entirely attributed to its actions as an inorganic non-selective VACC blocker, determined if the actions on spontaneous release of organic VACC blockers are equivalent to  $\text{Cd}^{2+}$ , and examined if VACC block affects spontaneous release at synapses in the brainstem. Our results indicate that the regulation of mEPSCs by VACCs is fundamentally different from that of mIPSCs at both small bouton-type and large calyx-type central synapses.

## **RESULTS**

VACCs mediate  $\text{Ca}^{2+}$  influx to trigger action potential-evoked neurotransmitter release. However, at resting membrane potential the probability of VACC opening is much lower so other mechanisms may regulate spontaneous release. One possibility is that reported differences in sensitivity to VACC blockers at cortical excitatory synapses may arise from differences attributable to cell culture. To remove this possible confounder, we examined spontaneous release of glutamate and GABA in acute neocortical slices. Using whole-cell recordings from neurons in layer 2/3 or 4, voltage-clamped at -70 mV, in the presence of 1  $\mu\text{M}$  tetrodotoxin (inhibitory or excitatory transmission blocked with gabazine or CNQX respectively), we found that that mEPSCs were unaffected by the inorganic, non-selective VACC blocker  $\text{Cd}^{2+}$  (Figure 11). The mEPSCs occurred as rapid, transient, down deflections in the current trace that were unaffected in rise-time,

decay, or amplitude (Figure 11a,b) by application of  $\text{Cd}^{2+}$  (100  $\mu\text{M}$ ). Similarly,  $\text{Cd}^{2+}$  did not affect mIPSC rise-time, decay, or amplitude (Figure 11c,d). The frequency of mEPSCs over time was unaffected by the addition of  $\text{Cd}^{2+}$  in the illustrated recording (Figure 11e, open circles). This was confirmed in the average diary plot (Figure 11e, solid circles, increased to  $92 \pm 2\%$  of basal; values represent mean  $\pm$  S.E.M.;  $n = 6$ ,  $p = 0.28$ ), indicating VACC were not triggering spontaneous release of glutamate. In contrast, mIPSC frequency clearly and reversibly decreased following  $\text{Cd}^{2+}$  application in the exemplar and average diary plots (Figure 11f). On average,  $\text{Cd}^{2+}$  reduced mIPSC frequency to  $50 \pm 6\%$  of basal frequency which was significantly different to its actions on spontaneous release of glutamate ( $n = 6$ ,  $p = 0.02$ ). These data indicate stochastic VACC activity did not contribute to spontaneous release at excitatory synapses but regulated a substantial fraction of spontaneous release at inhibitory synapses in neocortical slices.

### **Differences in Potency of $\text{Cd}^{2+}$ on Spontaneous Release and VACC currents**

Actions of  $\text{Cd}^{2+}$  at sites other than VACCs may make it an unreliable tool to investigate VACC coupling and spontaneous release (Ermolyuk et al. 2013). We postulated that if  $\text{Cd}^{2+}$  modulated mIPSC frequency via its action on VACC alone then the potency of  $\text{Cd}^{2+}$  on VACC currents and spontaneous release of GABA should be equivalent. To test this hypothesis we compared the concentration-effect relationships for  $\text{Cd}^{2+}$  on VACC currents and mIPSC frequency. Using cultured neocortical neurons, to improve voltage-clamp, we

examined the effects of  $\text{Cd}^{2+}$  on the VACC current elicited by depolarization from -70 to -10 mV every 10 seconds (Figure 12a). The VACC current amplitude was reversibly decreased by increasing concentrations of  $\text{Cd}^{2+}$  (Figure 12a-c). The plot of normalized inward current at the end of the depolarizing step versus time was used to estimate the block of VACC currents by external  $[\text{Cd}^{2+}]$  (Figure 12b). The steady state normalized inward current was used to measure the concentration-effect relationship for  $\text{Cd}^{2+}$  and VACC currents (Figure 12c,  $\text{IC}_{50} = 1.08 \pm 0.03 \mu\text{M}$ ,  $n = 12$ ). In other recordings, spontaneous release of GABA was isolated using TTX and CNQX to block action potentials and glutamatergic transmission, respectively. At -70 mV, mIPSC frequency decreased following the application of  $30 \mu\text{M}$   $\text{Cd}^{2+}$  (Figure 12d). The frequency of mIPSCs was estimated in contiguous 10 second bins and plotted versus time. Increasing external  $\text{Cd}^{2+}$  up to  $300 \mu\text{M}$  reversibly reduced mIPSC frequency (Figure 12e) and the plot of normalized steady state mIPSC frequency versus  $[\text{Cd}^{2+}]$  revealed a much lower potency (Figure 12;  $27 \pm 2.4 \mu\text{M}$ ,  $n = 9$ ) than that observed on VACC currents. This discrepancy was not simply explained by non-linear coupling between  $\text{Ca}^{2+}$  entry and the release machinery because, like VACC currents, action potential evoked GABA release was also highly sensitive to  $\text{Cd}^{2+}$  (Figure 12 g-i;  $\text{IC}_{50} = 4.0 \pm 0.03 \mu\text{M}$ ,  $n = 10$ ). If the only significant action of  $\text{Cd}^{2+}$  is to block VACCs what is the reason for the apparently lower potency of  $\text{Cd}^{2+}$  on mIPSCs? Could this difference be attributed to actions on VACC or did it result from effects at other targets?

$\text{Cd}^{2+}$  has been shown to have multiple voltage-dependent actions, blocking VACCs more effectively at depolarizing or hyperpolarizing potentials (Chow 1991; Thévenod & Jones 1992). Since these apparently contrasting results were obtained using different permeating ion conditions, we set out to determine the voltage-dependence of  $\text{Cd}^{2+}$  block of VACC currents under physiological  $[\text{Ca}^{2+}]_o$  and  $[\text{Mg}^{2+}]_o$ . We elicited VACC currents using a range of voltage steps from -70 mV (between -65 to 40 mV for 10 ms duration) in control conditions and in the presence of  $\text{Cd}^{2+}$  (1, 100, and 300  $\mu\text{M}$ ).  $[\text{Cd}^{2+}]$  at 100  $\mu\text{M}$  resulted in saturating VACC current block (unchanged by increasing  $[\text{Cd}^{2+}]$  to 300  $\mu\text{M}$ , data not shown). In order to isolate the  $\text{Cd}^{2+}$ -sensitive VACC current, currents recorded in 100  $\mu\text{M}$   $\text{Cd}^{2+}$  were subtracted from those measured in control conditions ( $I_{\text{Ctrl}}$ ) and 1  $\mu\text{M}$   $\text{Cd}^{2+}$  ( $I_{\text{Cd}}$ ; Figure 13a, b). Application of 1  $\mu\text{M}$   $\text{Cd}^{2+}$  reduced subtracted inward current amplitudes and this block was markedly enhanced at -10 mV compared with -40 mV (Figure 13a). Plotting these currents (mean over the last 2 ms of the step) versus voltage showed that block by 1  $\mu\text{M}$   $\text{Cd}^{2+}$  was ~90% at 0 mV but became more variable at positive voltage steps (Figure 13b,d). This could reflect reduced block by  $\text{Cd}^{2+}$  at positive potentials or contamination by outward currents through voltage-activated potassium channels despite use of 150 mM TEA in bath and cesium in pipette solutions (Thévenod & Jones 1992; Adelman & French 1978; Crouzy et al. 2001). Examination of the peak amplitude of the tail current versus the voltage of the step permitted us to further reduce the impact of any contaminating current. Tail currents ( $I_{\text{Tail}}$ ) recorded following steps to

voltages  $>0$  mV were stable in the presence of  $1 \mu\text{M Cd}^{2+}$ , and not decreased as expected if depolarization to  $>0$  mV reduced  $\text{Cd}^{2+}$  block of VACC currents (Figure 13c). The average voltage-dependence of block by  $1 \mu\text{M Cd}^{2+}$  was illustrated by replotting  $I_{\text{Cd}}/I_{\text{Ctrl}}$  versus voltage for both steady-state (red) and tail currents (blue, Figure 13d,  $n = 4$ ). Under these conditions, block by  $1 \mu\text{M Cd}^{2+}$  was  $89 \pm 5.4\%$  and  $73 \pm 6.2\%$  at  $\sim 0$  mV, respectively (Figure 13c,  $n = 4$ ) and did not decrease with further depolarizations. We looked more closely for evidence that  $\text{Cd}^{2+}$  was less effective at blocking VACC currents at positive membrane potentials by using strong depolarizations that have been shown to rapidly reverse block of VACCs by  $\text{Cd}^{2+}$  (Chow 1991; Thévenod & Jones 1992). In this set of experiments we compared VACC currents activated by a step to  $-10$  mV before (S1) and after (S2) a depolarization to  $130$  mV ( $1-15$  ms duration). S1 and S2 were reduced equally by the application of  $\text{Cd}^{2+}$  (Figure 13e,f) indicating the strong depolarizations did not reverse  $\text{Cd}^{2+}$  block of VACC currents—consistent with there being no rapidly occurring reduction in  $\text{Cd}^{2+}$  potency at depolarized potentials in these neurons. In addition, the middle pulse activated an outward current that was  $\text{Cd}^{2+}$ -sensitive and thus may account for the apparent variability of  $I_{\text{ss}}$  at positive voltages (Figure 13d). At potentials negative to  $-50$  mV,  $1 \mu\text{M Cd}^{2+}$  had no discernible effect on VACC tail currents. Since mIPSCs were recorded when the presynaptic membrane potential was presumably hyperpolarized ( $-70$  to  $-80$  mV) these results explain why higher concentrations of  $\text{Cd}^{2+}$  were required to inhibit mIPSCs (Figure 12f) than the VACC currents activated by steps to  $-10$



mV or stimulus-evoked IPSCs (Figure 12c, i) and obviates the need to propose off target effects of  $\text{Cd}^{2+}$  to explain its action on mIPSCs (Ermolyuk et al. 2013).

### **Specific blockers of VACCs on Spontaneous Release**

To further test the action of VACC activity on spontaneous release we used a structurally different type of VACC blocker, MVIIC, which is a peptide toxin specific for block of N- and P/Q-type VACCs. N-, P/Q-, and R-type VACCs are expressed in neocortical nerve terminals and have been shown to contribute to spontaneous and evoked release at these synapses (Cao & Tsien 2005; Bucurenciu et al. 2010). Application of a saturating concentration of MVIIC (5 $\mu\text{M}$ ) had no effect on mEPSC or mIPSC rise time, decay phase or amplitude (Figure 14 a-d). However MVIIC reduced mIPSC frequency to  $31 \pm 7\%$  of basal level while having no effect on mEPSC frequency ( $108 \pm 0.4\%$  of baseline) as illustrated by the exemplar and average diary plots (Figure 14e,f). Similar to the experiments using  $\text{Cd}^{2+}$  to block VACC currents (Figure 11) these findings confirmed that VACCs strongly regulate spontaneous synaptic transmission at inhibitory synapses but not at excitatory synapses. Moreover, the degree of reduction of mIPSC frequency by MVIIC seen here, is similar to that described previously using saturating doses of selective VACC blockers in cultured neurons (Williams et al. 2012).

### **Spontaneous Glutamate Release is Not Triggered by VACCs at the Calyx of Held**

How wide-ranging is the difference in regulation of spontaneous release from excitatory and inhibitory synapses? We asked if excitatory and inhibitory synapses in other areas of the CNS were regulated similarly. To answer this question we recorded from principal cells of the medial nucleus of the trapezoid body (MNTB) in acute mouse auditory brainstem slices (Figure 15). In voltage-clamp mode we acquired and resolved mEPSCs and mIPSCs simultaneously by employing bath and pipette solutions that widely separated the reversal potentials for excitatory and inhibitory transmission. At this developmental stage mIPSCs reflect spontaneous release of glycine and GABA (Awatramani et al. 2005). Application of  $\text{Cd}^{2+}$  (50  $\mu\text{M}$ ) blocked EPSCs evoked by afferent fiber stimulation (data not shown; Taschenberger & von Gersdorff 2000; also see (Mintz et al. 1995), but had no effect on the size or time course of the mEPSCs or mIPSCs (Figure 15a,b). However,  $\text{Cd}^{2+}$  reduced mIPSC frequency by  $73 \pm 12\%$  ( $p < 0.0001$ ) whereas it did not affect mEPSC frequency (Figure 15C-E;  $123 \pm 45\%$  of basal). These data are consistent with our observations in acute neocortical slices and cultured neocortical neurons and confirm and extend our findings that VACCs regulate spontaneous release at inhibitory but not at excitatory synapses.

### **Spontaneous Release at Excitatory Terminals and Excitability**

Previous reports suggesting VACCs regulate spontaneous release at excitatory synapses have utilized an external solution with higher glucose, HEPES,  $\text{Mg}^{2+}$  and  $\text{Ca}^{2+}$  concentrations and lower  $\text{K}^{+}$  concentration (Ermolyuk et al. 2013). We

tested if this alternative solution increased the sensitivity of spontaneous release of glutamate to VACC blockers (Figure 16; Vyleta & Smith 2011; Ermolyuk et al. 2013). We found that 100  $\mu\text{M}$   $\text{Cd}^{2+}$  did not elicit a decrease in mEPSC frequency in control Tyrode (Figure 16b;  $1.68 \pm 0.3$  Hz) or alternative Tyrode (Figure 16b;  $1.54 \pm 0.2$  Hz in  $\text{Cd}^{2+}$ ).  $\text{Cd}^{2+}$  slightly increased the mEPSC frequency, as reported previously (Vyleta & Smith 2011). This facilitation of spontaneous glutamate release may be due to activation of the  $\text{Ca}^{2+}$ -sensing receptor by  $\text{Cd}^{2+}$ , which has been suggested to be an agonist along with other divalent cations including  $\text{Mg}^{2+}$  and  $\text{Gd}^{2+}$  (Vyleta & Smith 2011; Smith et al. 2012). We did not examine if spontaneous release of glutamate became VACC-dependent after more prolonged exposure to the alternative solution.

## **DISCUSSION**

We previously determined that VACCs trigger spontaneous release at inhibitory but not excitatory central synapses in cultured neocortical (Vyleta & Smith 2011; Williams et al. 2012). More recently it was proposed that VACCs trigger spontaneous release at excitatory synapses in cultured hippocampal neurons and acute slices from the MNTB, and that the use of  $\text{Cd}^{2+}$  as a VACC blocker may have confounded our experiments (Ermolyuk et al. 2013; Dai et al. 2015). Here we describe experiments that confirm and extend our original findings that VACCs do not trigger spontaneous release at excitatory synapses, but play a major role in spontaneous release at inhibitory synapses. First, we established that the distinct actions of VACC blockade on excitatory and inhibitory spontaneous release were

apparent when VACCs are blocked using  $\text{Cd}^{2+}$  and by the specific N- and P/Q-type VACC blocker, MVIIC, obviating concern for off-target actions of  $\text{Cd}^{2+}$ . Second, these distinct actions of VACC inhibition occur in both acute brain slices from the neocortex and brainstem, as well as cultured neocortical neurons, consistent with this effect extending to other areas of the central nervous system. Third, we find that  $\text{Cd}^{2+}$  block is voltage dependent, and this likely contributes to discrepancies in VACC regulation of spontaneous and evoked release. Thus, through extensive study, we have confirmed that VACCs play a substantial role in regulating spontaneous release at inhibitory nerve terminals but not excitatory nerve terminals, where other mechanisms likely contribute to the  $\text{Ca}^{2+}$  dependence of release.

### **Differences between release at excitatory and inhibitory terminals**

Our findings that block of VACCs reduces spontaneous release at excitatory but not inhibitory synapses indicates that there may be important differences in regulation of spontaneous release of GABA and glutamate by VACCs. Other substantial differences in regulatory mechanisms between excitatory and inhibitory terminals have been identified. For example, agonists for endocannabinoid receptors suppress inhibitory activity-evoked release onto Purkinje cells in cerebellum, but only reduce spontaneous release at inhibitory and not excitatory synapses (Yamasaki 2006). Furthermore, inhibitory terminals in hippocampus were found to be more  $\text{Ca}^{2+}$ -sensitive than excitatory terminals synapsing on the same cell because of a deficiency in the SNARE protein

SNAP-25 (Verderio et al. 2004). Finally, differences in membrane ultrastructure that reflect the composition and organization of synaptic proteins have been observed between excitatory and inhibitory contacts (Landis & Reese 1974).

More studies are necessary to determine the mechanisms underlying this heterogeneity, which include potential differences in the resting membrane potential, number or type of VACCs, size of the  $\text{Ca}^{2+}$  domain for release, tightness of coupling between VACCs and vesicles, concentrations and potency of intracellular  $\text{Ca}^{2+}$  buffers, or the proteins that comprise the release machinery. Variation in experimental conditions could also make spontaneous release of glutamate susceptible to inhibition by VACC blockers. We addressed this hypothesis by determining what happened to spontaneous release of glutamate in acute brain slices from the neocortex and brainstem. Our slice and culture data were consistent validating our observation in culture.

Differences in external solution could alter resting membrane potential and thereby alter the response of excitatory terminals to VACC blockers. It has been demonstrated that depolarizing the resting membrane potential increases spontaneous release and hyperpolarizing has the opposite effect (Angleon & Betz 2001; Li et al. 2009; Williams et al. 2012). In addition, a high concentration of extracellular HEPES causes intracellular alkalinization, which can affect vesicular endocytosis (Zhang et al. 2010), synaptic cleft and vesicle acidification (Cho & von Gersdorff 2014), and elevated glucose has been demonstrated to lead to oxidative damage and apoptosis in neurons (Vincent et al. 2005). We thus tested

if altering the extracellular solution could account for the enhanced sensitivity of excitatory transmission observed by (Ermolyuk et al. 2013; Dai et al. 2015). The brief application of alternative solution had no effect on the response of excitatory terminals to  $\text{Cd}^{2+}$  and thus the cause of the difference remains unclear.

### **Variation in VACC regulation of neurotransmitter release**

The majority of investigators have reported that block of VACCs does not reduce spontaneous release of glutamate at central excitatory synapses. In cultured hippocampal neurons,  $\text{Cd}^{2+}$  did not affect mEPSC frequency (Abenavoli et al. 2002; Yamasaki 2006). In cultured neurons from neocortex, VACC block with  $\text{Cd}^{2+}$  or MVIIC did not reduce mEPSC frequency (Vyleta and Smith, 2011). In hippocampal slices, spontaneous release of glutamate was also independent of VACC activity (Eggermann et al. 2011). This contrasts with observations made at inhibitory synapses, where there have been numerous reports that VACC regulate spontaneous release of GABA. This finding has been confirmed in cultured neocortical neurons and acute hippocampal slices (Yamasaki 2006; Williams et al. 2012; Goswami et al. 2012).

Our findings at excitatory neocortical synapses are strengthened by a lack of effect of buffering  $[\text{Ca}^{2+}]_i$  with BAPTA, which points to other potential pathways for triggering release that are independent of transient changes in  $[\text{Ca}^{2+}]_i$  (Vyleta and Smith, 2011). This contrasts with observations in hippocampal cultures, where stochastic opening of VACCs triggered spontaneous release at excitatory synapses through transient (25-70 nm)  $\text{Ca}^{2+}$  microdomains

that are sensitive to BAPTA (Ermolyuk et al. 2013). They found that multiple subtypes of VACC participate in spontaneous release (namely P/Q-, N-, and R-type channels), but with a ratio of a single channel per vesicle due to the linear summation of block (see Mintz et al. 1995 for explanation). At other specialized synapses, spontaneous release of glutamate is clearly triggered by stochastic VACC openings, this includes hair cells which express VACC subtypes that are activated at relatively negative voltages and lack action potentials (Li et al. 2009; Graydon et al. 2011). But how do we explain the reported sensitivity of spontaneous release of glutamate to VACC blockers at hippocampal, neocortical, and brainstem synapses (Xu et al. 2009; Ermolyuk et al. 2013; Dai et al. 2015)? One explanation is that  $\text{Cd}^{2+}$  may be acting to impair synaptic transmission via off-target mechanisms (Ermolyuk et al. 2013). This idea arose because  $\text{Cd}^{2+}$  is known to permeate VACCs and directly increase Fluo-4 fluorescence (Hinkle et al. 1992; Spence & Johnson 2010; Lopin et al. 2012). We hypothesized that in the absence of off-target actions,  $\text{Cd}^{2+}$  would inhibit VACC currents and spontaneous release similarly. As we observed no effect of  $\text{Cd}^{2+}$  on spontaneous release of glutamate, we investigated its action at inhibitory synapses. We found  $\text{Cd}^{2+}$  was more potent on VACC currents than on spontaneous release (Figure 2), potentially refuting our hypothesis. However, previous studies showed that  $\text{Cd}^{2+}$  exhibits a voltage-dependent block—with  $\text{Cd}^{2+}$  being less effective at negative potentials in squid axon and depolarized potentials in frog sympathetic neurons (Chow, 1991; Thévenod and Jones, 1992). Since we studied the effects of  $\text{Cd}^{2+}$  on

VACC currents and spontaneous release at very different voltages (-10 mV and ~-75 mV respectively), we tested if Cd<sup>2+</sup> caused voltage-dependent block at the relevant concentration range (1-300 μM) and with 1.1 mM Ca<sup>2+</sup> and Mg<sup>2+</sup> in the external solution. While 100 and 300 μM Cd<sup>2+</sup> saturated the block of VACC currents, 1 μM Cd<sup>2+</sup> blocked ~50% of the VACC current at -10 mV but had no effect on VACC currents at the voltage range relevant to spontaneous release. Only by increasing the [Cd<sup>2+</sup>], and thus overcoming the voltage-dependent block, did we observe an effect on spontaneous release. Likewise, 3 μM Cd<sup>2+</sup> blocks 60% of the evoked EPSC at cerebellar granule cell to Purkinje cell synapses, indicating Cd<sup>2+</sup> is more effective when the nerve terminal is depolarized by stimulation (Mintz et al. 1995). This voltage dependence explains the discrepancy in potency of Cd<sup>2+</sup> on VACC currents and mIPSC frequency. Independent support for this hypothesis comes from our observations that the selective N- and P/Q-type VACC blocker, MVIIC, reduced mIPSC frequency but did not affect spontaneous release of glutamate in neocortical neurons in slice (Figure 14).

### **Alternatives to VACCs for Ca<sup>2+</sup> regulation**

Increases in [Ca<sup>2+</sup>]<sub>i</sub> independent of VACC has been shown to increase spontaneous release at excitatory and inhibitory synapses (Llano et al. 2000; Yamasaki, 2006; Vyleta and Smith, 2008). In addition, the lack of effect of strong buffering of [Ca<sup>2+</sup>]<sub>i</sub> on steady state mEPSC frequency pointed to a potential role for other pathways independent of [Ca<sup>2+</sup>]<sub>i</sub> (Vyleta and Smith, 2011). Consistent with this hypothesis, mEPSC frequency was proportional to external [Mg<sup>2+</sup>]



( $[Mg^{2+}]_o$ ), which might have been expected to reduce spontaneous release at excitatory and inhibitory synapses because it is a VACC blocker (Vyleta and Smith, 2011). Another possible pathway for  $Ca^{2+}$  regulation is activating metabotropic  $Ca^{2+}$  sensing receptor (CaSR), which is localized to the presynaptic membrane (Ruat et al. 1995; Chen et al. 2010). CaSR may trigger spontaneous vesicle fusion via a mechanism that is independent of  $[Ca^{2+}]_i$  but is sensitive to changes in  $[Ca^{2+}]_o$  and  $[Mg^{2+}]_o$ . A role for CaSR in spontaneous glutamate release was confirmed using CaSR agonists and CaSR null-mutants (Vyleta and Smith, 2011). Stimulation of CaSR may increase IP<sub>3</sub> and DAG and interestingly DAG analogs, have been shown to trigger spontaneous and evoked neurotransmission via a  $Ca^{2+}$ -independent mechanism (Parfitt and Madison, 1993; Wierda et al. 2007). Spontaneous release of glutamate may also be triggered by long lasting increases in basal  $[Ca^{2+}]_i$ , since  $Ca^{2+}$  chelators act by attenuating transient changes (Pethig et al. 1989).

## **Conclusions**

It is well established that activity-dependent neurotransmitter release is highly dependent on  $[Ca^{2+}]_o$ . Here we show that, while spontaneous release of GABA has much weaker  $[Ca^{2+}]_o$  dependence, VACCs are still the main  $Ca^{2+}$  source for release. This contrasts with the VACC independence of spontaneous at excitatory synapses, and these results are confirmed by a majority of studies from central synapses in culture and in slices. Understanding the mechanisms by which  $Ca^{2+}$

influences release of neurotransmitter will improve our knowledge of synaptic function in general and of disrupted transmission in disease states.

## **METHODS**

### **Slice preparation**

All animal procedures were approved by the VA Portland Health Care System and OHSU Institutional Animal Care and Use Committees (IACUC). Mouse pups of either sex were used to prepare acute slices from the neocortex or the medial nucleus of the trapezoid body (MNTB) at postnatal day P12-16 and P10-12, respectively, as described previously (Forsythe 1994; Borst & Sakmann 1996; Taschenberger & von Gersdorff 2000). Animals were anesthetized using isoflurane and decapitated. The brain was rapidly removed and placed in oxygenated ice-cold artificial cerebrospinal fluid (ACSF). ACSF for cortical pyramidal cells had the following composition (in mM): 129 NaCl, 3.2 KCl, 1.5 CaCl<sub>2</sub>, 1 MgCl<sub>2</sub>, 25 NaHCO<sub>3</sub>, 0.34 Na<sub>2</sub>HPO<sub>4</sub>, 0.44 KH<sub>2</sub>PO<sub>4</sub> and 5 glucose. For neurons of the MNTB we used: 125 NaCl, 2.5 KCl, 1.5 CaCl<sub>2</sub>, 1 MgCl<sub>2</sub>, 25 NaHCO<sub>3</sub>, 1.25 Na<sub>2</sub>HPO<sub>4</sub>, 2 Na-pyruvate, 3 myo-inositol, 0.44 ascorbic acid and 10 glucose. Slices (300 μm) were cut using Vibratome (VT 1200S; Leica, Nussloch, Germany) and kept in oxygenated (95% O<sub>2</sub> and 5% CO<sub>2</sub>, pH 7.3) in modified ACSF. For cortical slices NaCl was substituted by choline chloride in equimolar concentration at room temperature at least 1 hr before use. Individual slices were then transferred to the recording chamber where they were fully submerged and superfused with oxygenated ACSF at room temperature at a rate of 5–9 ml/min.

### **Neocortical culture preparation**

Neocortical neurons were isolated from postnatal day 1–2 mouse pups as described previously (Phillips et al. 2008). All animal procedures were approved by the VAPORHCS Institutional Animal Care and Use Committee in accordance with the U.S. Public Health Service Policy on Humane Care and Use of Laboratory Animals and the National Institutes of Health Guide for the Care and Use of Laboratory Animals. Animals were decapitated following general anesthetic with isoflurane and then the cerebral cortices were removed. Cortices were incubated in trypsin and DNase and then dissociated with a heat polished pipette. Dissociated cells were cultured in MEM plus 5% FBS on glass coverslips. Cytosine arabinoside (4  $\mu\text{M}$ ) was added 48 hours after plating to limit glial division. Cells were used after a minimum of 14 days in culture.

### **Electrophysiological recordings**

In sagittal neocortical slices, pyramidal cell recordings were made under visual control (layer 2/3 or 4 with Scientifica Pro 1000) using patch-clamp technique in the whole cell-configuration with an Axopatch 200B (Molecular Devices, Sunnyvale, CA). For spontaneous event recordings from slices, 1  $\mu\text{M}$  TTX was added to ACSF prior to the start of the experiment. Synaptic currents and agonist-evoked responses were acquired into a personal computer using ITC-16 analog-to-digital converter. To measure postsynaptic currents, we recorded with patch electrodes with a resistance of 5–10  $\text{M}\Omega$  and used two different intracellular solutions with compositions which allowed us to record spontaneous

release at  $-70\text{mV}$ . Excitatory events were recorded using a pipette solution of the following composition (in mM): 135 KGlucanate, 4  $\text{MgCl}_2$ , 10 HEPES, 4 Na-ATP, 0.3 Na-GTP, 10 creatine phosphate at pH 7.2 and 308 mOsm. Inhibitory events were recorded using a similar solution in which potassium gluconate was replaced with potassium chloride. Data were analyzed using Synaptosoft and IgorPro software. As a rule, we started recording no earlier than 10 minutes after forming whole-cell configuration to provide steady-state value for frequency of postsynaptic currents. Each point on dairy plots obtained by averaging frequency of events every 27 seconds for slice preparation and 10 seconds for culture preparation.

For recordings in transverse brainstem slices, principle neurons were identified under visual control (BX51 WI, Olympus, Japan) and recordings made using patch-clamp technique in the whole cell-configuration with an EPC 9/2 amplifier (HEKA Elektronik, Lambrecht, Germany). Currents were filtered at 2.9 kHz using a Bessel filter and sampled at 50 kHz. Series Resistance ( $R_s$ ) was monitored, and only recordings were  $R_s$  remained constant (less than 30% change during a recording) were used.  $R_s$  was compensated to 50-70%.

Microelectrodes had a resistance of 2.5–4  $\text{M}\Omega$  and filled with a solution of the following composition (in mM): 140 KGlucanate, 2 KCl, 5 EGTA, 10 HEPES, 4 Mg-ATP, 0.5 Na-GTP, 5 creatine phosphate, pH 7.2.  $\text{Na}^+$  and  $\text{Cl}^-$  ions had inwardly directed driving forces at  $-70\text{ mV}$  making it possible to distinguish them by their polarity Data were analyzed using IgorPro and Axograph.

For recordings in culture, cells were visualized with an Olympus IX70 inverted microscope. Recordings were made in whole-cell voltage clamp mode in neurons voltage-clamped at  $-70$  mV. Voltages were corrected for liquid junction potentials (Hughes et al. 1987). Extracellular solution contained the following (in mM): 150 NaCl, 4 KCl, 10 HEPES, 10 glucose, 1.1 CaCl<sub>2</sub>, 1.1 MgCl<sub>2</sub>, pH 7.35 with NaOH unless otherwise indicated. Recordings of mIPSCs were made in the presence of tetrodotoxin (TTX; 1  $\mu$ M) and CNQX (10  $\mu$ M), to block Na<sup>+</sup> channels and AMPA receptors respectively. Spontaneous release from excitatory synapses was resolved by blocking GABA with Gabazine (10  $\mu$ M). The alternative solution used in Figure 6 was (in mM): 125 NaCl, 2.5 KCl, 25 HEPES, 30 glucose, and 2 MgCl<sub>2</sub> and CaCl<sub>2</sub> at pH 7.35 as used in (Ermolyuk et al. 2013). Recordings of mIPSCs were made using a potassium chloride-rich intracellular solution containing the following (in mM): 118 KCl, 1 EGTA, 10 HEPES, 4 MgCl<sub>2</sub>, 1 CaCl<sub>2</sub>, 4 NaATP, 0.3 NaGTP, 14 creatinine phosphate, pH 7.2 with KOH. Electrodes had resistances of 3–7 M $\Omega$ . For VACC current recordings, 150 mM TEACl, 1  $\mu$ M TTX, and 10  $\mu$ M GABAzine and CNQX were added to standard extracellular solution; and the patch pipette was filled with a CsMeSO<sub>3</sub>-rich solution containing the following (in mM): 108 CsMeSO<sub>3</sub>, 9 EGTA, 10 HEPES, 4 MgCl<sub>2</sub>, 1 CaCl<sub>2</sub>, 4 NaATP, 0.3 NaGTP (pH was brought to 7.2 using TEAOH). Currents were recorded with a HEKA EPC9/2 amplifier and filtered at 1 kHz using a Bessel filter and sampled at 10 kHz. R<sub>s</sub> was monitored, and recordings were discarded if R<sub>s</sub>

changed significantly during a recording.  $R_s$  was compensated to ~70% in recordings of VACC currents.

### **Solution Application**

Solutions were gravity fed through a glass capillary (1.2 mm outer diameter) placed ~1 mm from the patch pipette tip. Toxin (Alomone Labs) stock solutions were all made at 1000-fold concentration with distilled water and stored at -20 °C. Cytochrome C (0.5 mg/ml) was also added to MVIIC-containing solutions to minimize non-selective toxin binding to the apparatus.

### **ACKNOWLEDGEMENTS**

CLW was supported by an NRSA from NINDS and other support was provided by Merit Review Award (BX002547) from U.S. Department of Veterans Affairs and NIGMS (R01 GM097433).

## FIGURES

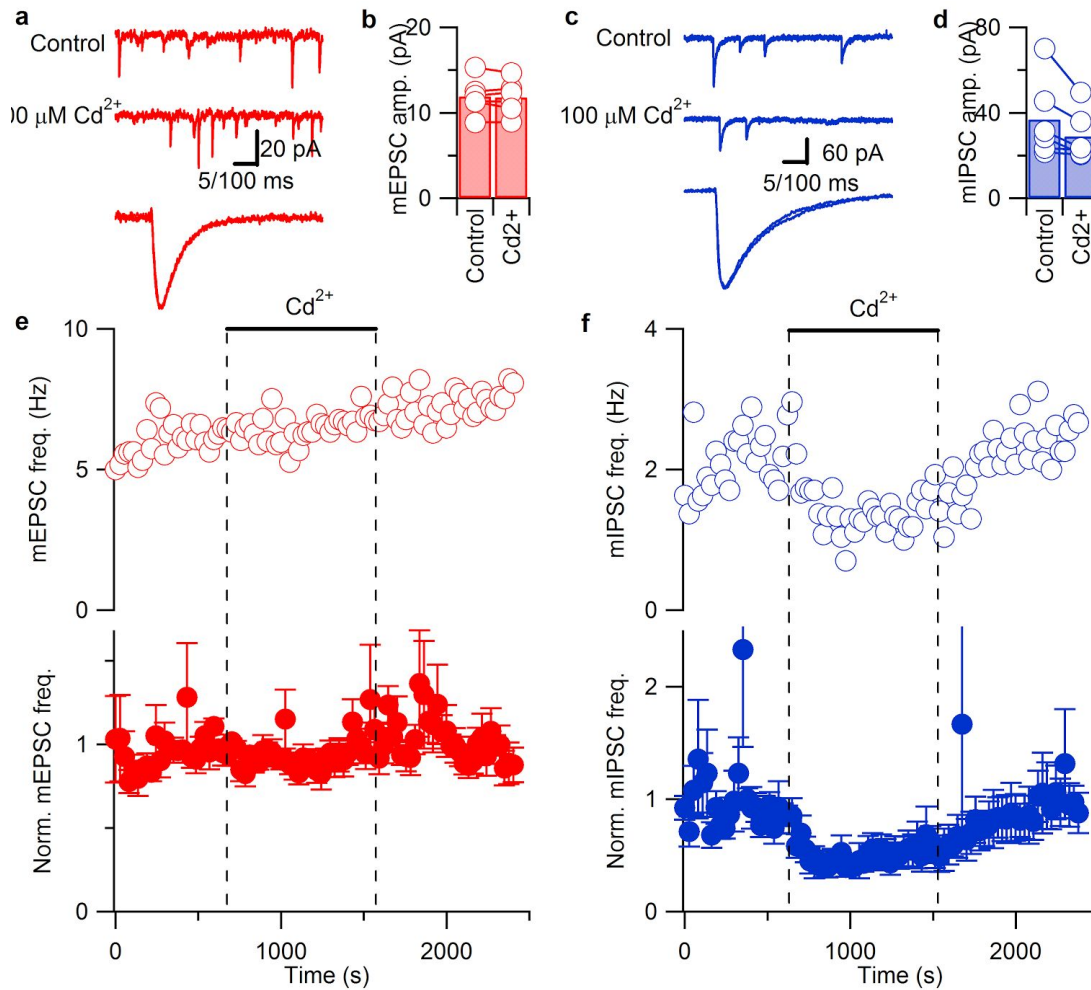


**Figure 11:  $\text{Cd}^{2+}$  has distinct actions on spontaneous release of glutamate and GABA in acute neocortical slices. a,c,** Exemplary traces of mEPSCs (red) and mIPSCs (blue) recorded under control conditions (top) and in the presence of 100  $\mu\text{M}$   $\text{Cd}^{2+}$  (scale bars are 20 pA for mEPSCs and 60 pA for mIPSCs versus 100 ms). Lower traces show superimposed average minis after normalization for amplitude (5 ms scale bar). **b,d,** Bar graph of average mEPSC (red) and mIPSC (blue) amplitude in control conditions and in the last 120 s of  $\text{Cd}^{2+}$  application ( $n = 6$ ). Open circles linked with lines represent average mEPSC amplitude from

individual experiments. **e,f**, Diary plots showing the effect of 100  $\mu\text{M}$   $\text{Cd}^{2+}$  (bar and dotted lines) on mEPSC (red) and mIPSC (blue) frequency (mean  $\pm$  S.E.M.) versus time in exemplary (open circles) and normalized average (closed circles).



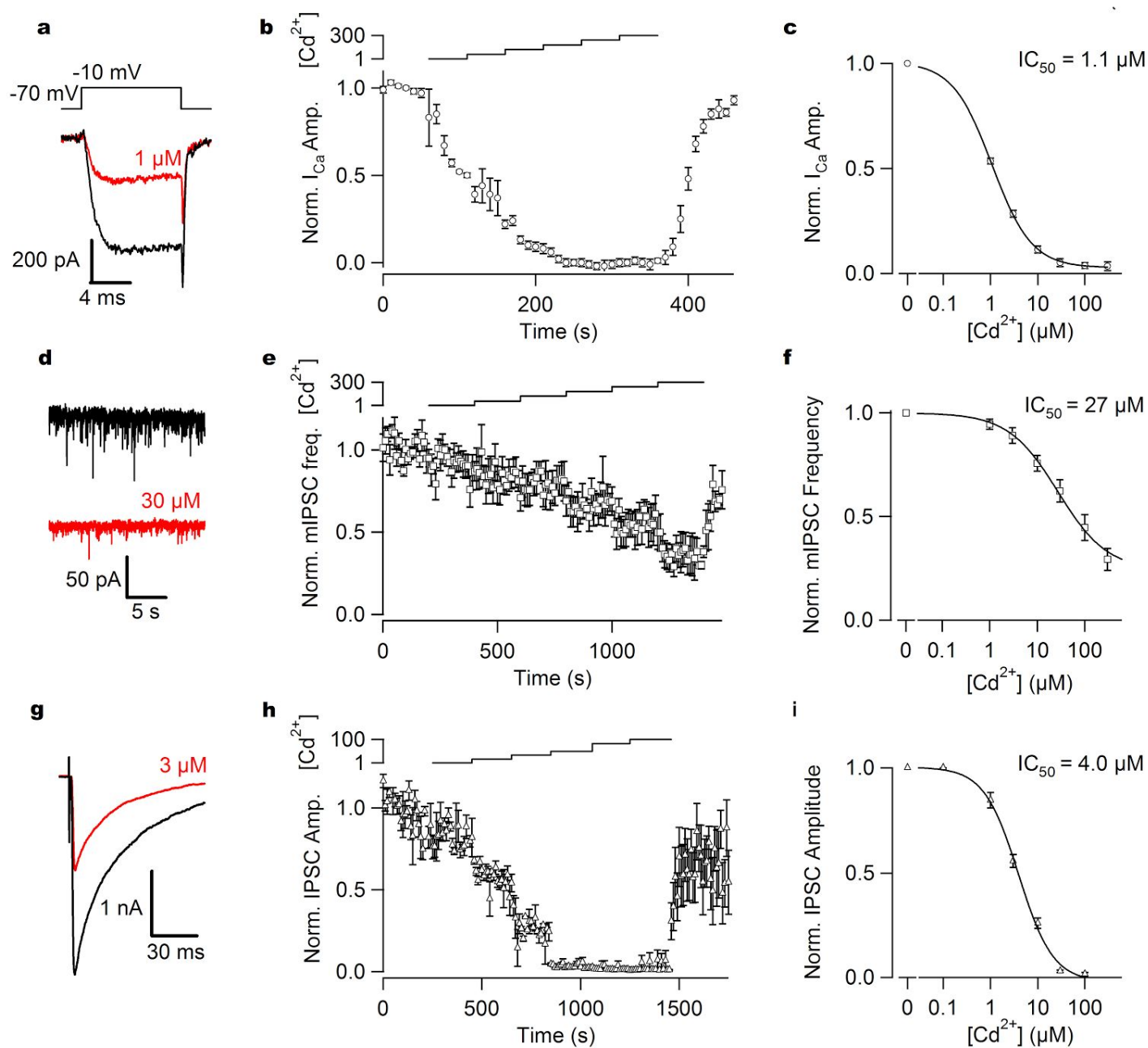


**Figure 12: Cd<sup>2+</sup> had a lower affinity for spontaneous release than evoked release or VACC currents in cultured neocortical neurons. a,d,g.** Exemplary traces of somatic VACC currents, stimulus-evoked IPSCs, and mIPSCs, respectively, in control and 1, 3, or 30 μM Cd<sup>2+</sup> (red). The concentration of Cd<sup>2+</sup> in the exemplary red traces was selected

to be close to the calculated  $IC_{50}$ s for each measurement (see c, f, and i). VACC currents were recorded stepping from -70 to -10mV. **b,e,h**, Average normalized diary plot of steady-state VACC current amplitude, mIPSC frequency, and stimulus-evoked IPSC amplitude, respectively, in 1, 3, 10, 30, 100, and 300  $\mu$ M  $Cd^{2+}$  (n = 12, 9, and 10). [ $Cd^{2+}$ ] is plotted above in  $\mu$ M. **c,f,i**, Dose response curves generated from the normalized diary plots in b,e, and h.  $IC_{50}$  values are stated beside each curve. Note the differences in  $IC_{50}$  for each measurement.

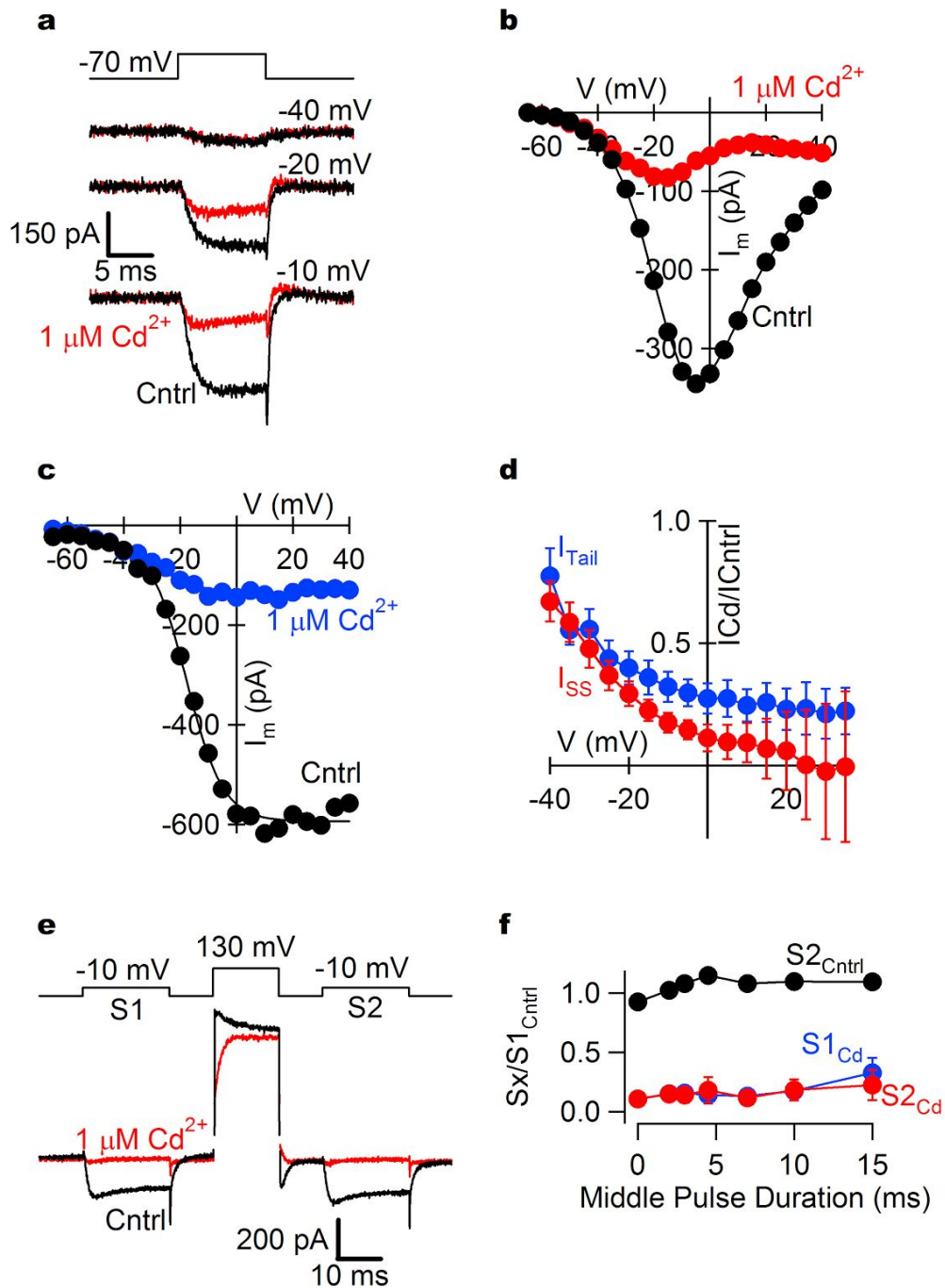


**Figure 13: Voltage-dependence of  $\text{Cd}^{2+}$  block of VACC currents.** **a**, Exemplary traces of  $100 \mu\text{M}$   $\text{Cd}^{2+}$ -subtracted currents recorded at  $-40$ ,  $-20$ , and  $-10$  mV voltage-step protocols under control conditions (black) and in  $1 \mu\text{M}$   $\text{Cd}^{2+}$  (red). Notice the decrease in block at more hyperpolarized steps. **b**, IV curve for  $\text{Cd}^{2+}$ -sensitive steady-state currents from the same

experiment in a. **c**, Plot of the peak amplitude of the tail current from the same experiment versus the magnitude of the voltage step from the same experiment in a. Tail currents recorded in control conditions are indicated in black and in the presence of  $1 \mu\text{M Cd}^{2+}$  in blue. **d**, Plot of steady-state VACC current amplitude (red) and tail current amplitude (blue) in  $1 \mu\text{M Cd}^{2+}$  divided by that measured in control conditions and plotted against membrane potential ( $n = 4$ ). Note the reduced block by  $\text{Cd}^{2+}$  and more hyperpolarized potentials and the increase in variability of the steady-state current at positive potentials. **e**, Exemplary traces of currents recorded in control (black) and in  $1 \mu\text{M Cd}^{2+}$  (red) with pre- and post-pulse currents (S1 and S2, respectively) recorded at  $-10 \text{ mV}$  where the current amplitude was maximal and the middle pulse to  $130 \text{ mV}$ . The middle pulse was increased in duration from 0 to 15 ms. Note the presence of the  $\text{Cd}^{2+}$ -sensitive outward current resulting from the middle pulse. **f**, Plot of the ratio of the peak amplitude of the steady-state current measured for S2 under control conditions (black) or in the presence of  $1 \mu\text{M Cd}^{2+}$  at either S1 (blue) or S2 (red) and the peak amplitude of the steady state current measured for S1 under control conditions versus the duration of the middle pulse in ms ( $n = 3$ ). Note that there is no relief of block even for longer middle pulse durations.

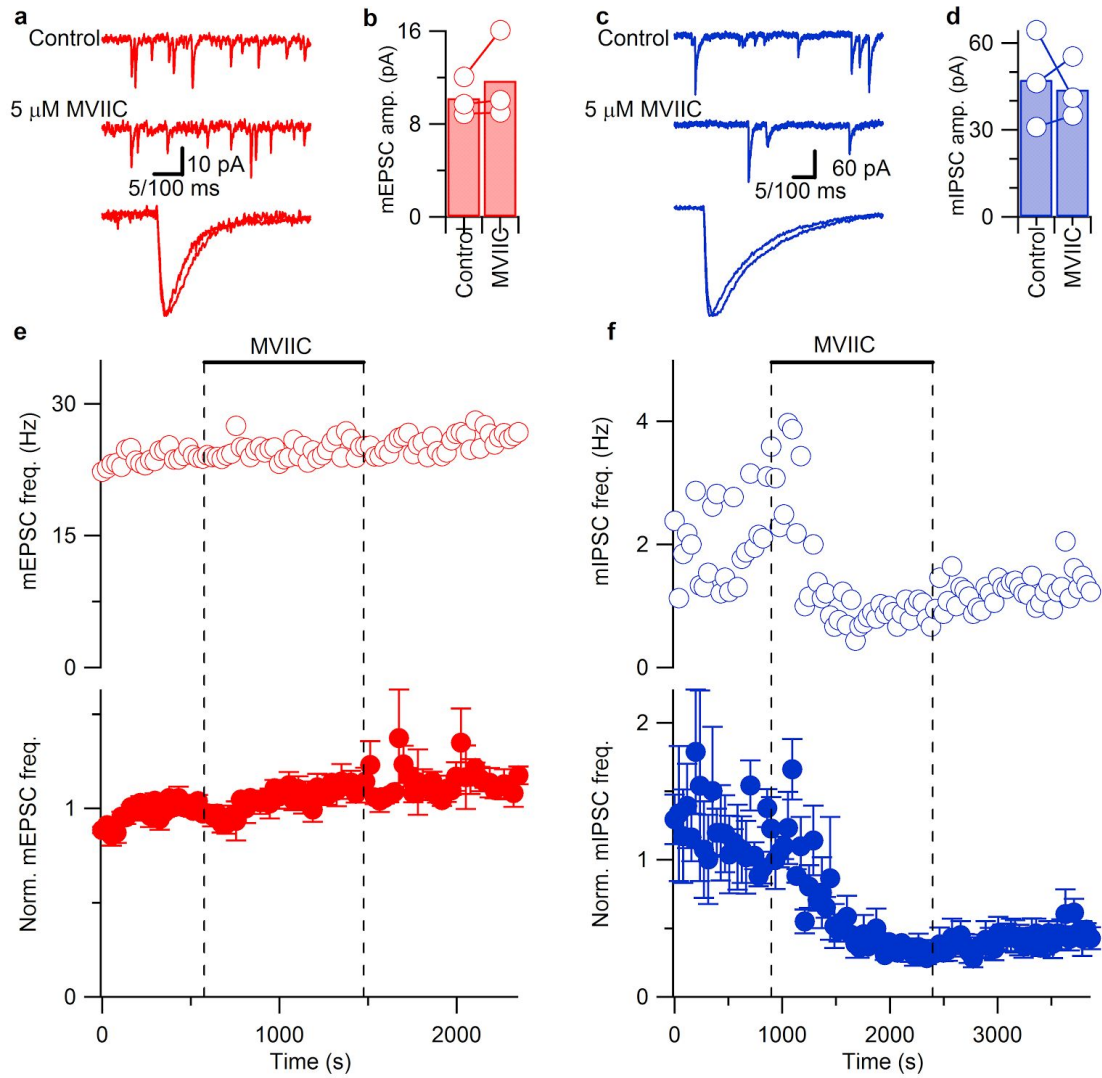


**Figure 14. The selective VACC blocker, MVIIC, substantially reduces spontaneous release of GABA but was ineffective on spontaneous release of glutamate. a,c,** Exemplary traces of mEPSCs (red) and mIPSCs (blue) recorded under control conditions (top) and in the presence of 5  $\mu$ M MVIIC. **b,d,** Bar graph of average mEPSC (red) and mIPSC (blue) amplitude in control conditions and in the last 100s of 5  $\mu$ M MVIIC application. Open circles linked with lines represent average mEPSC amplitude from individual experiments. **e,f,** Diary plots for exemplary experiments (top) and normalized average mEPSC

(red) or mIPSC (blue) frequency to show the time course of the response to 5  $\mu$ M MVIIC, as indicated by the black bar and dotted lines.

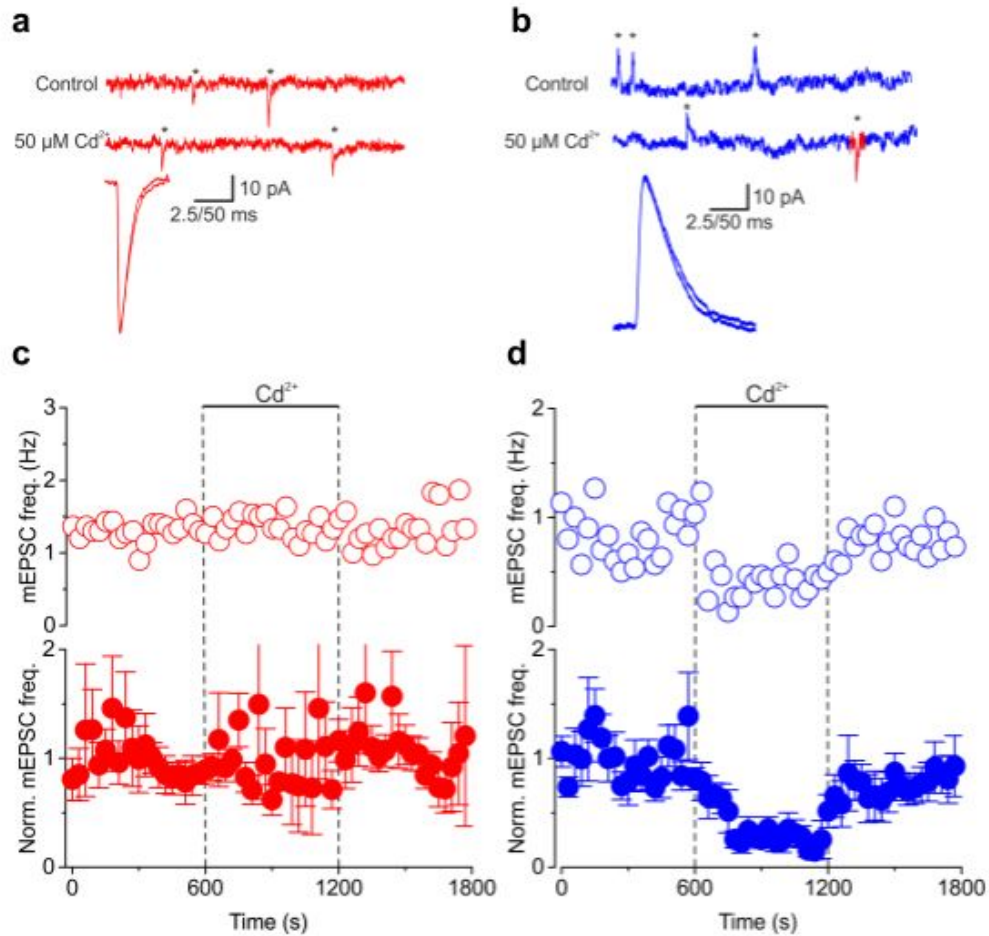


**Figure 15:  $\text{Cd}^{2+}$  reduces spontaneous release of GABA and glycine but not glutamate in acute auditory brainstem slices.** **a**, Exemplary current traces showing mEPSCs (red) before (upper trace) and during (middle trace) application of  $50 \mu\text{M Cd}^{2+}$  (10 pA and 50 ms scale bars). Asterisks denote individual release events. Lower trace shows superimposed average mEPSCs after normalization for amplitude (2.5 ms scale bar). **b**, Exemplary current traces showing mIPSCs (blue) before (upper trace) and during (middle trace) application of  $50 \mu\text{M Cd}^{2+}$  (10 pA and 50 ms scale bars). Note simultaneously recorded mEPSC denoted in red. Lower trace shows superimposed average mIPSCs after normalization for amplitude (2.5 ms scale bar). **c,d**, Diary plots showing the effect of  $50 \mu\text{M Cd}^{2+}$  (bar and dotted

lines) on mEPSC (red) and mIPSC (blue) frequency (mean  $\pm$  S.E.M.) versus time in exemplary (open circles) and normalized average (closed circles).



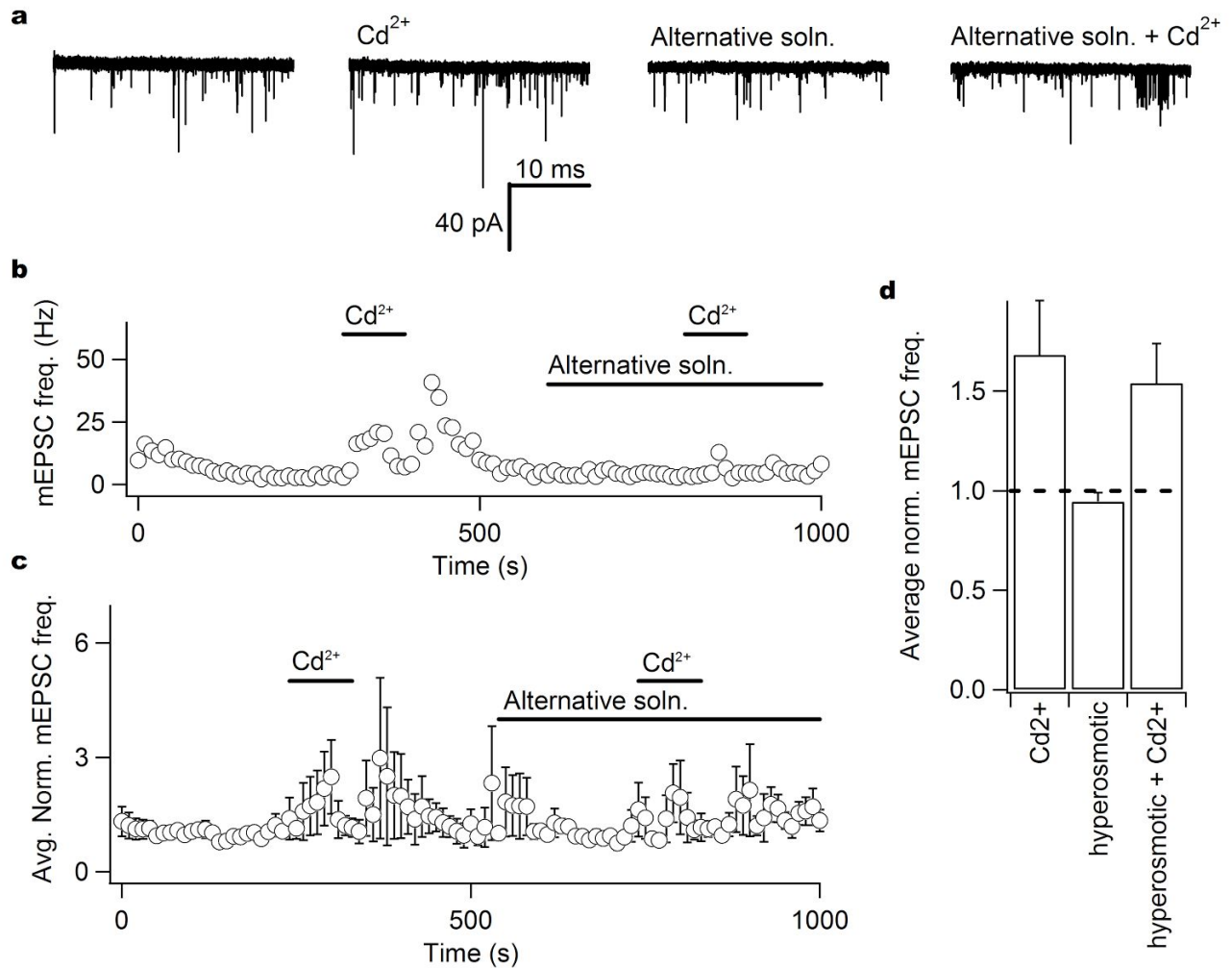


**Figure 16:  $\text{Cd}^{2+}$  does not reduce mEPSC frequency in neocortical culture, even in an alternative extracellular solution.** **a**, Exemplary traces of mEPSCs to show the response to 100  $\mu\text{M}$   $\text{Cd}^{2+}$  in control conditions and in an alternative extracellular solution which contained lower  $[\text{Na}^+]$  and higher  $[\text{glucose}]$  and  $[\text{HEPES}]$ . **b**, Exemplary diary plot from the same experiment to show the time course of the effects of  $\text{Cd}^{2+}$  application in control and alternative extracellular solutions. Note the increase produced by  $\text{Cd}^{2+}$  in control conditions. **c**, Averaged normalized diary plot of mEPSCs for all experiments using alternative extracellular

solution all similar experiments (n = 6). **d**, Bar graph from the same experiments in C showing the average effect of Cd<sup>2+</sup> in control and alternative solution.

## CHAPTER 3

---

### **Spontaneous and Evoked Vesicle Pools are Distinct at Inhibitory Terminals Where L-Type Ca<sup>2+</sup> Channels Participate in Release**

Courtney Williams<sup>1,2</sup> and Stephen M. Smith<sup>1,2</sup>

<sup>1</sup> Department of Medicine, Division of Pulmonary & Critical Care Medicine,  
Oregon Health & Science University, Portland, Oregon, 97239, USA.

<sup>2</sup> Section of Pulmonary & Critical Care Medicine, VA Portland Health Care  
System, Portland, Oregon, USA.

Address correspondence to: Stephen M. Smith, VA Portland Health Care  
System, 3710 SW U.S. Veterans Hospital Road, R&D 24, Portland, OR 97239.  
Phone: (503) 220 8262 extension 52361; E-mail: [smisteph@ohsu.edu](mailto:smisteph@ohsu.edu).

#### **ABSTRACT**

The Ca<sup>2+</sup> dependence of synaptic transmission has been well established. While it is known that action potential-evoked release of neurotransmitter occurs following the voltage-dependent gating of VACCs, the mechanism underlying spontaneous release of neurotransmitter has not been well described. Here we explore the differences in Ca<sup>2+</sup> dynamics of spontaneous and evoked release at inhibitory synapses. We find that spontaneous release is regulated by VACCs at

inhibitory synapses and that L-type channels play a role in triggering both spontaneous and evoked release. Additionally, vesicles that participate in evoked release are more loosely-coupled to VACCs and these spontaneous and evoked release of GABA arise from distinct vesicle pools.

## **INTRODUCTION**

Chemical synaptic transmission is essential for interneuronal communication. The initial step, release of neurotransmitter from vesicles stored in the presynaptic terminal, is  $\text{Ca}^{2+}$ -dependent, and occurs when synaptic vesicles fuse with the presynaptic membrane at the active zone (Katz & Miledi 1968; Borst & Sakmann 1996; Sudhof 2011). Once released, neurotransmitter diffuses across the synaptic cleft and binds to receptors on the postsynaptic cell membrane. The vesicle hypothesis for neurotransmission was developed with the assumption that vesicles engaged in evoked release were identical to those mediating spontaneous release (del Castillo & Katz 1954; Heuser 1989). However, spontaneous and evoked release at small cortical excitatory synapses arise from distinct vesicle pools, are released from the same active zones, and target different populations of postsynaptic receptors (Melom et al. 2013; Espinosa & Kavalali 2009; Sara et al. 2005; Ramirez & Kavalali 2011). Consistent with this, these two forms of release are regulated differently by VACCs. While evoked release at excitatory cortical synapses is dependent on VACC activity (Luebke et al. 1993; Takahashi & Momiyama 1993; Castillo et al. 1994; Wheeler et al. 1994), this is not the case for spontaneous release (Vyleta & Smith 2011; Yamasaki 2006; Scanziani et al.

1992). In contrast, at cortical inhibitory synapses VACCs regulate both evoked and spontaneous transmission (Williams et al; Cuo and Tsien) leading to a number of questions. What are the identity of the non P/Q- and N-type VACCs that trigger spontaneous release of GABA? Are VACC-vesicle coupling the same for evoked and spontaneous transmission? If not, are the vesicles undergoing spontaneous and evoked release from functionally distinct groups? We address these questions here and determine that L-type VACCs trigger release at inhibitory synapses and that spontaneous and evoked vesicle pools may be modulated independently.

## **MATERIALS AND METHODS**

### **Neuronal culture preparation**

Neocortical neurons were isolated from postnatal day 1–2 mouse pups as described previously (Phillips et al. 2008). All animal procedures were approved by the Portland Veteran Affairs Medical Center's Institutional Animal Care and Use Committee in accordance with the U.S. Public Health Service Policy on Humane Care and Use of Laboratory Animals and the National Institutes of Health Guide for the Care and Use of Laboratory Animals. Animals were decapitated following general anesthetic with isoflurane and then the cerebral cortices were removed. Cortices were incubated in trypsin and DNase and then dissociated with a heat polished pipette. Dissociated cells were cultured in MEM plus 5% FBS on glass coverslips. Cytosine arabinoside (4  $\mu$ M) was added 48

hours after plating to limit glial division. Cells were used after a minimum of 14 days in culture.

### **Electrophysiology**

Cells were visualized with an Olympus IX70 inverted microscope. Recordings were made in whole-cell voltage clamp mode in neurons voltage-clamped at  $-70$  mV. Voltages were corrected for liquid junction potentials (Hughes et al. 1987). In general and except where stated in the text, extracellular solution contained the following (in mM): 150 NaCl, 4 KCl, 10 HEPES, 10 glucose, 1.1  $\text{MgCl}_2$ , pH 7.35 with NaOH.  $\text{CaCl}_2$  was 1.1 mM unless otherwise indicated. Recordings of mIPSCs were made in the presence of tetrodotoxin (TTX; 1  $\mu\text{M}$ ) and CNQX (10  $\mu\text{M}$ ) to block  $\text{Na}^+$  channels and AMPA receptors, respectively. Recordings of mIPSCs were made using a potassium chloride-rich intracellular solution containing the following (in mM): 118 KCl, 9 EGTA, 10 HEPES, 4  $\text{MgCl}_2$ , 1  $\text{CaCl}_2$ , 4 NaATP, 0.3 NaGTP, 14 creatinine phosphate, pH 7.2 with KOH. Electrodes had resistances of 3–7  $\text{M}\Omega$ .

IPSCs were evoked using a theta stimulating electrode connected to a high-voltage stimulus isolator (World Precision Instruments, product #A365D). Theta glass was pulled to a tip of  $\sim 5$   $\mu\text{m}$  outer diameter and filled with extracellular solution. The electrode was positioned near to putative axons abutting the postsynaptic cell and stimulus intensity adjusted (0.3–0.5 mA, 0.1 ms duration) until IPSCs were recorded.

VACC currents were isolated using cesium methane-sulfonate rich solution as described previously (Vyleta & Smith 2011). Currents were recorded with a HEKA EPC9/2 amplifier and filtered at 1 kHz using a Bessel filter and sampled at 10 kHz. Series Resistance ( $R_s$ ) was monitored, and recordings were discarded if  $R_s$  changed more than 30% during the course of a recording.  $R_s$  was compensated to ~70% in recordings of VACC currents.

### **Solutions**

Solutions were gravity fed through a glass capillary (1.2 mm outer diameter) placed ~1 mm from the patch pipette tip. TTX and CNQX stock solutions were made at 1000X concentration with distilled water and stored at  $-20^\circ\text{C}$ .

BAPTA-AM (Invitrogen) was dissolved in DMSO at 50 mM stock concentration on the day of experiment. The BAPTA-AM stock was added to extracellular solution, incubated at  $30^\circ\text{C}$ , and then dissolved using ultrasonic agitation for  $\geq 30$  min. EGTA-AM (Invitrogen) was dissolved in DMSO at 50 mM stock concentration. Stock concanamycin solution was made at 10,000x concentration with DMSO and stored at  $-80^\circ\text{C}$ .

### **Analysis**

Data were acquired on a PIII computer and analyzed with IgorPro (Wavemetrics) software using a template matching algorithm. Miniature IPSC data were normalized to the basal level by dividing the mIPSC frequency measured over each ten second interval by the average mIPSC frequency over 100–200 s at the beginning of the experiment. Steady-state mIPSC frequency changes were the

averages measured over  $\geq 50$  s as a percentage of the basal level. Exemplar plots of mIPSC frequency versus time are shown as to illustrate the variability of basal mIPSC frequency rates which presumably reflect differences in the number of synapses and release probability. The average basal mIPSC frequency was  $5.3 \pm 0.6 \text{ s}^{-1}$  ( $n = 61$ ).

Data values are reported as mean  $\pm$  SEM. Pairwise comparison of data were performed using Student's t test or Mann-Whitney U-test if the data were not normally distributed (Microsoft EXCEL or Sigmaplot). Subsequent pairwise comparisons were performed with the Holm-Sidak method (Sigmaplot). Curve fitting was carried out using IgorPro (Wavemetrics).

## **RESULTS**

### **Extracellular $\text{Ca}^{2+}$ strengthens spontaneous release**

Spontaneous release of glutamate and GABA increases with rises in  $[\text{Ca}^{2+}]_o$  (Vyleta & Smith 2011; Williams et al. 2012). At hair cells, in the absence of action potentials, increased  $[\text{Ca}^{2+}]_o$  has been shown to stimulate multivesicular release (Graydon et al. 2011). In addition to an frequency of events,  $\text{Ca}^{2+}$  also synchronized vesicle fusion, increasing the event amplitude. We tested if increasing  $[\text{Ca}^{2+}]_o$  similarly affected spontaneous release of GABA release in neocortical neurons. Increasing  $[\text{Ca}^{2+}]_o$  from 1.1 to 6 mM resulted in a substantial reduction in the interevent interval from  $192 \pm 63$  ms ( $n = 8$ ) to  $118 \pm 32$  ms on average ( $n = 8$ , see Figure 17 for an exemplar). The increase in events was not associated with any change in the mIPSC amplitude, indicating that highly



synchronized multivesicular fusion was not triggered by external calcium at these synapses (Figure 17b). We next examined the interevent frequency of mIPSCs in greater detail to determine if VACC-mediated MVR or bursting of spontaneous fusion events accounted for the observed  $[Ca^{2+}]_o$ -dependent increases in release. This required long stable recordings and for convenience and to minimize non-uniformity of errors the data are shown in the logarithm transform of time versus square root of event number (Sigworth & Sine 1987). At rest, the distribution of mIPSC interevent intervals was described by sum of two exponential distributions with time constants of 46 and 140 ms (Figure 17b). The increased frequency at higher extracellular calcium resulted in a distribution well-described with double exponential with time constants of 34 and 89 ms. In other words, the increased frequency of mIPSCs was attributed to an average reduction in the inter-event interval of  $\sim 74$  ms and not the addition of another much shorter distribution indicating an additional pathway of vesicle fusion. This is substantially longer than the sub-millisecond delay that arises at the hair cell synapse, and indicates the increased frequency is unlikely to arise from the same multi-vesicular release mechanism identified in hair cells (Graydon et al. 2011). We next examined the dependence of mEPSC frequency on  $[Ca^{2+}]_o$  since this pathway does not involve VACCs. As expected mEPSC frequency increased with  $[Ca^{2+}]_o$ , but there was no increase in mEPSC amplitude (Figure 17b,c), and the inter-vent interval was reduced in a graded manner ( $231 \pm 44$  ms to  $85 \pm 13$  ms;  $n = 9$ ) similarly to that observed at inhibitory synapses.

## **L-type VACCs contribute to fast synaptic transmission**

N-type and P/Q-type VACCs are the major subtypes regulating release of GABA at neocortical synapses (Cao & Tsien 2005). However, ~25% of spontaneous release was still sensitive to the non-selective VACC blocker,  $\text{Cd}^{2+}$ , following saturating block of both P/Q- and N-type channels, indicating contribution by L- or R-type VACCs (Williams et al. 2012). A contribution of L-type VACCs to fast synaptic transmission would be surprising because L-type channels are primarily expressed in soma and dendrites, not nerve terminals (Hell et al. 1993; Ludwig et al. 1997; Lipscombe et al. 2004). However, L-type channels have been shown to contribute to spontaneous GABA release from hippocampal granule cells (Goswami et al. 2012).

Dihydropyridine antagonists of L-type VACCs have been shown to have off-target effects, including blocking action potential firing (Caro et al. 2011). To test both spontaneous and evoked release we used a non-dihydropyridine that is specific for L-type VACCs, diltiazem. We applied a saturating concentration of the selective L-type channel blocker, diltiazem (10  $\mu\text{M}$ ) to somatically recorded VACC currents to estimate the fraction of sensitive channels in our preparation.

Diltiazem reduced VACC currents by  $85 \pm 3\%$  on average (Figure 18). We then applied diltiazem while recording mIPSCs to determine if L-type channels contribute to spontaneous GABA release. Diltiazem (10  $\mu\text{M}$ ) reduced mIPSC frequency by  $68 \pm 5\%$  on average but did not significantly alter amplitude (Figure 19a) indicating that L-type channels do trigger spontaneous GABA

release. Additionally, diltiazem also reduced stimulus-evoked IPSC amplitude by  $68 \pm 12\%$  on average (Figure 19b), a similar degree to what was seen for spontaneous GABA release. L-type channel block had no effect on mEPSC frequency (data not shown).

### **A $\text{Ca}^{2+}$ microdomain triggers stimulus-evoked release**

BAPTA and EGTA have similar affinities for  $\text{Ca}^{2+}$ , but BAPTA has a 40-fold faster rate of binding so that it is able to disrupt diffusion of  $\text{Ca}^{2+}$  at mM concentrations if the diffusion distance is as short as 10-20 nm. EGTA will only have an effect if the distance is greater than 100 nm at the same concentration (Adler et al. 1991; Eggermann et al. 2011). Spontaneous release of GABA is reduced by BAPTA-AM but not EGTA-AM indicating tight coupling between VACCs and vesicles (Williams et al. 2012). We hypothesized that evoked release was similarly sensitive to  $\text{Ca}^{2+}$  buffers if the process utilizes the same pool of vesicles. We find that 50  $\mu\text{M}$  BAPTA-AM and 50  $\mu\text{M}$  EGTA-AM both reduced IPSC amplitude in 1.1 mM  $[\text{Ca}^{2+}]_o$  by  $34 \pm 7\%$  and  $30 \pm 8\%$  respectively (Figure 20). Both BAPTA-AM and EGTA-AM also reduce IPSC amplitude in elevated  $[\text{Ca}^{2+}]_o$  (Figure 20 c,f). When  $[\text{Ca}^{2+}]_o$  is increased to 6 mM, BAPTA-AM application resulted in a  $43 \pm 10\%$  decrease, and EGTA-AM decreased IPSC amplitude to  $25 \pm 6\%$  (Figure 20 c,f). This contrasts with what we see for spontaneous GABA release, where only BAPTA-AM reduces mIPSC frequency and EGTA-AM does not alter basal mIPSC frequency or the increase in mIPSC frequency in response to increasing  $[\text{Ca}^{2+}]_o$  (Williams et al. 2012). This difference between spontaneous and evoked release

of GABA indicates that spontaneous GABA release occurs from vesicles that are closer to VACCs than evoked released vesicles.

### **Spontaneous and evoked vesicle pools are independent**

Differences in vesicle-channel coupling for spontaneous and evoked release could result from at least two possible mechanisms: spontaneous and evoked release arise from distinct vesicle pools, or they arise from the same pool but vesicles are much more likely to be released spontaneously if they are tightly-coupled to channels (Figure 21b,c). We investigated whether we could separate spontaneous and evoked vesicle pools from one another by selectively depleting each of the vesicle pools with a vacuolar-type ATPase (V-ATPase) inhibitor, concanamycin A (Muroi et al. 1993; Nishihara et al. 1995). Concanamycin A blocks V-ATPase activity, preventing vesicles from refilling with GABA after they have been endocytosed (Zhou et al. 2000; Sara et al. 2005). First we applied 100 nM concanamycin A in the presence of TTX for 10 minutes to see if we could selectively deplete the spontaneously recycling vesicle pool. Following incubation with concanamycin A or vehicle control (0.01% DMSO) and TTX, we made recordings of mIPSCs and IPSCs (Figure 22a). The neurons exposed to concanamycin A showed a substantial reduction in mIPSC frequency (Figure 22b,f;  $4.0 \pm 0.8$  Hz compared to  $18.7 \pm 4.8$  Hz in control;  $p = 0.025$ ), while mIPSC amplitude was unchanged (Figure 22b,f;  $11.9 \pm 1.5$  pA compared to  $13.8 \pm 1.4$  pA in control;  $p = 0.378$ ). Evoked IPSC amplitude was also unaffected in neurons exposed to concanamycin A (Figure 22c,d;  $1.8 \pm 0.2$  nA versus  $2.5 \pm 0.8$

nA in control;  $p = 0.382$ ). mIPSC frequency is approximately 14 Hz at 35°C and therefore around 8000 vesicles should be released during the 10 minute incubation. It is not known if the spontaneous pool is completely depletable, however, the 10 minute exposure to concanamycin A reduces spontaneous release by ~80% while there is no change in evoked release.

Next we attempted to selectively deplete the evoked vesicle pool without affecting spontaneous release using concanamycin A. To minimize contamination of the spontaneous pool during this time, we attempted to define a period and frequency of stimulation that would be optimal for vesicle turnover. We recorded 100 IPSCs at stimulation frequencies of 1, 3, 10, and 30 Hz to measure the magnitude of synaptic depression (Figure 23a). Synaptic depression increased with stimulation frequency, but was rescued quickly following a brief 10 ms break in stimulation (Figure 23a, b). Stimulating at 10 and 30 Hz would allow for a very brief application of concanamycin A and thus minimize depletion of the spontaneous pool, but it results in significant and rapid synaptic depression ( $62 \pm 3\%$  and  $76 \pm 5\%$ , respectively  $n = 5$ ). 1 Hz stimulation for 100 IPSCs only gives  $19 \pm 4\%$  depression but takes a long time, allowing for spontaneously recycling vesicles to be exhausted. Using this protocol we could also estimate the size of the vesicle pool recycling during each stimulation protocol by plotting the cumulative IPSC amplitude by stimulus number (which gives a lower boundary for the estimate of the RRP, Figure 23c) or plotting the amplitude of each IPSC by the cumulative IPSC size (which gives an upper boundary for the estimate of the

RRP; Figure 23d; Neher 2015). From this analysis we estimate the RRP to be between  $\sim 385$  and  $410 \pm 160$  nA or containing  $\sim 3,500 - 3,000$  vesicles ( $n = 5$ ).

With these parameters in mind, we applied concanamycin A during a train of action potentials to determine if we could selectively deplete the stimulus-evoked dependent recycling pool. IPSC amplitude and mIPSC frequency were measured prior to and following exposure to concanamycin A or vehicle control (0.01% DMSO) during a 112.5 s 8 Hz stimulation protocol (Figure 24a). The stimulation protocol was kept brief to reduce exposure of spontaneously recycling vesicles to concanamycin A. Evoked IPSC amplitude was reduced substantially following the stimulation protocol in the presence of 100 nM concanamycin A but not during vehicle control (Figure 24b,c,f;  $92 \pm 10\%$  versus  $50 \pm 6\%$ ;  $p = 0.001$ ), indicating a substantial portion of our estimated  $\sim 3,000$  vesicles in the evoked recycling pool have been exhausted. Miniature IPSC frequency increased following the stimulation protocol in both treatment conditions, but was not significantly decreased in the group exposed to concanamycin A (Figure 24d;  $137 \pm 11\%$  in vehicle control versus  $123 \pm 11\%$  in concanamycin;  $p = 0.4$ ). From these results we conclude that spontaneous and evoked vesicles arise from distinct pools and recycle independently at neocortical synapses.

## **DISCUSSION**

In the present study we confirm that spontaneous release at excitatory and inhibitory synapses is enhanced by elevated levels of  $[Ca^{2+}]_o$ . At inhibitory

terminals, this enhancement is in part due to increased  $\text{Ca}^{2+}$  influx through L-type VACCs. Surprisingly, L-type channels also contribute proportionally to stimulus-evoked release at the same inhibitory terminals. Despite having similar contribution from the same VACC subtypes,  $\text{Ca}^{2+}$  diffuses farther from VACCs to trigger evoked release of GABA, as it has been previously shown that VACCs are tightly coupled to release machinery for spontaneous release (Goswami et al. 2012; Williams et al. 2012; Ermolyuk et al. 2013). This brings into question whether spontaneous and stimulus-evoked vesicles recycle independently at inhibitory terminals. We were able to deplete each pool using concanamycin A without affecting the other pool, indicating that spontaneous and evoked release result from distinct vesicle pools.

### **Mechanisms of $\text{Ca}^{2+}$ enhancement of spontaneous release**

Dissecting the pivotal role  $\text{Ca}^{2+}$  plays in synaptic transmission and the contributions of the component signaling pathways is essential to our understanding of neuronal communication. The results of this study suggest that spontaneous release is  $\text{Ca}^{2+}$  dependent at glutamatergic and GABAergic synapses in murine neocortical neurons. There are several possible mechanisms by which changes in  $[\text{Ca}^{2+}]_o$  may enhance tonic spontaneous release. At excitatory synapses in neocortex, a portion of the  $\text{Ca}^{2+}$ -dependence is mediated by a  $\text{Ca}^{2+}$  sensitive G-protein coupled receptor, CaSR (Vyleta & Smith 2011). Other GPCRs are possible candidates including metabotropic glutamate receptors and GPRC6A (Tabata & Kano 2004; Wellendorph & Bräuner-Osborne 2004). Another possible

mechanism is  $\text{Ca}^{2+}$  release from intracellular stores, which has been shown to promote spontaneous release in (Khodakhah & Ogden 1993; Llano et al. 2000; Wellendorph & Bräuner-Osborne 2004). However, stochastic opening of VACCs is likely a major contributor to the spontaneous release, and the number and types of channels contributing is under much debate (Scanziani et al. 1992; Eggermann et al. 2011; Goswami et al. 2012).

Stimulus-evoked release has been shown to have a steep dependence of  $[\text{Ca}^{2+}]_o$ , where 4-5  $\text{Ca}^{2+}$  ions cooperate to trigger release of each vesicle (Dodge & Rahamimoff 1967). This contrasts with what is observed for spontaneous release, where the relationship is much less steep (Vyleta & Smith 2011; Williams et al. 2012; Groffen et al. 2010; Xu et al. 2009). A weaker  $\text{Ca}^{2+}$  dependence suggests that spontaneous release may be more sensitive to small changes in  $[\text{Ca}^{2+}]_i$ —especially at low  $[\text{Ca}^{2+}]_i$ , as it does not require cooperative binding of multiple  $\text{Ca}^{2+}$  ions to release machinery (Lou et al. 2005; Sun et al. 2007). This apparent difference in  $\text{Ca}^{2+}$  dependence also raises the question of whether spontaneous and evoked release rely on the same release machinery. It has been suggested that spontaneous release is an extension of evoked release, and that they are both mediated by  $\text{Ca}^{2+}$  binding to synaptotagmin-1 (Xu et al. 2009). Interestingly, depletion of Synaptotagmin-1 or -2 has been shown to cause an increase in mini frequency, indicating this may not be true in all cases (Pang et al. 2011; Maximov & Südhof 2005; Sun et al. 2007). Other studies have indicated spontaneous release may use other  $\text{Ca}^{2+}$  sensing proteins, including Doc2 family



proteins (Groffen et al. 2010). Taken together, these studies indicate that the  $\text{Ca}^{2+}$  sensing mechanisms behind spontaneous release have not yet been elucidated.

### **L-type VACCs contribute to fast synaptic transmission**

There is debate over the number and type of VACCs that trigger both spontaneous and evoked release at a variety of synapses. Evoked release of GABA from neocortical synapses has been shown to be mediated by P/Q- > N- > R-types at cortical synapses the order of relative contribution (Cao & Tsien 2005). It is surprising that L-type calcium channels trigger fast synaptic transmission at our synapses. L-type channels are expressed throughout the CNS including cortex, hippocampus, spinal cord, cerebellum (Hell et al. 1993; Ludwig et al. 1997; Lipscombe et al. 2004). However, L-type channels are primarily localized in soma and dendrites of cortical neurons, making them unlikely candidates for contributing to exocytosis, excluding sensory terminals (Hell et al. 1993). Additionally, L-type channels are thought to open too slowly to contribute to action potential-induced  $\text{Ca}^{2+}$  influx (Helton et al. 2005). L-type channels have been shown to contribute to long-term cell changes like plasticity in hippocampal neurons and cell survival (Norris et al. 1998; Weisskopf et al. 1999; Galli et al. 1995; Mao et al. 1999). L-type channels also activate gene expression changes in the brain by activating CREB transcription factors (Weick et al. 2003; Dolmetsch et al. 2001). Yet, L-type channels have been shown to trigger spontaneous release of GABA and acetylcholine (Goswami et al. 2012; Losavio & Muchnik 1997). It

has been suggested that the contribution of L-type calcium channels to synaptic transmission may have been underestimated due to the voltage-dependence of many selective L-type channel blockers (Helton et al. 2005).

### **Independence of vesicle pools for different modes of release**

There is an emerging consensus for a distinct functional role of spontaneous release (Lee et al. 2010; Jakawich et al. 2010; Kavalali et al. 2011). Studies have shown that spontaneous and evoked release can be regulated independently by certain signaling pathways and potentially in opposite directions (Wasser et al. 2007; Zamir & Charlton 2006; Smith et al. 2012). Our finding that vesicle-channel coupling is looser for evoked release of GABA than it is for spontaneous release provides further insight into its independence from evoked release. One possible mechanism cells could use to tightly-couple spontaneous vesicles is to tether them to VACCs. RIM proteins have been shown to tether VACCs to active zones, allowing cells to maintain a nanodomain architecture (Kaesler et al. 2011). Recent studies show that VACCs may also tether to vesicles directly via their C-termini (Wong et al. 2014).

We are not the first to suggest that spontaneous and evoked vesicle pools recycle independently (Sara et al. 2005). Studies at the fly neuromuscular junction have used genetically encoded  $Ca^{2+}$  indicators to visualize independent release of spontaneous and evoked glutamate and determined that some terminals will release only spontaneous or evoked vesicles (Melom et al. 2013). Several vesicular membrane proteins have been indicated as possible targets for

segregation of vesicle pools, meaning that independent regulation is possible even within the same nerve terminals (Ramirez et al. 2012; Hua et al. 2011). By using different vesicle pools, the cell has another means by which to regulate spontaneous and evoked release independently and these two forms of release may represent distinct signals between cells.

### **ACKNOWLEDGEMENTS**

CLW was supported by an NRSA from NINDS and other support was provided by Merit Review Award (BX002547) from U.S. Department of Veterans Affairs and NIGMS (R01 GM097433).

## FIGURES

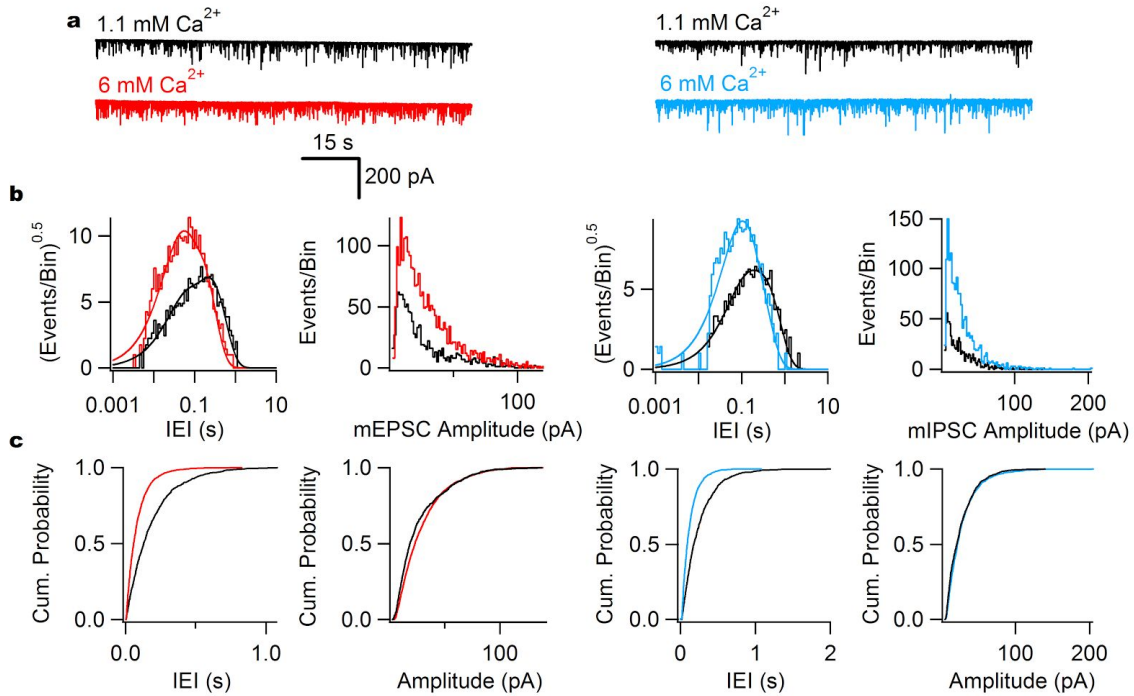


**Figure 17:  $Ca^{2+}$  enhancement of spontaneous glutamate and GABA release.**

**a**, Exemplary traces of mEPSCs and mIPSCs in 1.1 (black) or 6 mM  $[Ca^{2+}]_o$  (red or blue respectively). **b**, Histograms of mEPSC or mIPSC inter-event interval (IEI) and amplitude from exemplary experiments. Black traces indicate frequency and amplitude in 1.1 mM  $[Ca^{2+}]_o$ , while red and blue traces are measured in 6 mM  $[Ca^{2+}]_o$ . IEI is plotted on a logarithmic time scale and the variance is stabilized using a square root transformation to simplify interpretation and allow for better fitting of the probability density function (Sigworth & Sine 1987). **c**, Cumulative probability plots for IEI and amplitude from the same exemplars as in a and b.

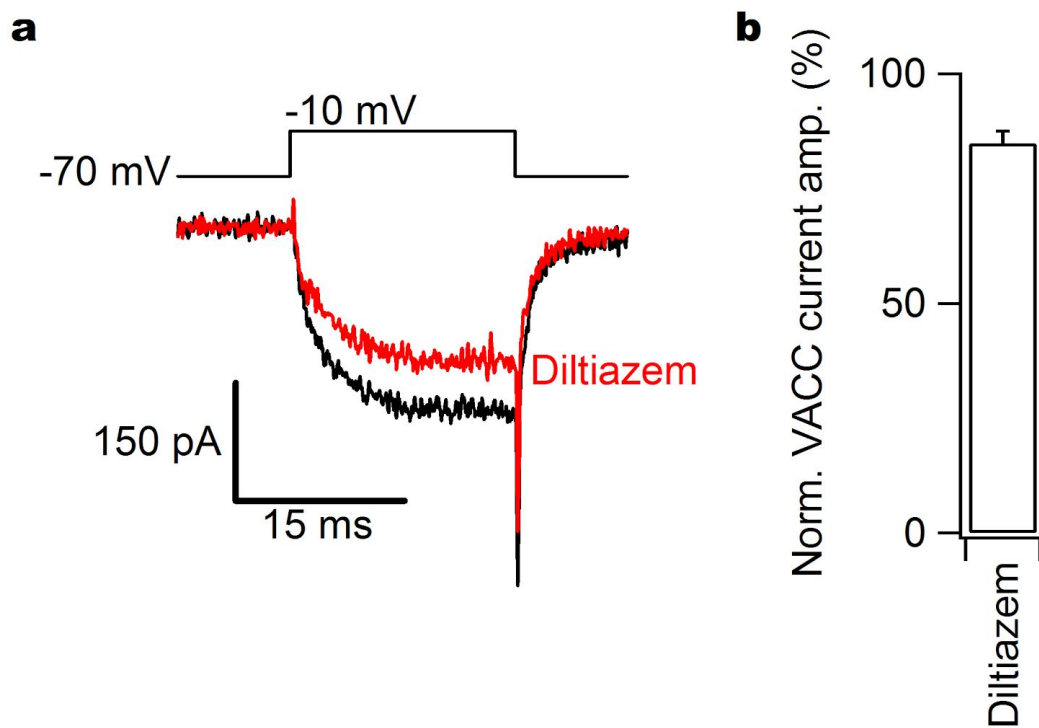


**Figure 18: Diltiazem selectively blocks L-type VACCs.** **a**, Exemplary traces of VACC currents recorded with a voltage step to -10 mV in control (black) and 10  $\mu$ M diltiazem (red). **b**, Bar graph of normalized VACC current amplitude in 10  $\mu$ M diltiazem (n = 6).

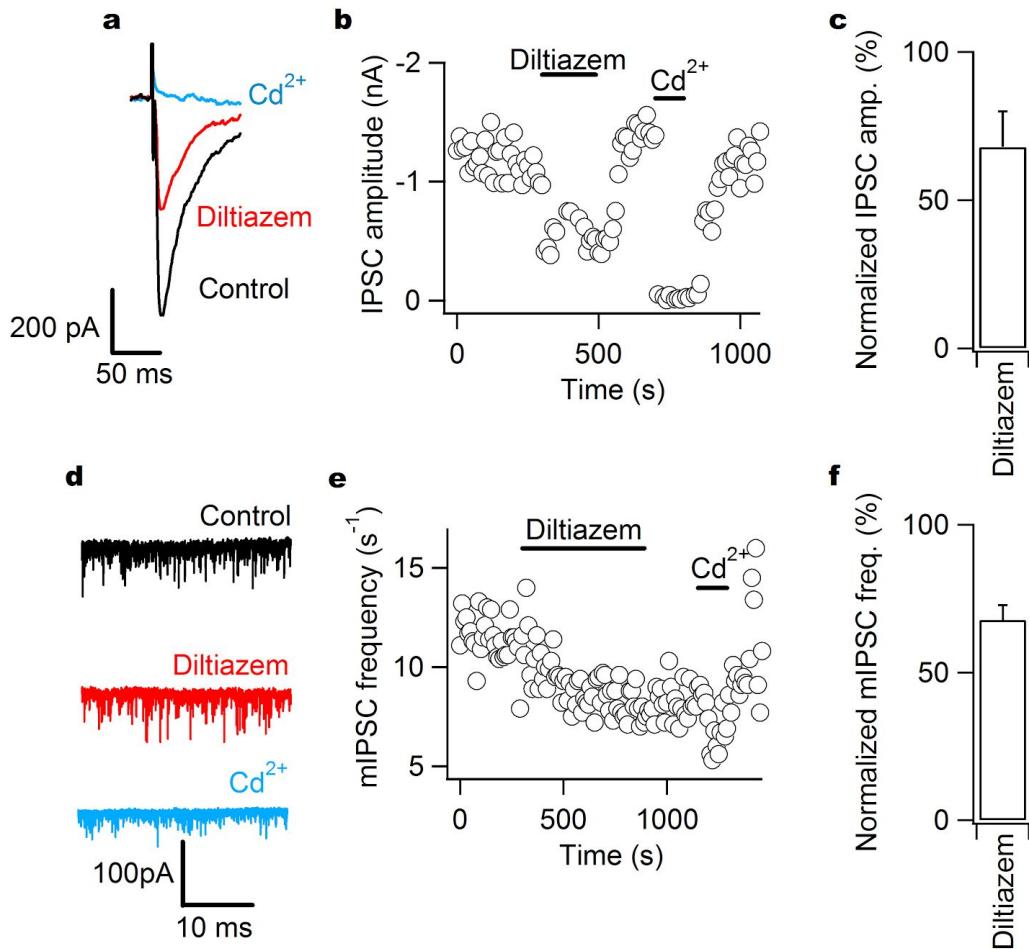


**Figure 19. L-type VACCs contribute to release of evoked and spontaneous release of GABA.** **a**, Exemplary traces of stimulus evoked IPSCs in control (black), 10  $\mu$ M diltiazem (red), and 100  $\mu$ M Cd<sup>2+</sup>. **b**, Diary plot from the same individual experiment to show the time course and reversibility of diltiazem and Cd<sup>2+</sup> applications. **c**, Bar graph of normalized IPSC amplitude in diltiazem (n = 6). **d**, Exemplary traces of mIPSCs in control (black), 10  $\mu$ M diltiazem (red), and 100  $\mu$ M Cd<sup>2+</sup>. **e**, Diary plot from the same individual experiment to show the time course and reversibility of diltiazem and Cd<sup>2+</sup> applications. **f**, Bar graph of normalized mIPSC frequency in diltiazem (n = 18).

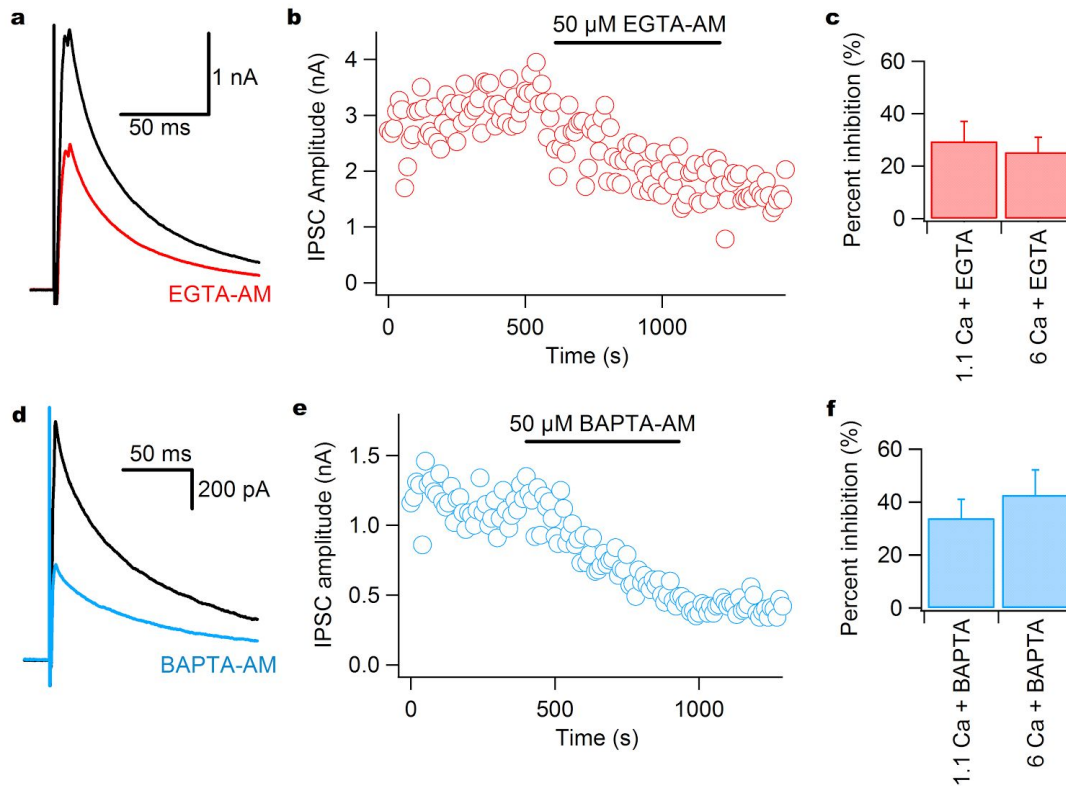


**Figure 20. VACCs trigger stimulus-evoked release of GABA through  $\text{Ca}^{2+}$**

**microdomain coupling.** **a** and **d**, Exemplary traces of stimulus evoked IPSCs in control (black) and 50  $\mu\text{M}$  EGTA-AM (red) or BAPTA-AM (blue) in 1.1 mM  $[\text{Ca}^{2+}]_o$ . **b** and **e**, Diary plot from the same individual experiment to show the time course of chelator application applications (EGTA-AM, red; BAPTA-AM, blue). **c** and **f**, Bar graphs of normalized IPSC amplitude in either EGTA-AM (red) or BAPTA-AM (blue) in 1.1 or 6 mM  $[\text{Ca}^{2+}]_o$  ( $n = 13, 17, 9,$  and  $12$  left to right and top to bottom).

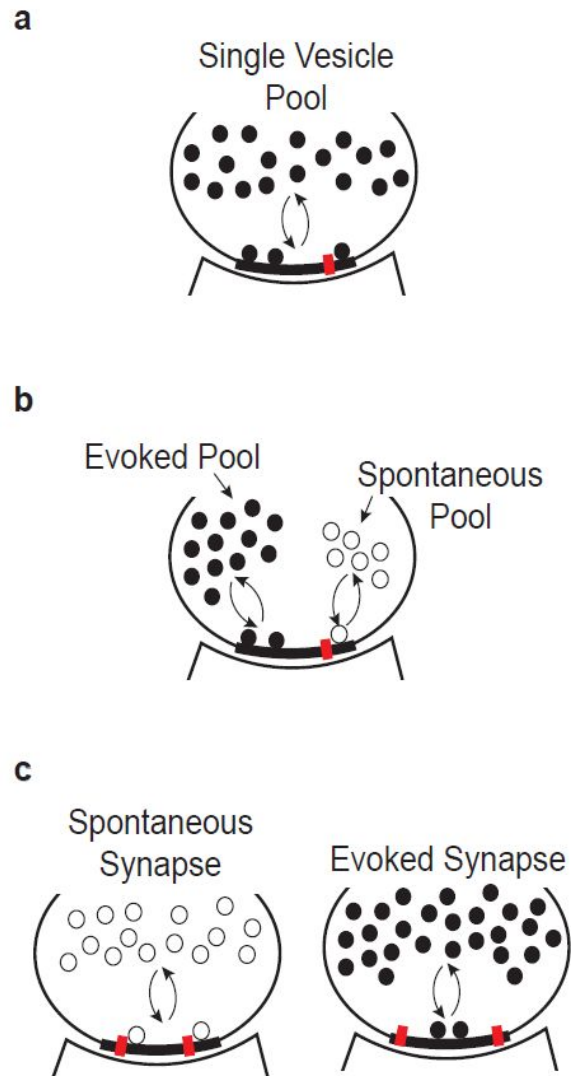


**Figure 21. Mechanisms of vesicle pool distinction.** **a**, Spontaneous and evoked vesicles arise from one vesicle pool, but vesicles are more likely to be released spontaneously if they are within 10-100nm from VACCs. **b**, Spontaneous and evoked vesicles recycle in independent vesicle pools at the same synapse, and spontaneous release occurs with vesicles that are close to VACCs. **c**, Spontaneous and evoked release are independent because they occur at different nerve terminals. At spontaneous terminals, VACCs are tightly-coupled to vesicle release machinery.



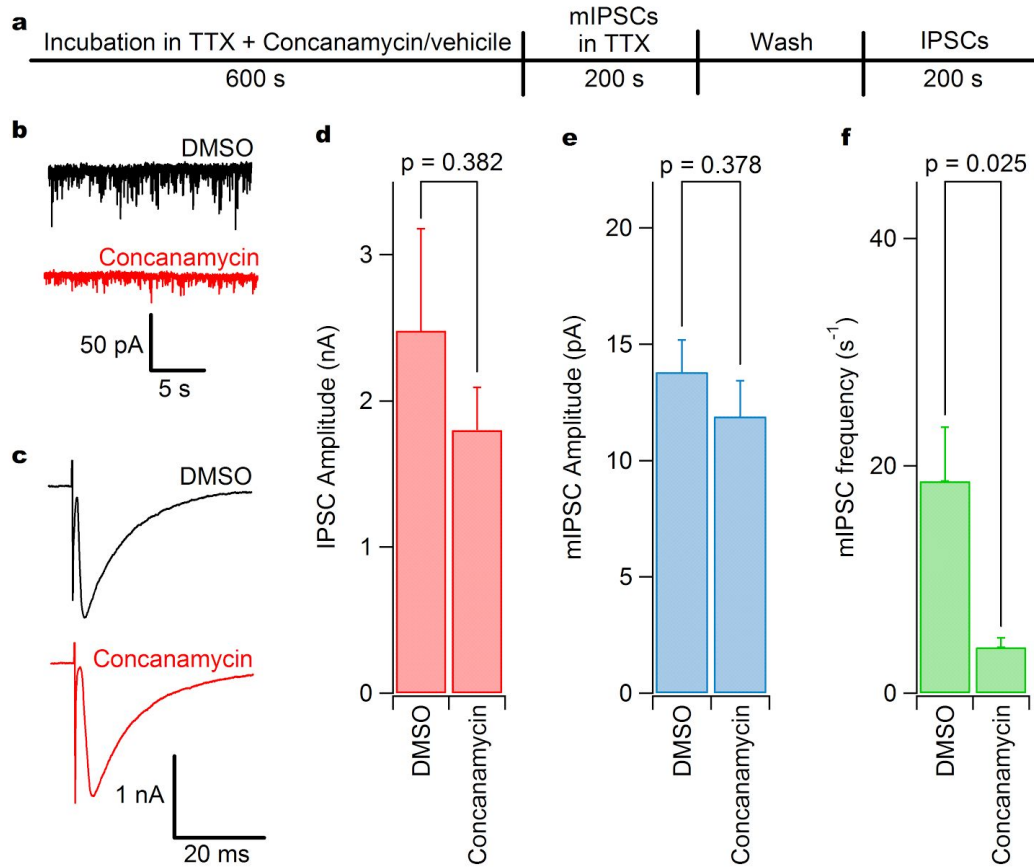


**Figure 22. Selective depletion of the spontaneous recycling pool by**

**inhibiting vesicle refilling.** **a**, Schematic representation of experiment protocol. Neurons were incubated for 10 minutes with 1  $\mu$ M TTX and either concanamycin A or 0.01% DMSO vehicle control. Neurons were then patched in whole-cell configuration and mIPSCs were recorded in TTX. TTX was washed out of the bath and stimulus-evoked IPSCs were recorded from the same cell. **b**, Exemplary traces of mIPSCs recorded in cells that were incubated in vehicle control (black) or concanamycin A (red). **c**, Exemplary traces of stimulus-evoked IPSCs recorded in cells that were incubated in vehicle control or concanamycin A. **d**, Bar graph of average IPSC amplitude from cells incubated in vehicle control or concanamycin A ( $n = 12$  and  $12$ , respectively). **e**, Bar graph of average mIPSC amplitude from the same cells incubated in vehicle control or

concanamycin A. **f**, Bar graph of average mIPSC frequency from the same cells incubated in vehicle control or concanamycin A.

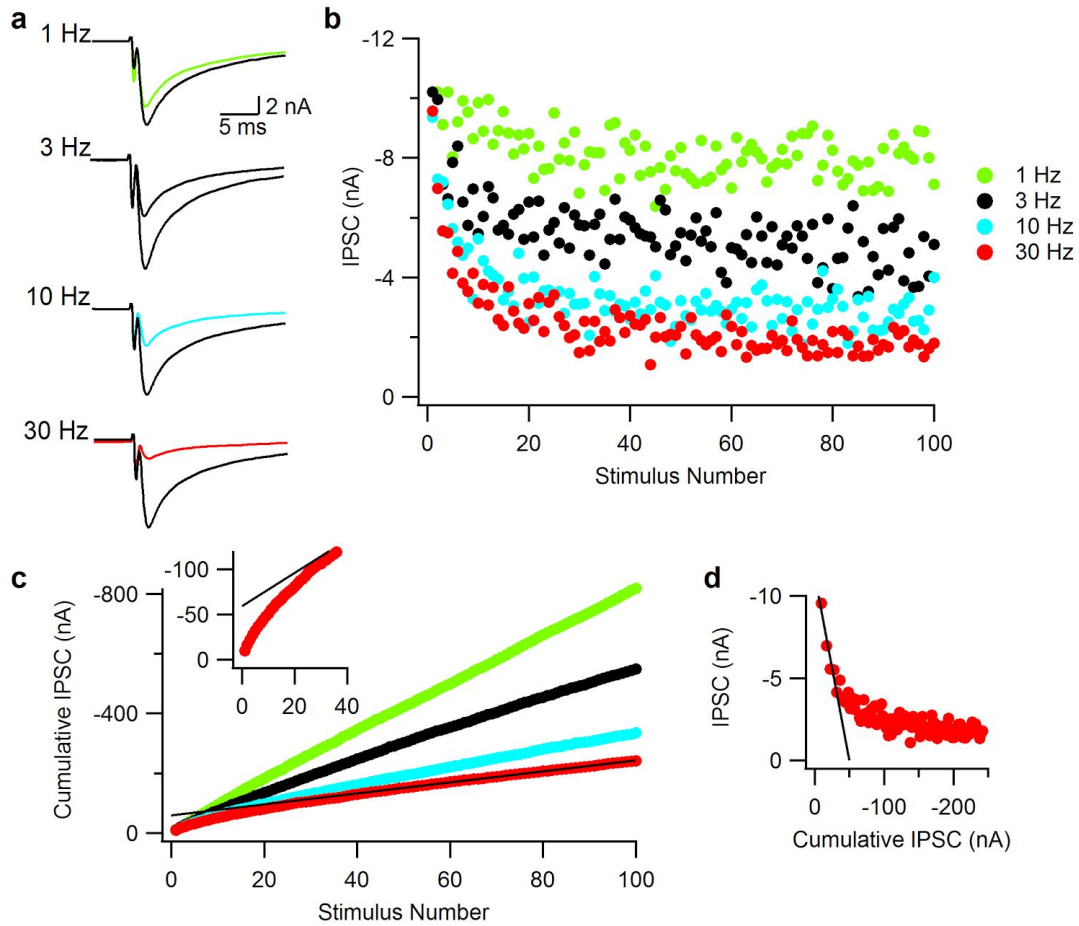


**Figure 23. The dependence of synaptic depression on stimulation**

**frequency and estimation of RRP sizes. a**, Exemplary IPSCs recorded before (black) and after a 100 action potential stimulation protocol at 1 (green), 3 (black), 10 (blue), or 30 (red) Hz. **b**, Plot of IPSC amplitude at 1 (green), 3 (black), 10 (blue), or 30 (red) Hz versus stimulus number. Note the increased synaptic depression with faster stimulation frequencies. **c**, Plot of cumulative IPSC amplitude versus stimulus number for various stimulation frequencies. The last 40 IPSCs are fit with a line that is back-extrapolated to the y-intercept (upper inset). **d**, Plot of IPSC amplitude versus cumulative IPSC amplitude for 30 Hz stimulation. The first 4 IPSCs are fit with a line that is extrapolated to the x-intercept.

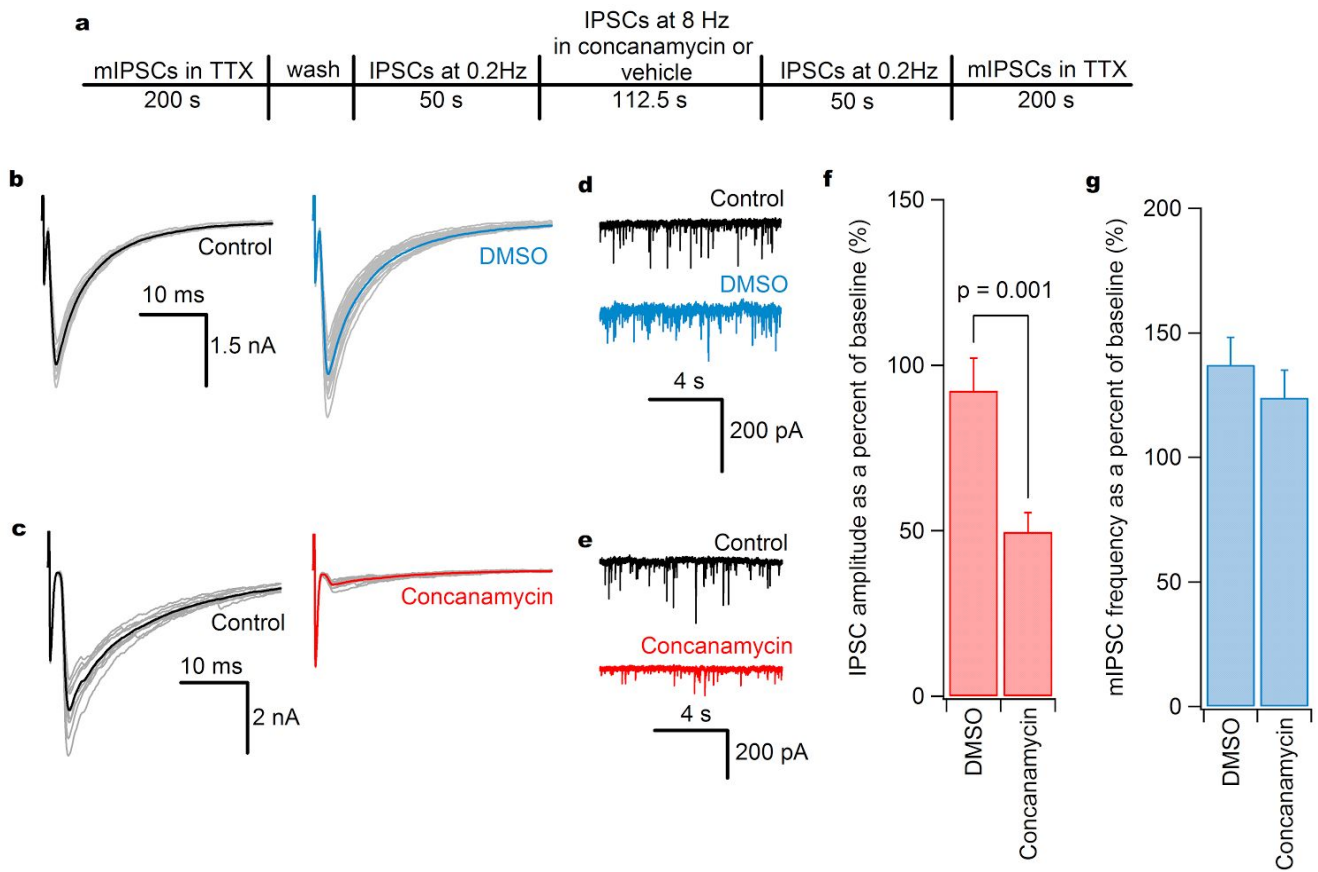


### Figure 24. Selective depletion of the evoked recycling pool by inhibiting

**vesicle refilling.** **a**, Schematic representation of experiment protocol. mIPSCs were recorded in 1  $\mu$ M TTX. TTX was washed out and IPSCs were evoked by stimulating at 0.2 Hz, a frequency that would not result in synaptic depression. IPSCs were then stimulated at 8 Hz in either concanamycin A or the same vehicle control from Figure 6. 8 Hz stimulation frequency was used because it minimized synaptic depression but allowed for quick mobilization of the entire evoked recycling pool (Xue et al. 2013). This minimized the amount of time the spontaneous recycling pool would be exposed to either condition. Following the stimulation protocol, IPSCs and mIPSCs were measured again. **b**, Exemplary traces of IPSCs (gray) measured before the stimulation protocol (left) or after the stimulation protocol in DMSO vehicle control (right). Average traces

are overlaid for before the protocol (control, black) and after stimulation in DMSO (blue). **c**, Exemplary traces of IPSCs (gray) measured before the stimulation protocol (left) or after the stimulation protocol in concanamycin A (right). Average traces are overlaid for before the protocol (control, black) and after stimulation in concanamycin A (red). **d**, Exemplary traces of mIPSCs measured before the stimulation protocol (black) or after the stimulation protocol in DMSO vehicle control (blue). **e**, Exemplary traces of mIPSCs measured before the stimulation protocol (black) or after the stimulation protocol in concanamycin A (red). **f**, Bar graph of average IPSC amplitude as a percent of baseline following the stimulation protocol in either DMSO or concanamycin A (n = 14 in concanamycin and 11 in DMSO treated). **g**, Bar graph of average mIPSC frequency as a percent of baseline following the stimulation protocol in either DMSO or concanamycin A from the same experiments as **f**.

## SUMMARY & CONCLUSIONS

---

Our work on spontaneous and evoked neurotransmission at murine neocortical synapses agrees with the growing consensus: that release of neurotransmitter may convey different messages to a postsynaptic neuron, depending on whether it is released spontaneously or in an activity-dependent manner. This divergence in postsynaptic signaling is facilitated by segregation of the presynaptic vesicle pools that mediate spontaneous and evoked release. Additionally, these processes may be managed independently by presynaptic regulatory mechanisms, in particular those involving VACCs. Signaling through parallel pathways that are kinetically distinct and independently regulated may enable the neurotrophic, homeostatic, and alternative functions of spontaneously released neurotransmitters to be isolated from their essential role in precise, action potential-driven information transfer. Future experiments are needed to fully characterize the molecular mechanisms that underlie spontaneous release events and allow selective manipulation of spontaneous release. Direct targeting of spontaneous neurotransmission will provide new insights into its function and address whether spontaneous release events can signal autonomously in the presence of activity. This information will be essential to understanding the synaptic processes that are affected by neuropsychiatric and neurological disorders that involve spontaneous neurotransmission in addition to those occurring under normal physiological conditions.

## **Functional significance of tight VACC coupling and cooperativity for spontaneous release**

This work shows that multiple VACCs of different subtypes cooperate to generate a nanodomain of  $\text{Ca}^{2+}$  that triggers spontaneous release at inhibitory terminals.

Nanodomain coupling between VACCs and release machinery offers several functional advantages (Eggermann et al. 2011). Tight coupling is suggested to increase the speed and temporal precision of synaptic transmission—as the duration of the  $\text{Ca}^{2+}$  transient detected by the  $\text{Ca}^{2+}$  sensor may be shorter in a nanodomain than in a microdomain coupling arrangement (Meinrenken et al. 2002; Bucurenciu et al. 2008; Eggermann et al. 2011). Another advantage of nanodomain coupling is that it increases synaptic efficacy and reduces the potential for ectopic release (Matsui & Jahr 2004). Tight coupling of a small number of VACCs is also energetically favorable because it reduces the total  $\text{Ca}^{2+}$  influx into presynaptic terminals (Eggermann et al. 2011).  $\text{Ca}^{2+}$  extrusion from the presynaptic terminal involves either  $\text{Na}^+/\text{Ca}^{2+}$  exchangers or  $\text{Ca}^{2+}$ -ATPase, both of which require the hydrolysis of ATP (Kim et al. 2005). Therefore, a nanodomain coupling configuration in which a small number of VACCs are tightly coupled to presynaptic  $\text{Ca}^{2+}$  sensors reduces the metabolic cost of synaptic transmission.

If coupling is tight, only a small number of  $\text{Ca}^{2+}$  channels may be needed to reach the effective  $[\text{Ca}^{2+}]$  threshold at the sensor. This should be even more pronounced for spontaneous release because the  $\text{Ca}^{2+}$  dependence is lower than

for evoked release, which requires 4-5  $\text{Ca}^{2+}$  ions to bind to the  $\text{Ca}^{2+}$ -sensor to trigger vesicle fusion (Williams et al. 2012; Vyleta & Smith 2011; Groffen et al. 2010; Dodge & Rahamimoff 1967). In Chapter 1, the number of VACCs involved in spontaneous release of GABA was estimated using a classical approach based on the relationship between presynaptic  $\text{Ca}^{2+}$  influx and neurotransmitter release during an experimental reduction in the number of open VACCs. Such a reduction of VACC number is achieved by application of peptide toxins, which are slow  $\text{Ca}^{2+}$  channel blockers (Eggermann et al. 2011; Mintz et al. 1995). This approach has been applied to evoked release at various other central synapses, including the calyx of Held and hippocampal basket cells (Fedchyshyn & Wang 2005; Wang et al. 2008; Wu et al. 1999; Bucurenciu et al. 2010). Yet this is the only study to date that has shown the relationship between spontaneous transmitter release and presynaptic  $\text{Ca}^{2+}$  currents during slow VACC block to be supralinear, suggesting the involvement of multiple VACCs (Goswami et al. 2012; Williams et al. 2012; Ermolyuk et al. 2013). If more than one VACC is required to trigger spontaneous fusion then what does this mean for the cell? An important physiological consequence of this would be a reduction in the basal rate of spontaneous GABA release due to stochastic channel openings and therefore an increase in the signal-to-noise ratio at the synapse.

The tight coupling for spontaneous release of GABA observed here is likely maintained by interactions between active zone proteins. Several candidate proteins include members of the SNARE, RIM, and ELKS families (Müller et al.



2010). Indeed, studies have indicated that t-SNARE proteins, syntaxin and SNAP25, directly interact with voltage-gated  $\text{Ca}^{2+}$  channels (Sheng et al. 1997; Bezprozvanny et al. 1995; Rettig et al. 1996; Zhong et al. 1999; Atlas 2001). Synaptotagmin, the  $\text{Ca}^{2+}$  sensor that triggers exocytosis, also interacts with the synaptic protein interaction site of VACCs in a  $\text{Ca}^{2+}$ -dependent manner (Sheng et al. 1997; Bezprozvanny et al. 1995; Rettig et al. 1996; Zhong et al. 1999). These interactions between  $\text{Ca}^{2+}$  channels and vesicle release machinery link the individual molecular elements within the nanodomain. VACCs that remain unbound or decoupled from the  $\text{Ca}^{2+}$  sensors are less likely to contribute to exocytosis (Eggermann et al. 2011). Additionally, co-expression of t-SNARES with VACCs reduces the channel open probability, whereas additional co-expression of synaptotagmin reverses this effect, indicating that these interactions between VACCs and SNARE proteins also alter VACC function (Zhong et al. 1999).

Neurexins also appear to be involved in the regulation of coupling between channels and  $\text{Ca}^{2+}$  sensors (Missler et al. 2003). Neurexins are polymorphic cell surface proteins that interact with neuroligins on the postsynaptic membrane and with both ELKS and synaptotagmin within the presynaptic terminal (Missler et al. 2003; Boucard et al. 2005). Deletion of neurexin reduces evoked transmitter release and the contribution of N-type VACCs to release, consistent with a role for neurexins in the regulation of  $\text{Ca}^{2+}$  channel–sensor coupling (Missler et al. 2003).

In addition, neurexin–neuroligin interactions may potentially explain the target cell specificity of coupling (Rozov et al. 2001)

Recent results suggest that RIMs have a organizational role in channel-sensor coupling (Han et al. 2011; Hibino et al. 2002). RIMs are multidomain proteins that interact with the C termini of P/Q- and N-type VACCs and other RIM-binding proteins (RIM-BPs) (Hibino et al. 2002). In inhibitory hippocampal synapses in culture, double knockout of RIM1 and RIM2, reduces the  $[Ca^{2+}]_o$  dependence of release attenuates the amplitude of evoked postsynaptic currents, suggesting that the coupling between VACCs and release machinery is disrupted (Kaesler et al. 2011). Similarly, in the calyx of Held, genetic deletion of RIM1 and RIM2 reduces both the presynaptic VACC density and the amplitude of the  $Ca^{2+}$  transient sensed by the release machinery (Han et al. 2011). Taken together, these results indicate that RIMs are crucial to the regulation of the coupling between  $Ca^{2+}$  channels and  $Ca^{2+}$  sensors of exocytosis at both excitatory and inhibitory central synapses.

Intriguingly, the tightness of the coupling not only depends on various release machinery proteins but may also depend on the subtype of VACC expressed at the synapse. In basket cell synapses of the hippocampus and cerebellum, as well as in the adult calyx of Held, tight coupling is associated with synapses that express predominantly P/Q- or L-type VACCs (Hefft & Jonas 2005; Bucurenciu et al. 2010; Iwasaki & Takahashi 1998; Forti et al. 2000; Stephens et al. 2001; Moser & Beutner 2000). Loose coupling is more often linked to the

involvement of N- or R-type VACCs in release (Hefft & Jonas 2005; Wu et al. 1999). However, the molecular mechanisms underlying this specificity remain unclear.

### **Differences in spontaneous release mechanisms at excitatory and inhibitory nerve terminals**

Chapter 2 confirms that neocortical excitatory synapses do not require  $\text{Ca}^{2+}$  entry via VACCs to trigger spontaneous release (Vyleta & Smith 2011). The basal spontaneous release rate was unaffected by block of VACCs with either the non-specific blocker  $\text{Cd}^{2+}$  or the specific blocker MVIIC. It was previously observed that increasing  $[\text{Ca}^{2+}]_o$  did not affect  $[\text{Ca}^{2+}]_i$  at rest in the majority of the nerve terminals observed, and spontaneous glutamate release was unaffected by the fast acting  $\text{Ca}^{2+}$  chelator BAPTA (Vyleta & Smith 2011). Spontaneous release at other excitatory synapses onto hippocampal and cerebellar neurons is also unaffected by blockade of VACCs (Abenavoli et al. 2002; Yamasaki et al. 2006). Together these results indicate that VACCs are not a source for  $\text{Ca}^{2+}$  in spontaneous glutamate release at these synapses. In contrast, at inhibitory synapses VACC blockers reduce spontaneous release of GABA in the hippocampus and neocortex (Eggermann et al. 2011; Xiao et al. 2006; Williams et al. 2012). Additionally, both the basal spontaneous release rate and the increase in  $[\text{Ca}^{2+}]_o$  were attenuated by intracellular  $\text{Ca}^{2+}$  chelators (Williams et al. 2012; Goswami et al. 2012). The differences in regulation between excitatory and inhibitory synapses in the cortex points to an unappreciated degree of

heterogeneity in regulation of the spontaneous pathway. Possible mechanisms underlying this heterogeneity include differences in the resting membrane potential, number or type of VACCs, size of the  $\text{Ca}^{2+}$  domain for release, tightness of coupling between VACCs and vesicles, concentrations and potency of intracellular  $\text{Ca}^{2+}$  buffers, or the proteins that comprise the release machinery. Striking contrasts in membrane structure between excitatory and inhibitory contacts have been observed, and it is presumed that these differences reflect alternative compositions and organization of functional synaptic proteins (Landis & Reese 1974).

In other parts of the nervous system, however, this contrast in the need for VACCs in spontaneous neurotransmission is not observed (for summary see Table 1). For example, cells that have ribbon synapses, including hair cells and retinal bipolar cells, release glutamate in the absence of action potentials and hence can be considered to employ spontaneous forms of release (Li et al. 2009; Jarsky et al. 2010; Bartoletti et al. 2011). At these synapses, very low-voltage-activated VACCs trigger glutamate release (Parsons et al. 1994). Even modest depolarization can trigger release at these synapses due to the left-shifted activation curve for these L-type VACC (Graydon et al. 2011; Trapani & Nicolson 2011; Helton et al. 2005). Conversely at other synapses, spontaneous release is dependent on  $\text{Ca}^{2+}$  release from intracellular stores and independent of VACC activity (Yamasaki et al. 2006; Llano et al. 2000; Vyleta & Smith 2008). This uniqueness in regulatory mechanisms for the  $\text{Ca}^{2+}$  dependence of spontaneous

release is paradoxical because evoked release mechanisms appear to be largely homogenous throughout the nervous system. They do, however, provide for independent regulation of spontaneous and evoked release at individual synapses.

### **Consequences of segregation of vesicle pools for spontaneous and evoked release**

In activity evoked release, presynaptic action potentials and electrical stimulation trigger synaptic vesicles exocytose, releasing neurotransmitters that induce large, synchronous currents in the postsynaptic cell (Kaesler & Regehr 2014). In contrast, small, miniature postsynaptic events are independent of action potential stimulation and occur when single synaptic vesicles fuse with the presynaptic membrane (Kavalali et al. 2011; Kaesler & Regehr 2014; Fatt & Katz 1952). These miniature events exhibit a seemingly random temporal pattern, and therefore have been referred to as spontaneous events despite their sensitivity to presynaptic calcium signaling (Glitsch 2008). Early work using the neuromuscular junction preparation disagreed on whether spontaneous and evoked vesicles resided at the same release sites, however, it is now clear that some synapses favor one form of release over the other, while many boutons produce both types of release (Colméus et al. 1982; Cherki-Vakil et al. 1995; Zefirov et al. 1995; Van der Kloot 1996; Macleod et al. 1999; Atasoy et al. 2008; Melom et al. 2013; Peled et al. 2014; Leitz & Kavalali 2014).

The ability to alter each form of fusion independently suggests that the vesicle pools are molecularly distinguishable (Kavalali 2015; Ramirez & Kavalali 2011). Vesicles released spontaneously can be modulated independently from those that are released in response to stimulation in several preparations (Sakaba 2006; Atasoy et al. 2008; Otsu & Murphy 2004; Otsu et al. 2004). For example, evoked neurotransmission recovers more easily than spontaneous neurotransmission in *Drosophila shibire* mutants, which undergo temperature-sensitive inhibition of neurotransmitter release (Koenig & Ikeda 1999). The GABA<sub>B</sub> receptor agonist baclofen inhibits evoked excitatory, spontaneous excitatory, and evoked inhibitory events but not spontaneous inhibitory events in hippocampal slice cultures and cerebellar slices (Scanziani et al. 1992; Dittman & Regehr 1996). Additionally Cd<sup>2+</sup>, a VACC blocker, inhibits evoked but not spontaneous neurotransmission in some preparations, suggesting that spontaneous and evoked events are differentially dependent upon Ca<sup>2+</sup> influx (Scanziani et al. 1992). Application of nitrosonium donors to cultured hippocampal neurons simultaneously inhibits evoked excitatory neurotransmission while enhancing spontaneous excitatory neurotransmission (Pan et al. 1996). Similarly a recent study in rat hindbrain slices demonstrated that cannabinoid receptor 1 activation selectively inhibits evoked but not spontaneous neurotransmission while TRPV1 receptor activation inhibits evoked neurotransmission and facilitates spontaneous neurotransmission (Shoudai et al. 2010; Fawley et al. 2014). These studies make it clear that spontaneous and

evoked neurotransmission are functionally separable under particular experimental contexts.

The differential modulation of these forms of vesicle release suggests that they originate from distinct vesicle pools. Investigators have tagged spontaneously recycled and stimulation-evoked vesicles independently with fluorescent probes or dyes and shown that the release properties of these tagged vesicles are substantially different, although other studies have detected complete overlap between the pools (Sara et al. 2005; Mathew et al. 2008; Fredj & Burrone 2009; Sara et al. 2011; Prange & Murphy 1999; Groemer & Klingauf 2007; Hua et al. 2010; Wilhelm et al. 2010). Blocking excitatory postsynaptic receptors activated by evoked neurotransmission does not inhibit receptors activated by spontaneous events and *vice versa*, suggesting that vesicles from different pools fuse to the plasma membrane at distinct locations, allowing their neurotransmitter molecules to bind separate postsynaptic receptors (Atasoy et al. 2008). To determine whether these vesicle pools are truly distinct, it has become necessary to molecularly dissect vesicle trafficking pathways. Proteins involved in endocytosis likely contribute to this vesicle sorting, and vesicle biogenesis mechanisms (Voglmaier & Edwards 2007; Chandrasekar et al. 2013; Evstratova et al. 2014; Kokotos & Cousin 2015; Rizzoli 2014; Morgan et al. 2013). Here the focus is on how vesicles are differentially trafficked to the plasma membrane for exocytosis.

The presence of molecularly and functionally distinct vesicle pools suggests that each form of neurotransmission has differential downstream effects on neuronal function. Information transfer throughout the nervous system has been classically assumed to depend on synchronous evoked release, due to its temporal precision, while asynchronous evoked and spontaneous release have been thought to modulate the information carried by the synchronous evoked signal (Smith et al. 2012; Kaeser & Regehr 2014). A recent study, however, showed that reducing synchronous evoked release in hippocampus, entorhinal cortex, or prefrontal cortex by knocking down *syt1* had only subtle effects on fear conditioning memory tests in mice, suggesting that asynchronous release is sufficient to deliver the majority of the informational signal (Xu et al. 2012). Spontaneous neurotransmission, in turn, modulates action potential generation in postsynaptic neurons and homeostatically scales postsynaptic receptor levels, which is thought to occur via activation of postsynaptic signaling cascades that are distinct from those activated by evoked release (Otmakhov et al. 1993; Carter & Regehr 2002; Sharma & Vijayaraghavan 2003; Frank et al. 2006; Sutton et al. 2006; Kavalali et al. 2011; Smith et al. 2012; Kavalali 2015). Inhibiting spontaneous neurotransmission also appears to be the mechanism by which glutamate receptor blockers induce fast-acting antidepressant behaviors in rodents, suggesting that spontaneous neurotransmission indeed exerts potent effects on neurotransmission (Autry et al. 2011; Nosyreva et al. 2013; Gideons et al. 2014). Each form of neurotransmission, therefore, works to refine the signal



being propagated through the circuit. Because of these distinct contributions to neurotransmission, determining the molecular basis of different vesicle pools is important for understanding nervous system function.

### **Physiological and pathophysiological importance of spontaneous neurotransmission**

Spontaneous neurotransmission is pronounced at young synapses and is crucial for synaptic development (Mozhayeva et al. 2002; Andreae et al. 2012; Hsia et al. 1998). Experiments show that activity independent postsynaptic receptor activation is required to cause developmental structural plasticity (McKinney et al. 1999; McAllister et al. 1996). At the *Drosophila* neuromuscular junction, complexin-null mutants show a conspicuous increase in spontaneous transmission and synaptic contacts (Yang et al. 2013). Additionally, loss-of-function and gain-of-function manipulations that alter spontaneous release indicate that spontaneous release—but not evoked release—is required for the normal structural maturation of *Drosophila* glutamatergic synapses (Choi et al. 2014). Although these studies support a key role for spontaneous neurotransmission in guiding synapse maturation, further work is needed to determine what mechanisms underlie the role of spontaneous release events in these developmental processes.

Spontaneous neurotransmitter release is also important in homeostasis (Kavalali 2015; Sutton & Schuman 2006). Homeostatic synaptic plasticity at the *Drosophila melanogaster* neuromuscular junction requires spontaneous release

(Frank et al. 2006). Furthermore, excitatory spontaneous release events trigger  $\text{Ca}^{2+}$  influx through NMDA receptors and thereby activate signaling cascades that suppress dendritic protein synthesis and stabilize synaptic function in cultured hippocampal neurons (Sutton et al. 2006; Sutton et al. 2007). One study suggested that this mechanism mediates the rapid antidepressant action of the NMDA receptor blocker ketamine (Autry et al. 2011), raising the possibility that manipulation of spontaneous neurotransmission may be used in the treatment of psychiatric disorders (Kavalali & Monteggia 2012). These results remain controversial, however, because ketamine metabolites have been shown to have similar actions that are independent of NMDA receptor activation (Zanos et al. 2016).

Spontaneous release may also play a part in mediating plasticity, especially under circumstances in which neuromodulators can augment the rate of spontaneous vesicle fusion (Hawkins 2013; Jin et al. 2012; Sharma & Vijayaraghavan 2003). Spontaneous neurotransmission may also have a permissive role in synaptic plasticity by increasing the sensitivity to activity-dependent signalling (Hawkins 2013). Unconventional ways in which spontaneous release may contribute to neuronal excitability have also been uncovered, including a new class of small mEPSCs—termed 'preminis'—that arise from retrograde signaling following spontaneous vesicle fusion (Trigo et al. 2010). The functional importance of preminis remains unclear, however, they

demonstrate that spontaneous neurotransmitter release can influence the presynaptic neuron in addition to its classical postsynaptic targets.

Despite the importance of spontaneous signaling in neuronal survival and structural stability of synaptic connections, an over-abundance of spontaneous release of excitatory neurotransmitters can lead to neuronal damage (Verhage et al. 2000). Excitotoxic neuronal death induced by excessive synaptic glutamate is implicated in the pathology of neurodegenerative diseases such as Alzheimer's and Huntington's diseases along with ischemia and epilepsy (Nishizawa 2001; Lo et al. 2003; Hynd et al. 2004; Andjus et al. 1997). Spontaneous GABA release may also be culpable in the pathophysiology of amyotrophic lateral sclerosis and epilepsy (Cossart et al. 2001; Hirsch et al. 1999). Furthermore, at synapses where spontaneous and evoked vesicle pools are shared, excess spontaneous release may cause presynaptic vesicle depletion and impair synaptic function. Thus, regulatory mechanisms are imperative as excess or reduced spontaneous neurotransmitter release may lead to adverse consequences.

## **Conclusions**

It is well established that action potential-evoked neurotransmitter release is highly dependent on  $[Ca^{2+}]_o$ . This work demonstrates that, while spontaneous release of GABA has much weaker  $[Ca^{2+}]_o$  dependence, VACCs are the main trigger. Strikingly, multiple, tightly-coupled VACCs of different subtypes cooperate to trigger spontaneous release of a single GABA-containing vesicle. This contrasts with the VACC independence of spontaneous glutamate release

and the loose vesicle-VACC coupling observed for evoked GABA release, despite being mediated by a similar population of VACC subtypes. Further, spontaneous release of GABA arises from an independent vesicle pool that can be manipulated without affecting evoked release. Knowledge of the mechanisms by which  $\text{Ca}^{2+}$  influences release of neurotransmitter will provide an improved understanding of synaptic function in general and contribute to a greater understanding of disrupted transmission in disease states.

## REFERENCES

---

- Abenavoli, A. et al., 2002. Multimodal quantal release at individual hippocampal synapses: evidence for no lateral inhibition. *The Journal of neuroscience: the official journal of the Society for Neuroscience*, 22(15), pp.6336–6346.
- Adelman, W.J., Jr & French, R.J., 1978. Blocking of the squid axon potassium channel by external caesium ions. *The Journal of physiology*, 276, pp.13–25.
- Adler, E.M. et al., 1991. Alien intracellular calcium chelators attenuate neurotransmitter release at the squid giant synapse. *The Journal of neuroscience: the official journal of the Society for Neuroscience*, 11(6), pp.1496–1507.
- Ahmed, M.S. & Siegelbaum, S.A., 2009. Recruitment of N-Type  $\text{Ca}^{2+}$  channels during LTP enhances low release efficacy of hippocampal CA1 perforant

path synapses. *Neuron*, 63(3), pp.372–385.

Andjus, P.R., Stevic-Marinkovic, Z. & Cherubini, E., 1997. Immunoglobulins from motoneurone disease patients enhance glutamate release from rat hippocampal neurones in culture. *The Journal of physiology*, 504 ( Pt 1), pp.103–112.

Andreae, L.C., Fredj, N.B. & Burrone, J., 2012. Independent vesicle pools underlie different modes of release during neuronal development. *The Journal of neuroscience: the official journal of the Society for Neuroscience*, 32(5), pp.1867–1874.

Angleson, J.K. & Betz, W.J., 2001. Intraterminal Ca(2+) and spontaneous transmitter release at the frog neuromuscular junction. *Journal of neurophysiology*, 85(1), pp.287–294.

Atasoy, D. et al., 2008. Spontaneous and evoked glutamate release activates two populations of NMDA receptors with limited overlap. *The Journal of neuroscience: the official journal of the Society for Neuroscience*, 28(40), pp.10151–10166.

Atlas, D., 2001. Functional and physical coupling of voltage-sensitive calcium channels with exocytotic proteins: ramifications for the secretion mechanism. *Journal of neurochemistry*. Available at:  
<http://onlinelibrary.wiley.com/doi/10.1046/j.1471-4159.2001.00347.x/full>.

- Augustine, G.J. & Charlton, M.P., 1986. Calcium dependence of presynaptic calcium current and post-synaptic response at the squid giant synapse. *The Journal of physiology*, 381(1), pp.619–640.
- Autry, A.E. et al., 2011. NMDA receptor blockade at rest triggers rapid behavioural antidepressant responses. *Nature*, 475(7354), pp.91–95.
- Awatramani, G.B., Price, G.D. & Trussell, L.O., 2005. Modulation of transmitter release by presynaptic resting potential and background calcium levels. *Neuron*, 48(1), pp.109–121.
- Bal, M. et al., 2013. Reelin mobilizes a VAMP7-dependent synaptic vesicle pool and selectively augments spontaneous neurotransmission. *Neuron*, 80(4), pp.934–946.
- Bao, J., Li, J.J. & Perl, E.R., 1998. Differences in Ca<sup>2+</sup> channels governing generation of miniature and evoked excitatory synaptic currents in spinal laminae I and II. *The Journal of neuroscience: the official journal of the Society for Neuroscience*, 18(21), pp.8740–8750.
- Bartoletti, T.M. et al., 2011. Release from the cone ribbon synapse under bright light conditions can be controlled by the opening of only a few Ca<sup>2+</sup> channels. *Journal of neurophysiology*, 106(6), pp.2922–2935.
- Bezprozvanny, I., Scheller, R.H. & Tsien, R.W., 1995. Functional impact of syntaxin on gating of N-type and Q-type calcium channels. *Nature*,

378(6557), pp.623–626.

Boland, L.M., Morrill, J.A. & Bean, B.P., 1994. omega-Conotoxin block of N-type calcium channels in frog and rat sympathetic neurons. *The Journal of neuroscience: the official journal of the Society for Neuroscience*, 14(8), pp.5011–5027.

Borst, J.G.G. & Sakmann, B., 1996. Calcium influx and transmitter release in a fast CNS synapse. *Nature*, 383(6599), pp.431–434.

Boucard, A.A. et al., 2005. A splice code for trans-synaptic cell adhesion mediated by binding of neuroligin 1 to alpha- and beta-neurexins. *Neuron*, 48(2), pp.229–236.

Boyd, I.A. & Martin, A.R., 1956. Spontaneous subthreshold activity at mammalian neuromuscular junctions. *The Journal of physiology*, 132(1), pp.61–73.

Broadie, K. et al., 1995. Syntaxin and synaptobrevin function downstream of vesicle docking in *Drosophila*. *Neuron*, 15(3), pp.663–673.

Brose, N., 2008. Altered complexin expression in psychiatric and neurological disorders: cause or consequence? *Molecules and cells*, 25(1), pp.7–19.

Brown, E.M. et al., 1993. Cloning and characterization of an extracellular Ca<sup>2+</sup>-sensing receptor from bovine parathyroid. *Nature*, 366(6455), pp.575–580.

Bucurenciu, I. et al., 2008. Nanodomain Coupling between Ca<sup>2+</sup> Channels and

Ca<sup>2+</sup> Sensors Promotes Fast and Efficient Transmitter Release at a Cortical GABAergic Synapse. *Neuron*, 57(4), pp.536–545.

Bucurenciu, I., Bischofberger, J. & Jonas, P., 2010. A small number of open Ca<sup>2+</sup> channels trigger transmitter release at a central GABAergic synapse. *Nature neuroscience*, 13(1), pp.19–21.

Cao, Y.-Q. & Tsien, R.W., 2005. Effects of familial hemiplegic migraine type 1 mutations on neuronal P/Q-type Ca<sup>2+</sup> channel activity and inhibitory synaptic transmission. *Proceedings of the National Academy of Sciences of the United States of America*, 102(7), pp.2590–2595.

Caro, A. et al., 2011. Nimodipine inhibits AP firing in cultured hippocampal neurons predominantly due to block of voltage-dependent potassium channels. *General physiology and biophysics*, 30 Spec No, pp.S44–53.

Carter, A.G. & Regehr, W.G., 2002. Quantal events shape cerebellar interneuron firing. *Nature neuroscience*, 5(12), pp.1309–1318.

del Castillo, J. & Katz, B., 1954. Quantal components of the end-plate potential. *The Journal of physiology*, 124(3), pp.560–573.

Castillo, P.E., Weisskopf, M.G. & Nicoll, R.A., 1994. The role of Ca<sup>2+</sup> channels in hippocampal mossy fiber synaptic transmission and long-term potentiation. *Neuron*, 12(2), pp.261–269.



- Chandrasekar, I. et al., 2013. Myosin II regulates activity dependent compensatory endocytosis at central synapses. *The Journal of neuroscience: the official journal of the Society for Neuroscience*, 33(41), pp.16131–16145.
- Chen, W. et al., 2010. Presynaptic External Calcium Signaling Involves the Calcium-Sensing Receptor in Neocortical Nerve Terminals. *PloS one*, 5(1), p.e8563.
- Cherki-Vakil, R., Ginsburg, S. & Meiri, H., 1995. The difference in shape of spontaneous and uniquantal evoked synaptic potentials in frog muscle. *The Journal of physiology*, 482 ( Pt 3), pp.641–650.
- Choi, B.J. et al., 2014. Miniature neurotransmission regulates Drosophila synaptic structural maturation. *Neuron*, 82(3), pp.618–634.
- Cho, S. & von Gersdorff, H., 2014. Proton-mediated block of Ca<sup>2+</sup> channels during multivesicular release regulates short-term plasticity at an auditory hair cell synapse. *The Journal of neuroscience: the official journal of the Society for Neuroscience*, 34(48), pp.15877–15887.
- Chow, R.H., 1991. Cadmium block of squid calcium currents. Macroscopic data and a kinetic model. *The Journal of general physiology*, 98(4), pp.751–770.
- Christie, J.M., Chiu, D.N. & Jahr, C.E., 2010. Ca<sup>2+</sup> -dependent enhancement of release by subthreshold somatic depolarization. *Nature neuroscience*, 14(1),

pp.62–68.

- Chung, C. et al., 2010. Acute Dynamin Inhibition Dissects Synaptic Vesicle Recycling Pathways That Drive Spontaneous and Evoked Neurotransmission. *Journal of Neuroscience*, 30(4), pp.1363–1376.
- Cohen, I. & Miles, R., 2000. Contributions of intrinsic and synaptic activities to the generation of neuronal discharges in in vitro hippocampus. *The Journal of physiology*, 524 Pt 2, pp.485–502.
- Colméus, C. et al., 1982. Discrepancies between spontaneous and evoked synaptic potentials at normal, regenerating and botulinum toxin poisoned mammalian neuromuscular junctions. *Proceedings of the Royal Society of London. Series B, Containing papers of a Biological character. Royal Society* , 215(1198), pp.63–74.
- Cossart, R. et al., 2001. Dendritic but not somatic GABAergic inhibition is decreased in experimental epilepsy. *Nature neuroscience*, 4(1), pp.52–62.
- Crawford, D.C. & Kavalali, E.T., 2015. Molecular underpinnings of synaptic vesicle pool heterogeneity. *Traffic* , 16(4), pp.338–364.
- Crouzy, S., Bernèche, S. & Roux, B., 2001. Extracellular Blockade of K<sup>+</sup> Channels by Tea. *The Journal of general physiology*, 118(2), pp.207–218.
- Dai, J. et al., 2015. Spontaneous Vesicle Release Is Not Tightly Coupled to

Voltage-Gated Calcium Channel-Mediated Ca<sup>2</sup> Influx and Is Triggered by a Ca<sup>2</sup> Sensor Other Than Synaptotagmin-2 at the Juvenile Mice Calyx of Held Synapses. *Journal of Neuroscience*, 35(26), pp.9632–9637.

Deak, F. et al., 2006. Structural Determinants of Synaptobrevin 2 Function in Synaptic Vesicle Fusion. *Journal of Neuroscience*, 26(25), pp.6668–6676.

Deák, F. et al., 2004. Synaptobrevin is essential for fast synaptic-vesicle endocytosis. *Nature cell biology*, 6(11), pp.1102–1108.

Deitcher, D.L. et al., 1998. Distinct requirements for evoked and spontaneous release of neurotransmitter are revealed by mutations in the *Drosophila* gene neuronal-synaptobrevin. *The Journal of neuroscience: the official journal of the Society for Neuroscience*, 18(6), pp.2028–2039.

Denker, A. & Rizzoli, S.O., 2010. Synaptic vesicle pools: an update. *Frontiers in synaptic neuroscience*, 2, p.135.

Dittman, J.S. & Regehr, W.G., 1996. Contributions of calcium-dependent and calcium-independent mechanisms to presynaptic inhibition at a cerebellar synapse. *The Journal of neuroscience: the official journal of the Society for Neuroscience*, 16(5), pp.1623–1633.

Dodge, F.A. & Rahamimoff, R., 1967. Co-operative action of calcium ions in transmitter release at the neuromuscular junction. *The Journal of physiology*,

193(2), pp.419–432.

Dolmetsch, R.E. et al., 2001. Signaling to the nucleus by an L-type calcium channel-calmodulin complex through the MAP kinase pathway. *Science*, 294(5541), pp.333–339.

Druzin, M. et al., 2002. Dual and opposing roles of presynaptic Ca<sup>2+</sup> influx for spontaneous GABA release from rat medial preoptic nerve terminals. *The Journal of physiology*, 542(Pt 1), pp.131–146.

Eggermann, E. et al., 2011. Nanodomain coupling between Ca<sup>2+</sup> channels and sensors of exocytosis at fast mammalian synapses. *Nature reviews. Neuroscience*, 13(1), pp.7–21.

Emptage, N.J., Reid, C.A. & Alan, F., 2001. Calcium Stores in Hippocampal Synaptic Boutons Mediate Short-Term Plasticity, Store-Operated Ca<sup>2+</sup> Entry, and Spontaneous Transmitter Release. *Neuron*, 29(1), pp.197–208.

Ermolyuk, Y.S. et al., 2013. Differential triggering of spontaneous glutamate release by P/Q-, N- and R-type Ca<sup>2+</sup> channels. *Nature neuroscience*, 16(12), pp.1754–1763.

Ertunc, M. et al., 2007. Fast Synaptic Vesicle Reuse Slows the Rate of Synaptic Depression in the CA1 Region of Hippocampus. *Journal of Neuroscience*, 27(2), pp.341–354.

Espinosa, F. & Kavalali, E.T., 2009. NMDA receptor activation by spontaneous glutamatergic neurotransmission. *Journal of neurophysiology*, 101(5), pp.2290–2296.

Evstratova, A. et al., 2014. Vesicles derived via AP-3-dependent recycling contribute to asynchronous release and influence information transfer. *Nature communications*, 5, p.5530.

Fatt, P. & Katz, B., 1952. Spontaneous subthreshold activity at motor nerve endings. *The Journal of physiology*, 117(1), pp.109–128.

Fatt, P., P., F. & B., K., 1950. Some Observations on Biological Noise. *Nature*, 166(4223), pp.597–598.

Fawley, J.A., Hofmann, M.E. & Andresen, M.C., 2014. Cannabinoid 1 and transient receptor potential vanilloid 1 receptors discretely modulate evoked glutamate separately from spontaneous glutamate transmission. *The Journal of neuroscience: the official journal of the Society for Neuroscience*, 34(24), pp.8324–8332.

Fedchyshyn, M.J. & Wang, L.-Y., 2005. Developmental transformation of the release modality at the calyx of Held synapse. *The Journal of neuroscience: the official journal of the Society for Neuroscience*, 25(16), pp.4131–4140.

Fernández-Chacón, R. et al., 2001. Synaptotagmin I functions as a calcium

regulator of release probability. *Nature*, 410(6824), pp.41–49.

Forsythe, I.D., 1994. Direct patch recording from identified presynaptic terminals mediating glutamatergic EPSCs in the rat CNS, in vitro. *The Journal of physiology*, 479 ( Pt 3), pp.381–387.

Forti, L., Pouzat, C. & Llano, I., 2000. Action potential-evoked Ca<sup>2+</sup> signals and calcium channels in axons of developing rat cerebellar interneurons. *The Journal of physiology*, 527 Pt 1, pp.33–48.

Frank, C.A. et al., 2006. Mechanisms underlying the rapid induction and sustained expression of synaptic homeostasis. *Neuron*, 52(4), pp.663–677.

Fredj, N.B. & Burrone, J., 2009. A resting pool of vesicles is responsible for spontaneous vesicle fusion at the synapse. *Nature neuroscience*, 12(6), pp.751–758.

Galli, C. et al., 1995. Apoptosis in cerebellar granule cells is blocked by high KCl, forskolin, and IGF-1 through distinct mechanisms of action: the involvement of intracellular calcium and .... *The Journal of*. Available at: <http://www.jneurosci.org/content/15/2/1172.short>.

Gideons, E.S., Kavalali, E.T. & Monteggia, L.M., 2014. Mechanisms underlying differential effectiveness of memantine and ketamine in rapid antidepressant responses. *Proceedings of the National Academy of Sciences of the United*

*States of America*, 111(23), pp.8649–8654.

Glitsch, M., 2006. Selective Inhibition of Spontaneous But Not Ca<sup>2+</sup>-Dependent Release Machinery by Presynaptic Group II mGluRs in Rat Cerebellar Slices. *Journal of neurophysiology*, 96(1), pp.86–96.

Glitsch, M.D., 2008. Spontaneous neurotransmitter release and Ca<sup>2+</sup>—How spontaneous is spontaneous neurotransmitter release? *Cell calcium*.

Available at:

<http://www.sciencedirect.com/science/article/pii/S0143416007000449>.

Goswami, S.P., Bucurenciu, I. & Jonas, P., 2012. Miniature IPSCs in Hippocampal Granule Cells Are Triggered by Voltage-Gated Ca<sup>2+</sup> Channels via Microdomain Coupling. *Journal of Neuroscience*, 32(41), pp.14294–14304.

Graydon, C.W. et al., 2011. Sharp Ca<sup>2+</sup> Nanodomains beneath the Ribbon Promote Highly Synchronous Multivesicular Release at Hair Cell Synapses. *The Journal of neuroscience: the official journal of the Society for Neuroscience*, 31(46), pp.16637–16650.

Groemer, T.W. & Klingauf, J., 2007. Synaptic vesicles recycling spontaneously and during activity belong to the same vesicle pool. *Nature neuroscience*, 10(2), pp.145–147.

Groffen, A.J. et al., 2010. Doc2b Is a High-Affinity Ca<sup>2+</sup> Sensor for Spontaneous

Neurotransmitter Release. *Science*, 327(5973), pp.1614–1618.

Han, Y. et al., 2011. RIM determines Ca<sup>2+</sup> channel density and vesicle docking at the presynaptic active zone. *Neuron*, 69(2), pp.304–316.

Hawkins, R.D., 2013. Possible contributions of a novel form of synaptic plasticity in *Aplysia* to reward, memory, and their dysfunctions in mammalian brain. *Learning & memory*, 20(10), pp.580–591.

Hefft, S. & Jonas, P., 2005. Asynchronous GABA release generates long-lasting inhibition at a hippocampal interneuron-principal neuron synapse. *Nature neuroscience*, 8(10), pp.1319–1328.

Hell, J.W. et al., 1993. Identification and differential subcellular localization of the neuronal class C and class D L-type calcium channel alpha 1 subunits. *The Journal of cell biology*, 123(4), pp.949–962.

Helton, T.D., Xu, W. & Lipscombe, D., 2005. Neuronal L-type calcium channels open quickly and are inhibited slowly. *The Journal of neuroscience: the official journal of the Society for Neuroscience*, 25(44), pp.10247–10251.

Herreros, J. et al., 1995. Tetanus toxin inhibits spontaneous quantal release and cleaves VAMP/synaptobrevin. *Brain research*, 699(2), pp.165–170.

Heuser, J.E., 1989. Review of electron microscopic evidence favouring vesicle exocytosis as the structural basis for quantal release during synaptic



transmission. *Quarterly journal of experimental physiology* , 74(7), pp.1051–1069.

Heuser, J.E. et al., 1979. Synaptic vesicle exocytosis captured by quick freezing and correlated with quantal transmitter release. *The Journal of cell biology*, 81(2), pp.275–300.

Heuser, J.E. & Reese, T.S., 1973. Evidence for recycling of synaptic vesicle membrane during transmitter release at the frog neuromuscular junction. *The Journal of cell biology*, 57(2), pp.315–344.

Hibino, H. et al., 2002. RIM binding proteins (RBPs) couple Rab3-interacting molecules (RIMs) to voltage-gated Ca(2+) channels. *Neuron*, 34(3), pp.411–423.

Hinkle, P.M., Shanshala, E.D., 2nd & Nelson, E.J., 1992. Measurement of intracellular cadmium with fluorescent dyes. Further evidence for the role of calcium channels in cadmium uptake. *The Journal of biological chemistry*, 267(35), pp.25553–25559.

Hirsch, J.C. et al., 1999. Deficit of quantal release of GABA in experimental models of temporal lobe epilepsy. *Nature neuroscience*, 2(6), pp.499–500.

Hofmann, M.E., Chinki, B. & Frazier, C.J., 2011. Cannabinoid receptor agonists potentiate action potential-independent release of GABA in the dentate gyrus through a CB1 receptor-independent mechanism. *The Journal of*

*physiology*, 589(15), pp.3801–3821.

Hsia, A.Y., Malenka, R.C. & Nicoll, R.A., 1998. Development of excitatory circuitry in the hippocampus. *Journal of neurophysiology*, 79(4), pp.2013–2024.

Hua, Y. et al., 2010. A common origin of synaptic vesicles undergoing evoked and spontaneous fusion. *Nature neuroscience*, 13(12), pp.1451–1453.

Hua, Z. et al., 2011. v-SNARE composition distinguishes synaptic vesicle pools. *Neuron*, 71(3), pp.474–487.

Hubbard, J.I., 1961. The effect of calcium and magnesium on the spontaneous release of transmitter from mammalian motor nerve endings. *The Journal of physiology*, 159(3), pp.507–517.

Hubbard, J.I., Jones, S.F. & Landau, E.M., 1968. On the mechanism by which calcium and magnesium affect the spontaneous release of transmitter from mammalian motor nerve terminals. *The Journal of physiology*, 194(2), pp.355–380.

Hughes, D. et al., 1987. Caesium ions activate chloride channels in rat cultured spinal cord neurones. *The Journal of physiology*, 392, pp.231–251.

Huntwork, S. & Littleton, J.T., 2007. A complexin fusion clamp regulates spontaneous neurotransmitter release and synaptic growth. *Nature*

*neuroscience*, 10(10), pp.1235–1237.

Hynd, M.R., Scott, H.L. & Dodd, P.R., 2004. Glutamate-mediated excitotoxicity and neurodegeneration in Alzheimer's disease. *Neurochemistry international*, 45(5), pp.583–595.

Iwasaki, S. & Takahashi, T., 1998. Developmental changes in calcium channel types mediating synaptic transmission in rat auditory brainstem. *The Journal of physiology*, 509 ( Pt 2), pp.419–423.

Jakawich, S.K. et al., 2010. Local presynaptic activity gates homeostatic changes in presynaptic function driven by dendritic BDNF synthesis. *Neuron*, 68(6), pp.1143–1158.

Jarsky, T., Tian, M. & Singer, J.H., 2010. Nanodomain control of exocytosis is responsible for the signaling capability of a retinal ribbon synapse. *The Journal of neuroscience: the official journal of the Society for Neuroscience*, 30(36), pp.11885–11895.

Jensen, K., Jensen, M.S. & Lambert, J.D., 1999. Post-tetanic potentiation of GABAergic IPSCs in cultured rat hippocampal neurones. *The Journal of physiology*, 519 Pt 1, pp.71–84.

Jin, I. et al., 2012. Spontaneous transmitter release recruits postsynaptic mechanisms of long-term and intermediate-term facilitation in Aplysia. *Proceedings of the National Academy of Sciences of the United States of*

*America*, 109(23), pp.9137–9142.

Jun, K. et al., 1999. Ablation of P/Q-type Ca<sup>2</sup> channel currents, altered synaptic transmission, and progressive ataxia in mice lacking the alpha 1A-subunit. *Proceedings of the National Academy of Sciences*, 96(26), pp.15245–15250.

Kaeser, P.S. et al., 2011. RIM proteins tether Ca<sup>2+</sup> channels to presynaptic active zones via a direct PDZ-domain interaction. *Cell*, 144(2), pp.282–295.

Kaeser, P.S. & Regehr, W.G., 2014. Molecular mechanisms for synchronous, asynchronous, and spontaneous neurotransmitter release. *Annual review of physiology*, 76, pp.333–363.

Katz, B. & Miledi, R., 1969. Spontaneous and evoked activity of motor nerve endings in calcium Ringer. *The Journal of physiology*, 203(3), pp.689–706.

Katz, B. & Miledi, R., 1968. The role of calcium in neuromuscular facilitation. *The Journal of physiology*, 195(2), pp.481–492.

Katz, B. & Miledi, R., 1967. The timing of calcium action during neuromuscular transmission. *The Journal of physiology*, 189(3), pp.535–544.

Kavalali, E.T. et al., 2011. Spontaneous neurotransmission: an independent pathway for neuronal signaling? *Physiology*, 26(1), pp.45–53.

Kavalali, E.T., 2015. The mechanisms and functions of spontaneous

neurotransmitter release. *Nature reviews. Neuroscience*, 16(1), pp.5–16.

Kavalali, E.T. & Monteggia, L.M., 2012. Synaptic mechanisms underlying rapid antidepressant action of ketamine. *The American journal of psychiatry*, 169(11), pp.1150–1156.

Khodakhah, K. & Ogden, D., 1993. Functional heterogeneity of calcium release by inositol trisphosphate in single Purkinje neurones, cultured cerebellar astrocytes, and peripheral tissues. *Proceedings of the National Academy of Sciences of the United States of America*, 90(11), pp.4976–4980.

Kim, M.-H. et al., 2005. Interplay between Na<sup>+</sup>/Ca<sup>2+</sup> exchangers and mitochondria in Ca<sup>2+</sup> clearance at the calyx of Held. *The Journal of neuroscience: the official journal of the Society for Neuroscience*, 25(26), pp.6057–6065.

Kimura, J. et al., 1999. Direction-independent block of bi-directional Na<sup>+</sup>/Ca<sup>2+</sup> exchange current by KB-R7943 in guinea-pig cardiac myocytes. *British journal of pharmacology*, 128(5), pp.969–974.

Koenig, J.H. & Ikeda, K., 1999. Contribution of active zone subpopulation of vesicles to evoked and spontaneous release. *Journal of neurophysiology*, 81(4), pp.1495–1505.

Kokotos, A.C. & Cousin, M.A., 2015. Synaptic vesicle generation from central

nerve terminal endosomes. *Traffic* , 16(3), pp.229–240.

Kombian, S.B. et al., 2000. Short-term potentiation of miniature excitatory synaptic currents causes excitation of supraoptic neurons. *Journal of neurophysiology*, 83(5), pp.2542–2553.

Koyama, S. et al., 1999. Presynaptic serotonergic inhibition of GABAergic synaptic transmission in mechanically dissociated rat basolateral amygdala neurons. *The Journal of physiology*, 518 ( Pt 2), pp.525–538.

Landis, D.M. & Reese, T.S., 1974. Differences in membrane structure between excitatory and inhibitory synapses in the cerebellar cortex. *The Journal of comparative neurology*, 155(1), pp.93–125.

Lee, M.-C., Yasuda, R. & Ehlers, M.D., 2010. Metaplasticity at single glutamatergic synapses. *Neuron*, 66(6), pp.859–870.

Leitz, J. & Kavalali, E.T., 2014. Fast retrieval and autonomous regulation of single spontaneously recycling synaptic vesicles. *eLife*, 3, p.e03658.

Li, G.-L. et al., 2009. The unitary event underlying multiquantal EPSCs at a hair cell's ribbon synapse. *The Journal of neuroscience: the official journal of the Society for Neuroscience*, 29(23), pp.7558–7568.

Lipscombe, D., Helton, T.D. & Xu, W., 2004. L-type calcium channels: the low down. *Journal of neurophysiology*, 92(5), pp.2633–2641.

- Liu, H. et al., 2009. Autapses and networks of hippocampal neurons exhibit distinct synaptic transmission phenotypes in the absence of synaptotagmin I. *The Journal of neuroscience: the official journal of the Society for Neuroscience*, 29(23), pp.7395–7403.
- Llano, I. et al., 2000. Presynaptic calcium stores underlie large-amplitude miniature IPSCs and spontaneous calcium transients. *Nature neuroscience*, 3(12), pp.1256–1265.
- Llano, I. & Gerschenfeld, H.M., 1993. Inhibitory synaptic currents in stellate cells of rat cerebellar slices. *The Journal of physiology*, 468, pp.177–200.
- Llinas, R., Sugimori, M. & Lin, J.W., 1989. Blocking and isolation of a calcium channel from neurons in mammals and cephalopods utilizing a toxin fraction (FTX) from funnel-web spider poison. *Proceedings of the*. Available at: <http://www.pnas.org/content/86/5/1689.short>.
- Lo, E.H., Dalkara, T. & Moskowitz, M.A., 2003. Mechanisms, challenges and opportunities in stroke. *Nature reviews. Neuroscience*, 4(5), pp.399–415.
- Long, A.A. et al., 2008. Presynaptic calcium channel localization and calcium-dependent synaptic vesicle exocytosis regulated by the Fuseless protein. *The Journal of neuroscience: the official journal of the Society for Neuroscience*, 28(14), pp.3668–3682.
- Lopin, K.V. et al., 2012. Cd<sup>2+</sup> Block and Permeation of CaV3.1 ( $\alpha$ 1G) T-Type

Calcium Channels: Candidate Mechanism for Cd<sup>2+</sup> Influx. *Molecular pharmacology*, 82(6), pp.1183–1193.

Losavio, A. & Muchnik, S., 1997. Spontaneous acetylcholine release in mammalian neuromuscular junctions. *The American journal of physiology*, 273(6 Pt 1), pp.C1835–41.

Lou, X. et al., 2005. Allosteric modulation of the presynaptic Ca<sup>2+</sup> sensor for vesicle fusion. *Nature*, 435(7041), pp.497–501.

Ludwig, A., Flockerzi, V. & Hofmann, F., 1997. Regional expression and cellular localization of the alpha1 and beta subunit of high voltage-activated calcium channels in rat brain. *The Journal of neuroscience: the official journal of the Society for Neuroscience*, 17(4), pp.1339–1349.

Luebke, J.I., Dunlap, K. & Turner, T.J., 1993. Multiple calcium channel types control glutamatergic synaptic transmission in the hippocampus. *Neuron*, 11(5), pp.895–902.

Macleod, G.T., Gan, J. & Bennett, M.R., 1999. Vesicle-associated proteins and quantal release at single active zones of amphibian (*Bufo marinus*) motor-nerve terminals. *Journal of neurophysiology*, 82(3), pp.1133–1146.

Malenka, R.C., Madison, D.V. & Nicoll, R.A., 1986. Potentiation of synaptic transmission in the hippocampus by phorbol esters. *Nature*, 321(6066),



pp.175–177.

Mao, Z. et al., 1999. Neuronal activity-dependent cell survival mediated by transcription factor MEF2. *Science*, 286(5440), pp.785–790.

Maravall, M. et al., 2000. Estimating Intracellular Calcium Concentrations and Buffering without Wavelength Ratioing. *Biophysical journal*, 78(5), pp.2655–2667.

Mathew, S.S., Pozzo-Miller, L. & Hablitz, J.J., 2008. Kainate modulates presynaptic GABA release from two vesicle pools. *The Journal of neuroscience: the official journal of the Society for Neuroscience*, 28(3), pp.725–731.

Matsui, K. & Jahr, C.E., 2004. Differential control of synaptic and ectopic vesicular release of glutamate. *The Journal of neuroscience: the official journal of the Society for Neuroscience*, 24(41), pp.8932–8939.

Matthews, G. & Wickelgren, W.O., 1977. On the effect of calcium on the frequency of miniature end-plate potentials at the frog neuromuscular junction. *The Journal of physiology*, 266(1), pp.91–101.

Matveev, V. et al., 2011. Calcium cooperativity of exocytosis as a measure of Ca<sup>2+</sup> channel domain overlap. *Brain research*, 1398, pp.126–138.

Maximov, A. & Südhof, T.C., 2005. Autonomous function of synaptotagmin 1 in

triggering synchronous release independent of asynchronous release.

*Neuron*, 48(4), pp.547–554.

McAllister, A.K., Katz, L.C. & Lo, D.C., 1996. Neurotrophin regulation of cortical dendritic growth requires activity. *Neuron*, 17(6), pp.1057–1064.

McKinney, R.A. et al., 1999. Miniature synaptic events maintain dendritic spines via AMPA receptor activation. *Nature neuroscience*, 2(1), pp.44–49.

McMahon, H.T. et al., 1995. Complexins: cytosolic proteins that regulate SNAP receptor function. *Cell*, 83(1), pp.111–119.

Meinrenken, C.J., Borst, J.G.G. & Sakmann, B., 2002. Calcium secretion coupling at calyx of Held governed by nonuniform channel-vesicle topography. *The Journal of neuroscience: the official journal of the Society for Neuroscience*, 22(5), pp.1648–1667.

Melom, J.E. et al., 2013. Spontaneous and Evoked Release Are Independently Regulated at Individual Active Zones. *Journal of Neuroscience*, 33(44), pp.17253–17263.

Mintz, I.M., Sabatini, B.L. & Regehr, W.G., 1995. Calcium control of transmitter release at a cerebellar synapse. *Neuron*, 15(3), pp.675–688.

Missler, M. et al., 2003. Alpha-neurexins couple Ca<sup>2+</sup> channels to synaptic vesicle exocytosis. *Nature*, 423(6943), pp.939–948.

- Mochida, S. et al., 1996. Inhibition of neurotransmission by peptides containing the synaptic protein interaction site of N-type Ca<sup>2+</sup> channels. *Neuron*, 17(4), pp.781–788.
- Morgan, J.R. et al., 2013. Presynaptic membrane retrieval and endosome biology: defining molecularly heterogeneous synaptic vesicles. *Cold Spring Harbor perspectives in biology*, 5(10), p.a016915.
- Moser, T. & Beutner, D., 2000. Kinetics of exocytosis and endocytosis at the cochlear inner hair cell afferent synapse of the mouse. *Proceedings of the National Academy of Sciences of the United States of America*, 97(2), pp.883–888.
- Mozhayeva, M.G. et al., 2002. Development of vesicle pools during maturation of hippocampal synapses. *The Journal of neuroscience: the official journal of the Society for Neuroscience*, 22(3), pp.654–665.
- Müller, C.S. et al., 2010. Quantitative proteomics of the Cav2 channel nano-environments in the mammalian brain. *Proceedings of the National Academy of Sciences of the United States of America*, 107(34), pp.14950–14957.
- Muroi, M. et al., 1993. Folimycin (concanamycin A), a specific inhibitor of V-ATPase, blocks intracellular translocation of the glycoprotein of vesicular stomatitis virus before arrival to the Golgi apparatus. *Cell structure and*

*function*, 18(3), pp.139–149.

Nachshen, D.A., Sanchez-Armass, S. & Weinstein, A.M., 1986. The regulation of cytosolic calcium in rat brain synaptosomes by sodium-dependent calcium efflux. *The Journal of physiology*, 381, pp.17–28.

Navedo, M.F. et al., 2010. Increased coupled gating of L-type Ca<sup>2+</sup> channels during hypertension and Timothy syndrome. *Circulation research*, 106(4), pp.748–756.

Neher, E., 2015. Merits and Limitations of Vesicle Pool Models in View of Heterogeneous Populations of Synaptic Vesicles. *Neuron*, 87(6), pp.1131–1142.

Neher, E. & Sakaba, T., 2008. Multiple roles of calcium ions in the regulation of neurotransmitter release. *Neuron*, 59(6), pp.861–872.

Nilsson, P. et al., 1993. Regional changes in interstitial K<sup>+</sup> and Ca<sup>2+</sup> levels following cortical compression contusion trauma in rats. *Journal of cerebral blood flow and metabolism: official journal of the International Society of Cerebral Blood Flow and Metabolism*, 13(2), pp.183–192.

Nishihara, T. et al., 1995. Specific inhibitors of vacuolar type H<sup>(+)</sup>-ATPases induce apoptotic cell death. *Biochemical and biophysical research communications*, 212(1), pp.255–262.

- Nishizawa, Y., 2001. Glutamate release and neuronal damage in ischemia. *Life sciences*, 69(4), pp.369–381.
- Norris, C.M., Halpain, S. & Foster, T.C., 1998. Reversal of age-related alterations in synaptic plasticity by blockade of L-type Ca<sup>2+</sup> channels. *The Journal of neuroscience: the official journal of the Society for Neuroscience*, 18(9), pp.3171–3179.
- Nosyreva, E. et al., 2013. Acute Suppression of Spontaneous Neurotransmission Drives Synaptic Potentiation. *Journal of Neuroscience*, 33(16), pp.6990–7002.
- Otmakhov, N., Shirke, A.M. & Malinow, R., 1993. Measuring the impact of probabilistic transmission on neuronal output. *Neuron*, 10(6), pp.1101–1111.
- Otsu, Y. et al., 2004. Competition between phasic and asynchronous release for recovered synaptic vesicles at developing hippocampal autaptic synapses. *The Journal of neuroscience: the official journal of the Society for Neuroscience*, 24(2), pp.420–433.
- Otsu, Y. & Murphy, T.H., 2004. Optical postsynaptic measurement of vesicle release rates for hippocampal synapses undergoing asynchronous release during train stimulation. *The Journal of neuroscience: the official journal of the Society for Neuroscience*, 24(41), pp.9076–9086.
- Pang, Z.P. et al., 2011. Doc2 Supports Spontaneous Synaptic Transmission by a

Ca<sup>2+</sup>-Independent Mechanism. *Neuron*, 70(2), pp.244–251.

Pang, Z.P. et al., 2006. Synaptotagmin-2 is essential for survival and contributes to Ca<sup>2+</sup> triggering of neurotransmitter release in central and neuromuscular synapses. *The Journal of neuroscience: the official journal of the Society for Neuroscience*, 26(52), pp.13493–13504.

Pan, Z.H., Segal, M.M. & Lipton, S.A., 1996. Nitric oxide-related species inhibit evoked neurotransmission but enhance spontaneous miniature synaptic currents in central neuronal cultures. *Proceedings of the National Academy of Sciences of the United States of America*, 93(26), pp.15423–15428.

Parsons, T.D. et al., 1994. Calcium-triggered exocytosis and endocytosis in an isolated presynaptic cell: capacitance measurements in saccular hair cells. *Neuron*, 13(4), pp.875–883.

Peled, E.S., Newman, Z.L. & Isacoff, E.Y., 2014. Evoked and spontaneous transmission favored by distinct sets of synapses. *Current biology: CB*, 24(5), pp.484–493.

Peters, J.H. et al., 2010. Primary Afferent Activation of Thermosensitive TRPV1 Triggers Asynchronous Glutamate Release at Central Neurons. *Neuron*, 65(5), pp.657–669.

Pethig, R. et al., 1989. On the dissociation constants of BAPTA-type calcium

buffers. *Cell calcium*, 10(7), pp.491–498.

Phillips, C.G. et al., 2008. Calcium-sensing receptor activation depresses synaptic transmission. *The Journal of neuroscience: the official journal of the Society for Neuroscience*, 28(46), pp.12062–12070.

Prange, O. & Murphy, T.H., 1999. Correlation of miniature synaptic activity and evoked release probability in cultures of cortical neurons. *The Journal of neuroscience: the official journal of the Society for Neuroscience*, 19(15), pp.6427–6438.

Ramirez, D.M.O. et al., 2012. Vti1a Identifies a Vesicle Pool that Preferentially Recycles at Rest and Maintains Spontaneous Neurotransmission. *Neuron*, 73(1), pp.121–134.

Ramirez, D.M.O. & Kavalali, E.T., 2011. Differential regulation of spontaneous and evoked neurotransmitter release at central synapses. *Current opinion in neurobiology*, 21(2), pp.275–282.

Rettig, J. et al., 1996. Isoform-specific interaction of the alpha1A subunits of brain Ca<sup>2+</sup> channels with the presynaptic proteins syntaxin and SNAP-25. *Proceedings of the National Academy of Sciences of the United States of America*, 93(14), pp.7363–7368.

Rizo, J., Josep, R. & Junjie, X., 2015. The Synaptic Vesicle Release Machinery.

*Annual review of biophysics*, 44(1), pp.339–367.

Rizzoli, S.O., 2014. Synaptic vesicle recycling: steps and principles. *The EMBO journal*, 33(8), pp.788–822.

Rizzoli, S.O. & Betz, W.J., 2005. Synaptic vesicle pools. *Nature reviews. Neuroscience*, 6(1), pp.57–69.

Rozov, A. et al., 2001. Transmitter release modulation by intracellular Ca<sup>2+</sup> buffers in facilitating and depressing nerve terminals of pyramidal cells in layer 2/3 of the rat neocortex indicates a target cell-specific difference in presynaptic calcium dynamics. *The Journal of physiology*, 531(Pt 3), pp.807–826.

Ruat, M. et al., 1995. Calcium sensing receptor: molecular cloning in rat and localization to nerve terminals. *Proceedings of the National Academy of Sciences of the United States of America*, 92(8), pp.3161–3165.

Saitoe, M. et al., 2001. Absence of junctional glutamate receptor clusters in *Drosophila* mutants lacking spontaneous transmitter release. *Science*, 293(5529), pp.514–517.

Sakaba, T., 2006. Roles of the fast-releasing and the slowly releasing vesicles in synaptic transmission at the calyx of Held. *The Journal of neuroscience: the official journal of the Society for Neuroscience*, 26(22), pp.5863–5871.



Sanchez-Armass, S. & Blaustein, M.P., 1987. Role of sodium-calcium exchange in regulation of intracellular calcium in nerve terminals. *The American journal of physiology*, 252(6 Pt 1), pp.C595–603.

Sara, Y. et al., 2005. An Isolated Pool of Vesicles Recycles at Rest and Drives Spontaneous Neurotransmission. *Neuron*, 45(4), pp.563–573.

Sara, Y. et al., 2011. Use-dependent AMPA receptor block reveals segregation of spontaneous and evoked glutamatergic neurotransmission. *The Journal of neuroscience: the official journal of the Society for Neuroscience*, 31(14), pp.5378–5382.

Scanziani, M. et al., 1992. Presynaptic inhibition of miniature excitatory synaptic currents by baclofen and adenosine in the hippocampus. *Neuron*, 9(5), pp.919–927.

Schiavo, G.G. et al., 1992. Tetanus and botulinum-B neurotoxins block neurotransmitter release by proteolytic cleavage of synaptobrevin. *Nature*, 359(6398), pp.832–835.

Schoch, S. et al., 2001. SNARE function analyzed in synaptobrevin/VAMP knockout mice. *Science*, 294(5544), pp.1117–1122.

Shahrezaei, V., Cao, A. & Delaney, K.R., 2006. Ca<sup>2+</sup> from one or two channels controls fusion of a single vesicle at the frog neuromuscular junction. *The Journal of neuroscience: the official journal of the Society for Neuroscience*,

26(51), pp.13240–13249.

Sharma, G. & Vijayaraghavan, S., 2003. Modulation of presynaptic store calcium induces release of glutamate and postsynaptic firing. *Neuron*, 38(6), pp.929–939.

Sheng, Z.H., Yokoyama, C.T. & Catterall, W.A., 1997. Interaction of the synprint site of N-type Ca<sup>2+</sup> channels with the C2B domain of synaptotagmin I. *Proceedings of the National Academy of Sciences of the United States of America*, 94(10), pp.5405–5410.

Shoudai, K. et al., 2010. Thermally active TRPV1 tonically drives central spontaneous glutamate release. *The Journal of neuroscience: the official journal of the Society for Neuroscience*, 30(43), pp.14470–14475.

Sidach, S.S. & Mintz, I.M., 2000. Low-affinity blockade of neuronal N-type Ca channels by the spider toxin omega-agatoxin-IVA. *The Journal of neuroscience: the official journal of the Society for Neuroscience*, 20(19), pp.7174–7182.

Sigworth, F.J. & Sine, S.M., 1987. Data transformations for improved display and fitting of single-channel dwell time histograms. *Biophysical journal*, 52(6), pp.1047–1054.

Smith, S.M. et al., 2012. Calcium regulation of spontaneous and asynchronous

neurotransmitter release. *Cell calcium*, 52(3-4), pp.226–233.

Spence, M. & Johnson, I.D., 2010. The molecular probes handbook: a guide to fluorescent probes and labeling technologies.

Stanley, E.F., 1993. Single calcium channels and acetylcholine release at a presynaptic nerve terminal. *Neuron*, 11(6), pp.1007–1011.

Stanley, E.F., 1997. The calcium channel and the organization of the presynaptic transmitter release face. *Trends in neurosciences*, 20(9), pp.404–409.

Stanley, E.F., 2016. The Nanophysiology of Fast Transmitter Release. *Trends in neurosciences*, 39(3), pp.183–197.

Stephens, G.J. et al., 2001. The Cav2.1/ $\alpha$ 1A (P/Q-type) voltage-dependent calcium channel mediates inhibitory neurotransmission onto mouse cerebellar Purkinje cells. *The European journal of neuroscience*, 13(10), pp.1902–1912.

Sudhof, T.C., 2011. Calcium Control of Neurotransmitter Release. *Cold Spring Harbor perspectives in biology*, 4(1), pp.a011353–a011353.

Südhof, T.C., 2013. Neurotransmitter release: the last millisecond in the life of a synaptic vesicle. *Neuron*, 80(3), pp.675–690.

Sun, J. et al., 2007. A dual-Ca<sup>2+</sup>-sensor model for neurotransmitter release in a

central synapse. *Nature*, 450(7170), pp.676–682.

Sutton, M.A. et al., 2006. Miniature neurotransmission stabilizes synaptic function via tonic suppression of local dendritic protein synthesis. *Cell*, 125(4), pp.785–799.

Sutton, M.A. et al., 2007. Postsynaptic decoding of neural activity: eEF2 as a biochemical sensor coupling miniature synaptic transmission to local protein synthesis. *Neuron*, 55(4), pp.648–661.

Sutton, M.A. & Schuman, E.M., 2006. Dendritic protein synthesis, synaptic plasticity, and memory. *Cell*, 127(1), pp.49–58.

Swartz, K.J. et al., 1993. Protein kinase C modulates glutamate receptor inhibition of Ca<sup>2+</sup> channels and synaptic transmission. *Nature*, 361(6408), pp.165–168.

Tabata, T. & Kano, M., 2004. Calcium dependence of native metabotropic glutamate receptor signaling in central neurons. *Molecular neurobiology*, 29(3), pp.261–270.

Takahashi, T. & Momiyama, A., 1993. Different types of calcium channels mediate central synaptic transmission. *Nature*, 366(6451), pp.156–158.

Takamori, S. et al., 2006. Molecular Anatomy of a Trafficking Organelle. *Cell*, 127(4), pp.831–846.

- Taschenberger, H. & von Gersdorff, H., 2000. Fine-tuning an auditory synapse for speed and fidelity: developmental changes in presynaptic waveform, EPSC kinetics, and synaptic plasticity. *The Journal of neuroscience: the official journal of the Society for Neuroscience*, 20(24), pp.9162–9173.
- Thévenod, F. & Jones, S.W., 1992. Cadmium block of calcium current in frog sympathetic neurons. *Biophysical journal*, 63(1), pp.162–168.
- Trapani, J.G. & Nicolson, T., 2011. Mechanism of spontaneous activity in afferent neurons of the zebrafish lateral-line organ. *The Journal of neuroscience: the official journal of the Society for Neuroscience*, 31(5), pp.1614–1623.
- Trigo, F.F. et al., 2010. Presynaptic miniature GABAergic currents in developing interneurons. *Neuron*, 66(2), pp.235–247.
- Van der Kloot, W., 1996. Spontaneous and unquantal-evoked endplate currents in normal frogs are indistinguishable. *The Journal of physiology*. Available at: <http://onlinelibrary.wiley.com/doi/10.1113/jphysiol.1996.sp021297/full>.
- Verderio, C. et al., 2004. SNAP-25 modulation of calcium dynamics underlies differences in GABAergic and glutamatergic responsiveness to depolarization. *Neuron*, 41(4), pp.599–610.
- Verhage, M. et al., 2000. Synaptic assembly of the brain in the absence of neurotransmitter secretion. *Science*, 287(5454), pp.864–869.

- Vincent, A.M. et al., 2005. Cell culture modeling to test therapies against hyperglycemia-mediated oxidative stress and injury. *Antioxidants & redox signaling*, 7(11-12), pp.1494–1506.
- Virmani, T. et al., 2005. Phorbol esters target the activity-dependent recycling pool and spare spontaneous vesicle recycling. *The Journal of neuroscience: the official journal of the Society for Neuroscience*, 25(47), pp.10922–10929.
- Voglmaier, S.M. & Edwards, R.H., 2007. Do different endocytic pathways make different synaptic vesicles? *Current opinion in neurobiology*, 17(3), pp.374–380.
- Vyleta, N.P. & Smith, S.M., 2008. Fast Inhibition of Glutamate-Activated Currents by Caffeine. *PloS one*, 3(9), p.e3155.
- Vyleta, N.P. & Smith, S.M., 2011. Spontaneous Glutamate Release Is Independent of Calcium Influx and Tonically Activated by the Calcium-Sensing Receptor. *Journal of Neuroscience*, 31(12), pp.4593–4606.
- Wang, L.-Y., Neher, E. & Taschenberger, H., 2008. Synaptic vesicles in mature calyx of Held synapses sense higher nanodomain calcium concentrations during action potential-evoked glutamate release. *The Journal of neuroscience: the official journal of the Society for Neuroscience*, 28(53), pp.14450–14458.
- Wasser, C.R., Ertunc, M. & Liu, X., 2007. Cholesterol-dependent balance

between evoked and spontaneous synaptic vesicle recycling. *The Journal of*

Available at:

<http://onlinelibrary.wiley.com/doi/10.1113/jphysiol.2006.123133/full>.

Wasser, C.R. & Kavalali, E.T., 2009. Leaky synapses: regulation of spontaneous neurotransmission in central synapses. *Neuroscience*, 158(1), pp.177–188.

Watano, T. et al., 1996. A novel antagonist, No. 7943, of the Na<sup>+</sup>/Ca<sup>2+</sup> exchange current in guinea-pig cardiac ventricular cells. *British journal of pharmacology*, 119(3), pp.555–563.

Waters, J. & Smith, S.J., 2000. Phorbol esters potentiate evoked and spontaneous release by different presynaptic mechanisms. *The Journal of neuroscience: the official journal of the Society for Neuroscience*, 20(21), pp.7863–7870.

Weick, J.P. et al., 2003. Interactions with PDZ proteins are required for L-type calcium channels to activate cAMP response element-binding protein-dependent gene expression. *The Journal of neuroscience: the official journal of the Society for Neuroscience*, 23(8), pp.3446–3456.

Weingarten, J. et al., 2014. The proteome of the presynaptic active zone from mouse brain. *Molecular and cellular neurosciences*, 59, pp.106–118.

Weisskopf, M.G., Bauer, E.P. & LeDoux, J.E., 1999. L-type voltage-gated calcium channels mediate NMDA-independent associative long-term

potentiation at thalamic input synapses to the amygdala. *The Journal of neuroscience: the official journal of the Society for Neuroscience*, 19(23), pp.10512–10519.

Wellendorph, P. & Bräuner-Osborne, H., 2004. Molecular cloning, expression, and sequence analysis of GPRC6A, a novel family C G-protein-coupled receptor. *Gene*, 335, pp.37–46.

Wheeler, D., Randall, A. & Tsien, R., 1994. Roles of N-type and Q-type Ca<sup>2+</sup> channels in supporting hippocampal synaptic transmission. *Science*, 264(5155), pp.107–111.

Wierda, K.D.B. & Sorensen, J.B., 2014. Innervation by a GABAergic Neuron Depresses Spontaneous Release in Glutamatergic Neurons and Unveils the Clamping Phenotype of Synaptotagmin-1. *Journal of Neuroscience*, 34(6), pp.2100–2110.

Wilhelm, B.G. et al., 2014. Composition of isolated synaptic boutons reveals the amounts of vesicle trafficking proteins. *Science*, 344(6187), pp.1023–1028.

Wilhelm, B.G., Groemer, T.W. & Rizzoli, S.O., 2010. The same synaptic vesicles drive active and spontaneous release. *Nature neuroscience*, 13(12), pp.1454–1456.

Williams, C. et al., 2012. Coactivation of multiple tightly coupled calcium channels triggers spontaneous release of GABA. *Nature neuroscience*,



15(9), pp.1195–1197.

Wong, F.K. et al., 2014. Synaptic vesicle tethering and the CaV2.2 distal C-terminal. *Frontiers in cellular neuroscience*, 8, p.71.

Wu, L.G. et al., 1999. Calcium channel types with distinct presynaptic localization couple differentially to transmitter release in single calyx-type synapses. *The Journal of neuroscience: the official journal of the Society for Neuroscience*, 19(2), pp.726–736.

Xiao, C. et al., 2006. Pb<sup>2+</sup> impairs GABAergic synaptic transmission in rat hippocampal slices: a possible involvement of presynaptic calcium channels. *Brain research*, 1088(1), pp.93–100.

Xue, L. et al., 2013. Most vesicles in a central nerve terminal participate in recycling. *The Journal of neuroscience: the official journal of the Society for Neuroscience*, 33(20), pp.8820–8826.

Xu, J. et al., 2009. Synaptotagmin-1 functions as a Ca<sup>2+</sup> sensor for spontaneous release. *Nature neuroscience*, 12(6), pp.759–766.

Xu, W. et al., 2012. Distinct neuronal coding schemes in memory revealed by selective erasure of fast synchronous synaptic transmission. *Neuron*, 73(5), pp.990–1001.

Yamasaki, M., 2006. Miniature Synaptic Events Elicited by Presynaptic Ca<sup>2+</sup> Rise

Are Selectively Suppressed by Cannabinoid Receptor Activation in Cerebellar Purkinje Cells. *Journal of Neuroscience*, 26(1), pp.86–95.

Yamasaki, M., Hashimoto, K. & Kano, M., 2006. Miniature synaptic events elicited by presynaptic Ca<sup>2+</sup> rise are selectively suppressed by cannabinoid receptor activation in cerebellar Purkinje cells. *The Journal of neuroscience: the official journal of the Society for Neuroscience*, 26(1), pp.86–95.

Yang, X. et al., 2010. Complexin clamps asynchronous release by blocking a secondary Ca(2+) sensor via its accessory  $\alpha$  helix. *Neuron*, 68(5), pp.907–920.

Yang, X., Cao, P. & Südhof, T.C., 2013. Deconstructing complexin function in activating and clamping Ca<sup>2+</sup>-triggered exocytosis by comparing knockout and knockdown phenotypes. *Proceedings of the National Academy of Sciences of the United States of America*, 110(51), pp.20777–20782.

Yao, J. et al., 2011. Doc2 Is a Ca<sup>2+</sup> Sensor Required for Asynchronous Neurotransmitter Release. *Cell*, 147(3), pp.666–677.

Zamir, O. & Charlton, M.P., 2006. Cholesterol and synaptic transmitter release at crayfish neuromuscular junctions. *The Journal of physiology*, 571(Pt 1), pp.83–99.

Zanos, P. et al., 2016. NMDAR inhibition-independent antidepressant actions of

ketamine metabolites. *Nature*, 533(7604), pp.481–486.

Zefirov, A. et al., 1995. Localization of active zones. *Nature*, 376(6539), pp.393–394.

Zhang, Z. et al., 2010. Vesicular ATPase inserted into the plasma membrane of motor terminals by exocytosis alkalinizes cytosolic pH and facilitates endocytosis. *Neuron*, 68(6), pp.1097–1108.

Zhong, H. et al., 1999. Reciprocal regulation of P/Q-type Ca<sup>2+</sup> channels by SNAP-25, syntaxin and synaptotagmin. *Nature neuroscience*, 2(11), pp.939–941.

Zhou, Q., Petersen, C.C. & Nicoll, R.A., 2000. Effects of reduced vesicular filling on synaptic transmission in rat hippocampal neurones. *The Journal of physiology*, 525 Pt 1, pp.195–206.

Zucker, R., 1989. Short-Term Synaptic Plasticity. *Annual review of neuroscience*, 12(1), pp.13–31.

Zucker, R.S., 2005. Minis: whence and wherefore? *Neuron*, 45(4), pp.482–484.